

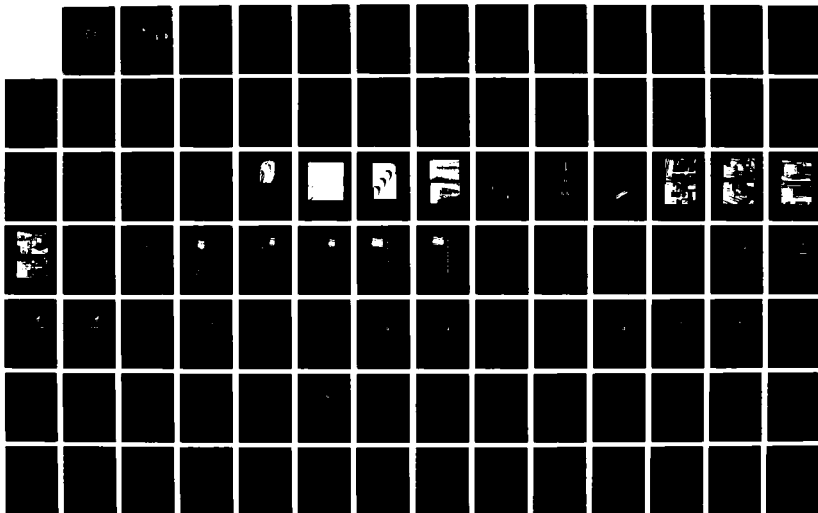
AD-A183 428

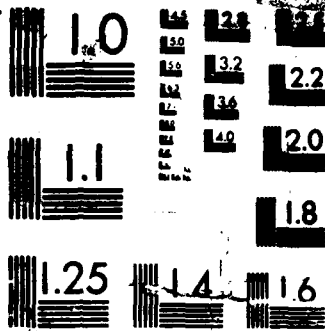
STUDY OF VORTICES EMBEDDED IN BOUNDARY LAYERS WITH FILM 1/2
COOLING(U) NAVAL POSTGRADUATE SCHOOL MONTEREY CA
D L EVANS MAR 87 NIPR-FY-1455-86-N0616

UNCLASSIFIED

F/8 28/4

NL





MICROCOPY RESOLUTION TEST CHART

AD-A183 428

DTIC FILE COPY ②

NAVAL POSTGRADUATE SCHOOL

Monterey, California



S DTIC
ELECTE **D**
AUG 17 1987
E

THESIS

STUDY OF VORTICES
EMBEDDED IN BOUNDARY
LAYERS WITH FILM COOLING

by

David L. Evans

March 1987

Thesis Advisor

Phillip M. Ligrani

Approved for public release; distribution is unlimited.

033

UNCLASSIFIED

SECURITY CLASSIFICATION OF THIS PAGE

A183 428

REPORT DOCUMENTATION PAGE

1a REPORT SECURITY CLASSIFICATION UNCLASSIFIED		1b RESTRICTIVE MARKINGS	
2a SECURITY CLASSIFICATION AUTHORITY		3 DISTRIBUTION/AVAILABILITY OF REPORT Approved for public release; distribution is unlimited	
2b DECLASSIFICATION/DOWNGRADING SCHEDULE		5 MONITORING ORGANIZATION REPORT NUMBER(S)	
4 PERFORMING ORGANIZATION REPORT NUMBER(S)		7a NAME OF MONITORING ORGANIZATION Wright Aeronautical Laboratories	
6a NAME OF PERFORMING ORGANIZATION NAVAL POSTGRADUATE SCHOOL	6b OFFICE SYMBOL (if applicable) Code 69	7b ADDRESS (City, State, and ZIP Code) Wright-Patterson Air Force Base Ohio 45433	
6c ADDRESS (City, State, and ZIP Code) Monterey, California 93943-5000		9 PROCUREMENT INSTRUMENT IDENTIFICATION NUMBER Mipr. No. FY 1455-86-N0616	
8a NAME OF FUNDING/SPONSORING ORGANIZATION Wright Aeronautical Lab.	8b OFFICE SYMBOL (if applicable)	10 SOURCE OF FUNDING NUMBERS	
8c ADDRESS (City, State, and ZIP Code) Wright-Patterson Air Force Base Ohio 45433		PROGRAM ELEMENT NO	PROJECT NO
		TASK NO	WORK UNIT ACCESSION NO
11 TITLE (Include Security Classification) STUDY OF VORTICES EMBEDDED IN BOUNDARY LAYERS WITH FILM COOLING			
12 PERSONAL AUTHOR(S) Evans, David L.			
13a TYPE OF REPORT Master's Thesis	13b TIME COVERED FROM _____ TO _____	14 DATE OF REPORT (Year, Month, Day) 1987 March	15 PAGE COUNT 101
16 SUPPLEMENTARY NOTATION			
17 COSATI CODES		18 SUBJECT TERMS (Continue on reverse if necessary and identify by block number)	
FIELD	GROUP	Embedded vortex, film cooling	
	SUB-GROUP		
19 ABSTRACT (Continue on reverse if necessary and identify by block number)			
<p>Measurements are presented of boundary layers with embedded vortices and with film cooling for freestream velocities of 15, and 11 m/s. Measurements of a boundary layer with embedded vortex and and no film cooling, and of a boundary layer with film cooling but no vortex are presented for freestream velocity of 15 m/s. Plots of total velocity, V, streamwise velocity, V_x, secondary flow vectors, total pressure, P_o, and streamwise vorticity are presented for many of these test conditions.</p> <p>The results show that the embedded vortices completely dominate the flow field in boundary layers with film cooling. This is indicated from the plots of V, V_x, and P_o which show the effects of film cooling to be completely decimated in the vicinity of the vortex.</p>			
20 DISTRIBUTION/AVAILABILITY OF ABSTRACT <input checked="" type="checkbox"/> UNCLASSIFIED/UNLIMITED <input type="checkbox"/> SAME AS RPT <input type="checkbox"/> DTIC USERS		21 ABSTRACT SECURITY CLASSIFICATION UNCLASSIFIED	
22a NAME OF RESPONSIBLE INDIVIDUAL Phillip M. Ligrani		22b TELEPHONE (Include Area Code) (408) 646-3382	22c OFFICE SYMBOL Code 69L1

DD FORM 1473, 84 MAR

83 APR edition may be used until exhausted
All other editions are obsoleteSECURITY CLASSIFICATION OF THIS PAGE
UNCLASSIFIED

19. ABSTRACT (cont.)

In order to conduct this study, a five-hole pressure probe was calibrated for pitch and yaw. The probe was then used to measure five pressures associated with the flow. From these pressures, total velocity and the x, y, and z components of velocity were determined.

A boundary layer profile was conducted to verify the calibration of the pressure probe, measurement procedures, and velocity computations. The results show expected boundary layer behavior with a small V_y and V_z component. ()

Approved for public release; distribution is unlimited.

Study of Vortices
Embedded in Boundary
Layers with Film Cooling

by

David L. Evans
Lieutenant Commander, United States Navy
B.S., United States Naval Academy, 1974

Submitted in partial fulfillment of the
requirements for the degree of

MASTER OF SCIENCE IN MECHANICAL ENGINEERING

from the

NAVAL POSTGRADUATE SCHOOL
March 1987

Accession For	
NTIS GRA&I	<input checked="" type="checkbox"/>
DTIC TAB	<input type="checkbox"/>
Unannounced	<input type="checkbox"/>
Justification	
By _____	
Distribution/ _____	
Availability Codes	
Dist	Avail and/or Special
A-1	

Author:

David L. Evans
David L. Evans

Approved by:

Phillip M. Ligrani
Phillip M. Ligrani, Thesis Advisor

Anthony J. Healy
Anthony J. Healy, Chairman,
Department of Mechanical Engineering

G. E. Schacher
G. E. Schacher,
Dean of Science and Engineering



ABSTRACT

Measurements are presented of boundary layers with embedded vortices and with film cooling for freestream velocities of 15, and 11 m/s. Measurements of a boundary layer with embedded vortex and no film cooling, and of a boundary layer with film cooling but no vortex are presented for freestream velocity of 15 m/s. Plots of total velocity, V , streamwise velocity, V_x , secondary flow vectors, total pressure, P_o , and streamwise vorticity are presented for many of these test conditions.

The results show that the embedded vortices completely dominate the flow field in boundary layers with film cooling. This is indicated from the plots of V , V_x , and P_o which show the effects of film cooling to be completely decimated in the vicinity of the vortex.

In order to conduct this study, a five-hole pressure probe was calibrated for pitch and yaw. The probe was then used to measure five pressures associated with the flow. From these pressures, total velocity and the x, y, and z components of velocity were determined.

A boundary layer profile was conducted to verify the calibration of the pressure probe, measurement procedures, and velocity computations. The results show expected boundary layer behavior with a small V_y and V_z component.

TABLE OF CONTENTS

I.	INTRODUCTION	10
II.	EXPERIMENTAL APPARATUS	12
	A. WIND TUNNEL	12
	1. Description	12
	2. Qualification and Performance	12
	B. INJECTION SYSTEM	13
	C. FIVE-HOLE PRESSURE PROBE	14
	D. DATA ACQUISITION SYSTEM	15
	1. Transducers and Demodulators	15
	2. Computers and Hardware	15
III.	CALIBRATION AND MEASUREMENT PROCEDURES	17
	A. COORDINATE SYSTEM	17
	B. EXPERIMENTAL PROCEDURES	17
	C. CALIBRATION COEFFICIENTS	18
	D. RESULTS	19
	E. INTERPOLATION AND APPLICATION	20
	F. VELOCITY COMPONENT DETERMINATION	22
	G. SPATIAL RESOLUTION CORRELATION	23
	H. SOFTWARE	23
IV.	EXPERIMENTAL RESULTS	25
	A. BASELINE RESULTS	25
	B. 15M S FREESTREAM VELOCITY RESULTS	25
	1. Boundary layer with film cooling	26
	2. Boundary layer with vortex	26
	3. Boundary layer with vortex and film cooling	26
	C. 20 M S AND 10 M S FREESTREAM VELOCITY RESULTS	27

V. SUMMARY AND CONCLUSIONS	28
APPENDIX A: FIGURES	29
APPENDIX B: SOFTWARE	75
APPENDIX C: UNCERTAINTY ANALYSIS	98
LIST OF REFERENCES	99
INITIAL DISTRIBUTION LIST	100

LIST OF FIGURES

1.1	Endwall secondary flows	29
1.2	Smoke and oil visulization for rotor blade	30
1.3	Secondary flow deflection	31
1.4	Rotation of passage and corner vortices in turbine cascade	32
2.1	Photographs of wind tunnel	33
2.2	Schematic of injection air flow	34
2.3	Schematic of injection plenum	35
2.4	Photographs of pressure probe	36
2.5	Manual traversing device	37
2.6	Automated traversing mechanism	38
2.7	Photographs of Two-Axis Motion Controller	39
2.8	Photographs of data acquistion system	40
3.1	Coordinate system for flow measurement	41
3.2	Repeatability of calibration results at different freestream velocities for $C_{p_{yaw}}$ vs. yaw angles	42
3.3	Probe calibration, $C_{p_{yaw}}$ vs. yaw angles, freestream velocity of 21 m/s	43
3.4	Probe calibration, $C_{p_{pitch}}$ vs. pitch angle for -20° to -4° yaw, freestream velocity of 21 m/s	44
3.5	Probe calibration, $C_{p_{pitch}}$ vs. pitch angle for 0° to +20° yaw, freestream velocity of 21 m/s	45
3.6	Probe calibration, $C_{p_{static}}$ vs. pitch angles, freestream velocity of 21 m/s	46
3.7	Probe calibration, $C_{p_{total}}$ vs. pitch angles, freestream velocity of 21 m/s	47
3.8	Interpolation for pitch angles	48
3.9	Interpolation for yaw angles	49
3.10	Interpolation for local $C_{p_{total}}$	50
3.11	Interpolation for local $C_{p_{static}}$	51
4.1	Baseline boundary layer results for streamwise velocity, V_x	52
4.2	Baseline boundary layer results for spanwise velocity, V_z	53

4.3	Baseline boundary layer results for corrected V_y	54
4.4	Baseline boundary layer results for uncorrected V_y	55
4.5	Streamwise velocity for boundary layer without embedded vortex, 75% film cooling, freestream velocity 15 m/s	56
4.6	Total velocity for boundary layer without embedded vortex 75% film cooling, freestream velocity 15 m/s	57
4.7	Total pressure for boundary layer without embedded vortex, 75% film cooling, freestream velocity 15 m/s	58
4.8	Secondary flow vectors for boundary layer without embedded vortex, 75% film cooling, freestream velocity 15 m/s	59
4.9	Streamwise velocity for boundary layer with embedded vortex, without film cooling, freestream velocity 15 m/s	60
4.10	Total velocity for boundary layer with embedded vortex, without film cooling, freestream velocity 15 m/s	61
4.11	Total pressure for boundary layer with embedded vortex, without film cooling, freestream velocity 15 m/s	62
4.12	Secondary flow vectors for boundary layer with embedded vortex, without film cooling, freestream velocity 15 m/s	63
4.13	Vorticity contours for boundary layer with embedded vortex, without film cooling, freestream velocity 15 m/s	64
4.14	Streamwise velocity for boundary layer with embedded vortex and film cooling, freestream velocity 15 m/s	65
4.15	Total velocity for boundary layer with embedded vortex and film cooling, freestream velocity 15 m/s	66
4.16	Total pressure for boundary layer with embedded vortex and film cooling, freestream velocity 15 m/s	67
4.17	Secondary flow vectors for boundary layer with embedded vortex and film cooling, freestream velocity 15 m/s	68
4.18	Vorticity contours for boundary layer with embedded vortex and film cooling, freestream velocity 15 m/s	69
4.19	Stanton number ratio for vortex at $z = -4.79\text{cm}$ with film cooling	70
4.20	Streamwise velocity for embedded vortex without film cooling, freestream velocity 20 m/s	71
4.21	Secondary flow vectors for embedded vortex without film cooling, freestream velocity 20 m/s	72
4.22	Streamwise velocity for embedded vortex with film cooling, freestream velocity 11 m/s	73
4.23	Secondary flow vectors for embedded vortex with film cooling, freestream velocity 11 m/s	74

ACKNOWLEDGEMENTS

This work was supported by the Wright Aeronautical Laboratories, Wright-Patterson Air Force Base, MIPR number Fy 1455-86-N0616. Dr. Charles Mac Arthur was program monitor. The Shear Layer Research Facility and other apparatus were purchased from the NPS Research Foundation. Technical contributions were made by Dr. R. V. Westphal.

I wish to thank my God for providing me with faith, persistence, and patience required to complete this thesis. I am grateful to the United States Navy for providing me with this chance of a lifetime, and to the staff and faculty of the Naval Postgraduate School for the fine education. In particular, I wish to thank Professor Phil Ligrani for his assistance, infinite patience, and for the many long hours he spent helping me. *Because of his efforts, this has been a most rewarding and interesting study.* Additionally, I want to acknowledge Tom McCord for his assistance and suggestions and Charles Crow for his fine workmanship. Most importantly, I am forever grateful to Sunny, Elizabeth, and Sarah for their love, and support.

I. INTRODUCTION

The increasing need for greater efficiency in gas turbine engines has resulted in higher turbine inlet temperatures. Consequently, combustor liners and turbine blading are subjected to greater amounts of thermal stress, thermal fatigue, and creep. At present, gas turbines, such as those associated with military applications, have inlet temperatures as high as 1800 - 2000 degrees C (3270 - 3632 F) with pressures of 40 atmospheres.

Turbine parts may be protected from heat loads resulting from exposure to gas at high temperatures by using a coolant within turbine passages and along turbine surfaces. Convection cooling, impingement cooling, transpiration cooling, and film cooling are used for this purpose. Although it is possible for the cooling medium to be a substance such as liquid water or Freon - 12, most gas turbine arrangements utilize engine air bled off from the compressor and rerouted to the turbine nozzles and blading. With film cooling, compressor air is ejected from surfaces of blades and vanes. The film coolant then protects metal surfaces by forming a protective insulating film between the blades and the mainstream, and by acting as a heat sink.

The flow through a turbine cascade is extremely complex. Efforts to analytically model the flow are successful only when the fluid is considered to be inviscid. When the effects of viscosity are included, the analysis is much less effective [Ref. 1]. Because of the difficulty involved in analytical representation of the viscous portions of cascade flows, much of the work in this area is experimental in nature.

Flow visualization studies by Herzig, et al., [Ref. 2] were among the first to show the complexity of flow within the cascade. Flow visualization studies by Langston, et al., [Ref. 3] and Marchal and Sieverding, [Ref. 4] also show the detailed development and complexity of the flow through the turbine cascade. More recently, Sieverding and Van Den Bosche, [Ref. 5] have used color smoke-visualization to study the evolution of flow in cascades.

Figure 1.1 from [Ref. 6] shows the various secondary flows associated with flow in turbine cascades. As the inlet boundary layer approaches the blade's leading edge, a horseshoe vortex is formed. The point at which this formation occurs is the saddle point which is clearly shown in Figure 1.2 from [Ref. 4]. One leg of the horseshoe

vortex moves initially near the side of the blade, and then through the blade passage where it is referred to as the passage vortex. In cascade flow, the passage vortex is composed of 1) fluid from the pressure side leg of the horseshoe vortex, 2) the crossflow from the endwall boundary layer, and 3) entrained fluid from the mainstream flow, [Ref. 7]. As the passage vortex continues through the cascade, it is forced by the pressure gradient to the opposite side of the passage near the suction side of the adjacent blade. This shift is clearly shown in Figure 1.3 from [Ref. 2]. The second leg of the horseshoe vortex follows the suction side of the blade and has a sense of rotation opposite to that of the pressure side vortex. This vortex moves away from the corner and is generally believed to be smaller in size than the passage vortex. As can be seen from Figure 1.4 from [Ref. 8] the passage vortex makes approximately one rotation as it passes through the cascade. In Figure 1.1 the number of revolutions has been exaggerated for clarity.

The objective of this thesis is to study the effects of embedded vortices on a film cooled turbulent boundary layer. In order to understand the effects that this complex flow field has upon heat transfer, vortex characteristics and their interaction with surrounding flow must be understood. In this study, a five-hole pressure probe is used to measure vortex characteristics.

Extensive procedures for calibration and qualification of the five-hole pressure probe, and its use in measuring three-dimensional flows are first discussed. Results of six different test are then given: 1) a baseline measurement in a developing boundary layer, 2) a boundary layer with film cooling only at a freestream velocity of 15m s, 3) a boundary layer with a single embedded vortex and without film cooling at a freestream velocity of 15 m/s, 4) a boundary layer with embedded vortex and film cooling at a freestream velocity of 15 m/s, 5) a boundary layer with an embedded vortex and no film cooling at a freestream velocity of 20 m/s, and 6) a boundary layer with embedded vortex and film cooling at a freestream velocity of 11 m/s. Cases 3, and 4 provide the most informative results of the study; cases 5 and 6 are incidental.

II. EXPERIMENTAL APPARATUS

A. WIND TUNNEL

The wind tunnel pictured in Figure 2.1 is now described. It is an open-circuit blower tunnel used to provide uniform flow at the nozzle exit.

1. Description

The wind tunnel is designated the NPS Shear Layer Research Facility (SLRF) and was built by Aerolab. It is designed to provide uniform flow with a minimum amount of turbulence intensity. It is designed with numerous pressure taps and four 38 x 20.3 cm (15 x 8 in.) access ports along each of the of the side walls. The height of the top wall is adjustable to permit changes in the pressure gradient along the length of the test section. Additionally, the top wall contains numerous instrument ports for the measurement of various flow characteristics.

The air speed through the tunnel can be adjusted from 5 m/s to 40 m/s. The blower exit slips into the inlet end of the wide-angle diffuser with 1.6 mm of clearance so that the fan is isolated from the body of the wind tunnel. The diffuser inlet contains a filter and nozzle. The test section is 3.048 m (10 ft.) long and 0.6096 m (2 ft.) wide. The top is fabricated from Lexan sheet (4.76 mm thick), continuously sealed with neoprene along the edges. The tunnel's bottom wall consists of one 1.2192 m (4 ft.) long and three 0.6096 m (2 ft.) long removeable and replaceable sections. These sections are all 0.6096 m (2 ft.) wide and are sealed with "O" rings around the sides. Further discussions of the wind tunnel are contained in [Ref. 9] and [Ref. 10: p. 38].

2. Qualification and Performance

Extensive qualification test of the Shear Layer Research Facility were conducted by Ligrani, [Ref. 11]. Results show that the variation of total pressure at the exit plane of the nozzle is less than 0.4% at 26 m/s and 34 m/s. Mean velocity varies less than 0.7% for the same mean freestream speeds. From five-hole pressure probe measurements, the velocity angle deviation is nowhere greater than about 0.6 degrees at the nozzle exit plane.

Profile measurements of the mean velocity and longitudinal turbulence intensity in the turbulent boundary layer developing at 20 m/s indicate normal, spanwise uniform behavior. For this qualification test, and all results which follow, the

boundary layer was tripped near the exit of the nozzle with a 1.5 mm high strip of tape. Total pressure measurements along the test section surface at the nozzle exit were uniform within 0.5% indicating spanwise uniform skin friction.

Freestream turbulence intensity was measured to be 0.00085 (8.5 one-hundredths of one percent or .085 percent) at 20 m/s increasing to 0.00095 at 30 m/s.

B. INJECTION SYSTEM

Ordinarily, the injection system provides film coolant at temperatures above ambient. The freestream air is at ambient temperature; therefore, the heat transfer would then be in a direction opposite to that which occurs in gas turbines. The coolant is injected into the boundary layer through a single row of injection holes. The injection holes are scaled relative to boundary layer thickness to be similar to those used in current turbine blade design.

For the present tests, all injected air was at ambient temperatures.

Injection system air is provided by an 71TD Ingersoll-Rand air compressor. The air is discharged from the compressor into three large storage tanks. As the schematic, Figure 2.2, shows the air flows from the storage tank through an adjustable regulator, a cut-off valve, moisture separator, flow regulator, a Fisher and Portor rotometer (full scale $9.345E-3$ m³/s, 19.8 SCFM, model 10A3565A). The rotometer which controls the volumetric flow rate, discharges the film coolant through a diffuser and into the injection heat exchanger and plenum chamber.

The heat exchanger and plenum chamber shown in Figure 2.3 is 0.305 x 0.508 x 0.457 m (23 x 20 x 18 in.) and is constructed of 1.27 cm (1/2 in.) plexiglass. Injection air flows over three metal plates 0.381 x 0.508 m (15 x 20 in.). The two lower plates are covered by silicon rubber heaters, 0.381 x 0.483 m (15 x 19 in.), rated at 120 volts. The heaters are controlled through a type 136 Powerstat variable autotransformer. The top surface of the chamber contains 13 plexiglass injection tubes each being 8 cm (3.15 in.) in length and with an inner diameter of 0.95 cm (3/8 in.). This corresponds to a length to diameter ratio of 8.42. The 13 injection holes discharge the coolant into the boundary layer at a 30 degree angle. There is a three-diameter spanwise spacing between the center of each hole.

Further discussion of the qualification and performance of the injection system can be found in [Ref. 10: p.23].

C. FIVE-HOLE PRESSURE PROBE

Multi-hole pressure probes are invaluable in the investigation and measurement of complex, three-dimensional flows. In particular, the five-hole probe is well suited for measurement of three mean velocity components in low speed incompressible flows.

The five-hole pressure probe used to measure pressure in this study is manufactured by United Sensors and Control Corp. (drawing number DA-125-24-F-22-CD). The probe shown in Figure 2.4 is 0.6096 m (2 ft.) in overall length with a probe diameter of 0.318 cm (0.125 in.). It is constructed of corrosion-resistant, non-magnetic stainless steel.

The five pressure holes are arranged in two different planes which intersect at the mutual hole, P_1 . The probe tip is prismatic in geometry, as shown in Figure 2.4. The centrally located P_1 hole is normal to the freestream. The pitch plane consists of P_1 , P_4 , and P_5 pressure holes. While pressure holes P_1 , P_2 , P_3 constitute the yaw plane. The distance separating P_2 and P_3 is 0.178 cm (0.070 in.), P_4 and P_5 are 0.155 cm (0.061 in.) apart. The central hole P_1 is 0.648 cm (0.255 in.) from the bottom of the probe tip. These distances were measured using a micrometer.

For calibration, the probe was positioned in a manual traversing unit manufactured by United Sensor and Control Corp., Figure 2.5. The unit was modified by the user to include a compass rose with a radius of 15.24 cm (6 in.) and a range of yaw angles from -40 to +40 degrees (0.25 degree accuracy). Additionally, the manual traversing unit positions the probe vertically in the mainstream 0 - 30.48 cm (0 - 12 in.) range. The manual traversing unit is mounted on top of a spanwise, horizontal sled. The sled is 62.23 cm (24.5 in.) wide and is designed to set in place on top of the wind tunnel's side walls. The spanwise mounting sled is designed such that the probe can be positioned 10.16 cm (4 in.) either side of centerline in increments of 0.635 cm (0.25 in.). In addition to spanwise positioning, the spanwise sled could be rotated through a range of pitch angles from -15 to +15 degrees with an accuracy of 0.5 degrees.

After the completion of the probe calibration, an automated traversing mechanism, Figure 2.6, was used for probe positioning while measuring the pressures in the experimental test cases. The probe is fixed into the automated traversing mechanism in a position of zero yaw. The traversing mechanism has two degrees of movement which allows a thorough measurement of the flow field to be conducted. Both the spanwise and vertical traversing blocks are mounted on a 20-thread per inch drive screw and two ground steel, case-hardened steel guide support shafts. Each drive

shaft is directly coupled to a SLO-SYN type MO92-FD310 stepping motor. The motors are controlled by a MITAS Two-Axis Motion Controller, Figure 2.7 The stepping motors and the controller are manufactured by Superior Electric Company. The controller directs the movement the probe in both the spanwise and vertical directions. The MITAS controller comes equipped with 2K bytes of memory and an MC68000, 16-bit microprocessor which allows the user to program the start, stop, duration, speed, acceleration and deceleration of the stepping motors.

D. DATA ACQUISITION SYSTEM

The data acquisition system, shown in Figure 2.8 rapidly acquires the voltages associated with each pressure, converts each voltage to pressure.

1. Transducers and Demodulators

The probe is connected through reinforced plastic tubing to five Celesco model LCVR differential pressure transducers. These transducers have a designed pressure range of 0 -20 cm (0 - 7.85 in.) water and produce a 15 to 45 mV volt output signal. The transducer output signal is converted to a proportional DC signal by Celesco CD 10D carrier demodulators. Each demodulator has a maximum frequency response of -3dB at 500 Hz and a maximum out put noise of 10mV, peak to peak. Each transducer carrier demodulator combination was calibrated against a Meridian 1.27 cm (0.5 in.) horizontal manometer with an accuracy of 0.002 cm (.005 in.) of water, to give typical calibration of approximately 1.0 volt per inch of water differential pressure.

2. Computers and Hardware

A Hewlett-Packard 85 microcomputer was used to acquire and process data for the calibration of the pressure probe. Configured with 64K bytes of memory and a single magnetic tape cartridge drive, the HP-85 was used to collect, store, display, and print the majority of the data required during the course of probe calibration.

For the measurement of the flow field, a Hewlett-Packard Series 300, Model 9836S computer was dedicated to the data acquisition process. The HP 9836S is equipped with a MC68000, 8 MHz 16 32-bit processor, Dual 5-1/4 inch floppy disk drives, and 1M bytes of memory. A HP 7470 two pen plotter was used for the graphic representation of data.

Each transducer carrier demodulator combination is connected directly to a HP 3498A extender which is controlled by a HP-3497A data acquisition control unit. The HP-3497A which provides precision measurement and process monitoring, is equipped with analog multiplexing and a digital voltmeter with 1 μ V sensitivity.

Six software programs were developed for use during the thesis. PROCAL was developed for use with the HP-85 and was used during the probe calibration phase. PRSACQ, VEL, VELC, PLOT, VECTOR were developed for use with the HP 9836S. PRSACQ is used to measure the pressures in the various flow fields. VEL and VELC are used to compute the velocity components. PLOT and VECTOR are used for the plotting of results. A thorough discussion of the programs requires an understanding of the calibration procedures and the velocity measurement techniques as discussed in Chapter Three.

III. CALIBRATION AND MEASUREMENT PROCEDURES

Prior to using the five-hole pressure probe to measure flow velocities, it is necessary to calibrate the probe to determine the dependence of yaw, pitch, static, and total coefficients on yaw and pitch angles.

A. COORDINATE SYSTEM

A right hand coordinate system, Figure 3.1 was established for use throughout the course of study. The X-axis is parallel to the streamwise direction and is positive in the downstream direction. The Y-axis is in the vertical plane and is positive from the wind tunnel's bottom wall. The Z-axis is in the spanwise direction and is positive from the wind tunnel's bottom wall. The origin of the coordinate system is located on the centerline line of the bottom wall.

Yaw, β , is defined as rotation about the Y-axis and was arbitrarily defined as positive when the direction of the flow resulted in pressure P_3 being greater than P_2 . This condition corresponds to positive component of velocity in Z direction. The pitch angle, α , is defined as rotation about the Z-axis and is defined as positive when P_4 is greater than P_5 . This condition results in a positive component of velocity in the Y direction.

B. EXPERIMENTAL PROCEDURES

The five-hole pressure probe was calibrated using the method described by Treaster and Yocum, [Ref. 12].

To perform the calibration, the probe is placed in the manual traversing unit which is mounted on top of the spanwise horizontal sled as described in Chapter Two. The probe is normal to the freestream when P_2 is equal to P_3 which gives β equal to zero.

The probe was manually fixed at a predetermined yaw angle and then rotated through the pitch plane. At each point, the data acquisition system records the five pressures. Four pressure coefficients are then calculated by the PROCAL program.

Calibration of the probe was conducted over a range of yaw angles from -20 degrees to +20 degrees in four-degree increments. The pitch angle was varied from -15 degrees to +15 degrees in five-degree increments. This provided a cone of angles

which was sufficient for the flows to be studied in this thesis. Calibration was performed in the NPS Shear Layer Tunnel at a freestream velocity of approximately 21 m/s (68.89 ft/sec). The probe was located 1.6 m (5.3ft) from the boundary layer trip. This equates to a Reynolds number of 1.97×10^6 based on downstream distance. Static pressure was obtained from a static pressure tap on the tunnel side wall and total pressure from a Kiel probe inserted into the flow through the top wall. Static and total pressures are measured once per set of calibration points. Atmospheric pressure is used as the reference pressure.

C. CALIBRATION COEFFICIENTS

To use the probe for measurement of complex flows, it is necessary to determine the flow angles, α and β , and the local static and total pressures. This can be done by determining four non-dimensional pressure coefficients over a range of angles in both the yaw and pitch planes. The four calibration coefficients are defined as:

$$C_{p_{yaw}} = (P_2 - P_3) (P_1 - \bar{P}) \quad (\text{eqn 3.1})$$

$$C_{p_{pitch}} = (P_4 - P_5) (P_1 - \bar{P}) \quad (\text{eqn 3.2})$$

$$C_{p_{total}} = (P_1 - P_{total}) (P_1 - \bar{P}) \quad (\text{eqn 3.3})$$

$$C_{p_{static}} = (\bar{P} - P_{static}) (P_1 - \bar{P}) \quad (\text{eqn 3.4})$$

where

$$\bar{P} = (P_2 + P_3 + P_4 + P_5) / 4 \quad (\text{eqn 3.5})$$

To be of value in measuring a flow field, the calibration coefficients must be a function of flow angle only, independent of velocity and repeatable. Figure 3.2 shows that the calibration is both independent of velocity and repeatable in the yaw plane.

As previously stated, probe calibration was conducted by fixing the yaw angle and varying the pitch angle. Theoretically, a calibration procedure of fixing the pitch angle and rotating through the yaw angles should provide identical results. However, in this study when the fixed pitch vary yaw method was attempted, the results were not identical. The trend of $C_{p_{pitch}}$ vs. pitch angle showed significant scatter, and $C_{p_{total}}$ vs. pitch angle was not constant for each yaw angle.

D. RESULTS

Figure 3.3 shows the variation of $C_{p_{yaw}}$ with the yaw angles for various pitch angles. The response is nearly linear for all yaw angles. The results show that values of $C_{p_{yaw}}$ for various pitch angles collapse on top of each other for yaw angles of -12 degrees to +8 degrees. This means that $C_{p_{yaw}}$ is independent of pitch angle in this range. From -23 degrees to -15 degrees and from +8 degrees to +15 degrees, there are slight variations in the results indicating that $C_{p_{yaw}}$ has a slight dependency on the pitch angle. The fact that yaw is only slightly dependent on the pitch angle allows data to be more easily processed in determination of flow velocity.

The variation of $C_{p_{pitch}}$ vs. pitch angle, Figures 3.4 and 3.5, show that this coefficient is dependent on both yaw and pitch angles. The trend of $C_{p_{pitch}}$ vs. pitch angle is generally linear but there are variations from that linearity for each yaw angle, and unlike the yaw plane, these variations are not restricted to any particular region.

Figures 3.4 and 3.5 show that the range of values for $C_{p_{pitch}}$ is small over the range of α shown compared to the variation of $C_{p_{yaw}}$ with β . [Ref. 12: pp. 27-28] attributes this to the types of surfaces on which the holes in the pitch and yaw plane are connected. Large yaw angles result in one hole being nearly aligned with the flow. This hole senses a pressure nearly equal to the total pressure of the freestream. The other hole is then blocked from the freestream and, consequently, reads a pressure much less than the freestream static pressure. The holes in the pitch plane have a different response to variation in the pitch angle. When pitched, one hole reads a pressure which is near the total pressure of the freestream, but the second hole senses a pressure which is greater than the freestream static pressure. Thus, $C_{p_{yaw}}$ is a much larger number than $C_{p_{pitch}}$. The small range of $C_{p_{pitch}}$ increases the scatter and uncertainty of pitch angle measurements.

The plot of $C_{p_{static}}$ vs. pitch angle, Figure 3.6, shows that $C_{p_{static}}$ has weak dependency on yaw and pitch angles.

$C_{p_{total}}$ vs. pitch angle, Figure 3.7, indicates that for any given yaw angle, $C_{p_{total}}$ is constant throughout the range of pitch angles. Here, $C_{p_{total}}$ also shows a weak dependency on yaw and pitch angles.

E. INTERPOLATION AND APPLICATION

After the probe has been calibrated and the operating characteristics of the probe are known, it is possible to determine the pitch angle, yaw angle, local static and total pressures for any flow field,

The probe is positioned normal to the freestream, and at any location in the flow field, the five pressures can be measured. These five pressures are now used to calculate the experimental or local coefficients of yaw, pitch, static pressure, and total pressure.

A fifth order polynomial was fitted to the average values of $C_{p_{yaw}}$. The resulting polynomial computed using a FORTRAN program based on the least-squares method is:

$$\beta_{app} = -.158 - 7.36(M_1) + 0.135(M_1)^2 + 0.304(M_1)^3 + 0.009(M_1)^4 - 0.031(M_1)^5 \quad (\text{eqn 3.5})$$

Here, β_{app} is the approximate yaw angle, and M_1 is the local coefficient of yaw.

Knowing the approximate yaw angle and the local $C_{p_{pitch}}$, a computerized interpolation is performed to determine the pitch angle. Since the value of the pitch angle is dependent on the local $C_{p_{pitch}}$ and on the yaw angle, it is necessary to perform a double interpolation. Referring to Figure 3.8, the two yaw angles, β_1 and β_2 , which bracket the approximate yaw angle are first determined. Next, the local $C_{p_{pitch}}$, M_{2a} and M_{2b} , is located between known values of $C_{p_{pitch}}$ from the calibration data for each yaw angle. In Figure 3.8, these values are designated C_{11} , C_{12} , C_{21} , and C_{22} which correspond to pitch angles from the calibration data of α_{11} , α_{12} , α_{21} , and α_{22} . The bracketing pitch angle α_{1f} is determined by the following interpolation

$$(C_{11} - M_{2a})(C_{11} - C_{12}) = (\alpha_{11} - \alpha_{1f})(\alpha_{11} - \alpha_{12}) \quad (\text{eqn 3.6})$$

which rearranged gives

$$\alpha_{1f} = \alpha_{11} - (\alpha_{11} - \alpha_{12}) \frac{(C_{11} - M_{2a})}{(C_{11} - C_{12})} \quad (\text{eqn 3.7})$$

The other bracketing pitch angle α_{2f} is found in a similar manner which gives

$$\alpha_{2f} = \alpha_{21} - (\alpha_{21} - \alpha_{22}) \frac{(C_{21} - M_{2b})}{(C_{21} - C_{22})} \quad (\text{eqn 3.8})$$

The pitch angle for the flow α_f is found through a second interpolation which results in the relationship

$$\alpha_f = \alpha_{1f} - (\alpha_{1f} - \alpha_{2f}) \frac{(\beta_1 - \beta_{app})}{(\beta_1 - \beta_2)} \quad (\text{eqn 3.9})$$

Because $C_{p_{yaw}}$ has a slight dependency on pitch, it is necessary to refine the approximate yaw angle once the local pitch angle is known. This is done with a computerized interpolation routine which is very similar to that used for the pitch angle. As shown in Figure 3.9, the pitch angles from the calibration data, α_1 and α_2 , which bracket the local pitch angle, α_f are first determined. The local $C_{p_{yaw}}$, M_{1b} , is then located between the values of $C_{p_{yaw}}$ from the calibration data for α_1 . This results in C_{31} and C_{21} which correspond to yaw angles β_{11} and β_{12} . Then, by linear interpolation β_{1f} is found

$$(C_{31} - M_{1b}) \frac{(C_{31} - C_{21})}{(C_{31} - C_{21})} = ((\beta_{11} - \beta_{1f}) \frac{(\beta_{11} - \beta_{12})}{(\beta_{11} - \beta_{12})}) \quad (\text{eqn 3.10})$$

or

$$\beta_{1f} = \beta_{11} - (\beta_{11} - \beta_{12}) \frac{(C_{31} - M_{1b})}{(C_{31} - C_{21})} \quad (\text{eqn 3.11})$$

The same interpolation is done for α_2 which gives

$$\beta_{2f} = \beta_{21} - (\beta_{21} - \beta_{22}) \frac{(C_{32} - M_{1a})}{(C_{32} - C_{22})} \quad (\text{eqn 3.12})$$

β_{2f} and β_{1f} are the yaw angles which bracket the yaw angle of the flow. The flows yaw angle, β_f , can be found by a second interpolation which results in the relationship

$$\beta_f = \beta_{2f} - (\beta_{2f} - \beta_{1f}) \frac{(\alpha_2 - \alpha_f)}{(\alpha_2 - \alpha_1)} \quad (\text{eqn 3.13})$$

Since local total and static pressures are not measured at each probe location, it is necessary to perform another double interpolation to compute their values. From the calibration data, the values of $C_{p_{total}}$ for each of the bracketing yaw angles and pitch angles are known. In Figure 3.10, these points are designated C_{11} , C_{12} , C_{21} , and C_{22} . An interpolation is performed to determine the $C_{p_{total}}$ corresponding to the local pitch angle. These points are designated, C_{1f} and C_{2f} . The local $C_{p_{total}}$, M_3 , is found using the relationship

$$(C_{1f} - M_3)(C_{1f} - C_{2f}) = (\beta_1 - \beta_f)(\beta_1 - \beta_2) \quad (\text{eqn 3.14})$$

which when rearranged as shown below gives the local $C_{p_{total}}$ for the flow

$$M_3 = C_{1f} - (C_{1f} - C_{2f}) \frac{(\beta_1 - \beta_f)}{(\beta_1 - \beta_2)} \quad (\text{eqn 3.15})$$

The local $C_{p_{static}}$, M_4 is found in a similar manner. Referring to Figure 3.11, the relationship for determining the local $C_{p_{static}}$ is then given by

$$M_4 = C_{3f} - (C_{3f} - C_{4f}) \frac{(\beta_1 - \beta_f)}{(\beta_1 - \beta_2)} \quad (\text{eqn 3.16})$$

F. VELOCITY COMPONENT DETERMINATION

Once the values of the local $C_{p_{total}}$ and $C_{p_{static}}$ have been determined, the local total and static pressure can be calculated and, subsequently, the total velocity at the probe tip can be determined.

The defining relationships for $C_{p_{total}}$ and $C_{p_{static}}$ can be rearranged to determine P_{total} and P_{static} :

$$P_{total} = P_1 - (C_{p_{total}})(P_1 - \bar{P}) \quad (\text{eqn 3.17})$$

$$P_{static} = \bar{P} - (C_{p_{static}})(P_1 - \bar{P}) \quad (\text{eqn 3.18})$$

By using Bernoulli's equation, the magnitude of the local total velocity is:

$$V = \sqrt{2(P_{\text{total}} - P_{\text{static}}) \rho} \quad (\text{eqn 3.19})$$

The three components of velocity can now be determined using the total velocity vector and the local pitch and yaw angles. Referring to Figure 3.1, these velocity components are given by,

$$V_x = V \cos \alpha \cos \beta \quad (\text{eqn 3.20})$$

$$V_y = V \sin \alpha \quad (\text{eqn 3.21})$$

$$V_z = V \cos \alpha \sin \beta \quad (\text{eqn 3.22})$$

G. SPATIAL RESOLUTION CORRELATION

The calculation of V_y may be influenced by the local total velocity gradient. Corrections for this effect may be made using the following relationship

$$V_{yf} = V_{yo} + (\partial U / \partial x)(ly) \quad (\text{eqn 3.23})$$

Here V_{yo} is the uncorrected value of V_y and V_{yf} is the value of V_y corrected for spatial resolution. The value of ly used was slightly greater than the distance between P_4 and P_5 (0.155 cm): a value of 0.200 cm gave constant V_y through the two-dimensional boundary layer.

H. SOFTWARE

Six programs were developed for use during this study. They are PROCAL, PRSACQ, VEL VELC, PLOT, and VECTOR. Each program is written in BASIC. PROCAL was used with the HP-85, all others were written for the HP-9836S. All of the programs are listed in Appendix C.

PROCAL is a BASIC program used for the calibration of the pressure probe. The program begins by computing the correction factor for random noise associated

with each transducer. The user is then prompted to manually calibrate each transducer against a horizontal monometer. Static pressures are input utilizing a static pressure tap on the side wall and one of the transducers. Total pressure of the freestream is input using a Keil probe inserted into freestream and a transducer. The user is next prompted to input the ambient pressure in inches of mercury. After the user has positioned the probe at the desired angles of yaw and pitch, those angles are input into the program.

The computer then acquires the five voltages from the data acquisition system, converts each voltage to a pressure in inches of water, and then calculates the yaw, pitch, total, and static coefficients of pressure. Finally, the yaw angle, pitch angle, and the four coefficients are stored on a separate file and printed out utilizing the HP-85's internal printer.

PRSACQ was used to acquire the pressures during the experiment. PRSACQ begins by prompting the user for the number spanwise and vertical data points and the resolution. A matrix of data point location is then computed. Next, the transducers are corrected for noise and calibrated against the manometer. Freestream static and total pressures are measured and ambient conditions are input. The program enters a loop which samples each pressure ten times per probe location. The local $C_{p_{yaw}}$ and $C_{p_{pitch}}$ are computed. Probe position, $C_{p_{yaw}}$, and $C_{p_{pitch}}$, P_1 and P_{total} are stored in a matrix. At the end of the data collection run, these values are read into a data file on a floppy disk.

VEL is used to process the raw data acquired by PRSACQ. The data is first read into computer memory. The program computes an approximate $C_{p_{yaw}}$ using a polynomial fit. Next, double interpolation subroutine is used to compute local $C_{p_{pitch}}$. A second interpolation subroutine is used to refine the value of $C_{p_{yaw}}$. The values of the $C_{p_{pitch}}$ and $C_{p_{yaw}}$ are used in a third interpolation subroutine to compute the local $C_{p_{static}}$ and $C_{p_{total}}$. The total pressure is found from the definition of $C_{p_{total}}$. The velocity at the probe tip is computed, and the x, y, and z components of velocity are determined. Probe position (y and z coordinates), total pressure, total velocity, and V_x , V_y , and V_z are stored in a matrix and then read into a data file.

VELC corrects the V_y component for spatial resolution. PLOT is used to generate graphs of streamwise velocity, total velocity, and total pressure. VECTOR is used to plot the secondary flow vectors.

IV. EXPERIMENTAL RESULTS

The study was conducted in three parts. The first was the measurement of baseline data consisting of boundary layer profiles in a two-dimensional mean flow field. The second was the measurement of the boundary layer characteristics at a freestream velocity of 15 m/s with 1) film cooling only, 2) with embedded vortex only, and 3) with both film cooling and embedded vortex. The third part was the measurement of boundary layer with vortex at 20 m/s, and measurement of boundary layer with vortex and film cooling at a freestream velocity of 11 m/s.

A. BASELINE RESULTS

The baseline boundary layer profiles were conducted at a freestream velocity of 22 m/s. For these tests, the top wall of the wind tunnel was adjusted at 20 m/s freestream velocity so that a zero pressure gradient existed within 0.15 mm water along the length of the test section. Profiles were taken at three spanwise locations $z = +2.54$ cm, $z = 0$ cm, and $z = -2.54$ cm. Figure 4.1 shows measurements of the streamwise velocity, V_x . Figure 4.2 shows measurements of V_z . Figures 4.3 and 4.4 show measurements of the normal velocity, V_y . The results of the baseline measurements indicate behavior expected of a 2-D turbulent boundary layer, since the figures show mean profiles to be spanwise uniform for all three velocity components. Figures 4.2 and 4.3 show that the V_z and the corrected V_y components are small and nearly zero as would be expected. Figure 4.4 is the plot of V_y uncorrected for spatial resolution.

B. 15M/S FREESTREAM VELOCITY RESULTS

The investigation of the flow field was conducted by using the five-hole pressure probe to measure pressures at 800 points in a spanwise plane. Data was taken at 20 different vertical locations, each having 40 spanwise locations. All 15 m/s measurements were taken at a location of 1.49 meters from the boundary layer trip or 0.39 meters from the heat transfer plate leading edge. The film cooling cases were conducted with injection air at 75% of full scale on the rotometer which corresponds to a blowing ratio (ratio of coolant to mass fluxes) of 0.50.

1. Boundary layer with film cooling

The results of boundary layer with film cooling only and no vortex are shown in Figures 4.5 to 4.8. Figure 4.5 shows contours of the streamwise velocity, Figure 4.6 shows total velocity contours, Figure 4.7 is the plot for total pressure, and Figure 4.8 shows the secondary flow vectors. Away from the wall, outside the boundary layer, the first three figures show spatially uniform behavior for V_x , V , and P_0 . Secondary flow vectors are very small everywhere in Figure 4.8. Near the wall deficits of V_x , V , and P_0 correspond to locations of the film cooling jets which are located about every 3.0 cm from tunnel centerline.

2. Boundary layer with vortex

The vortex is generated by using a half-delta wing which is 3.0 cm high with 7.5 cm chord and an angle of 18° . It is identical to vortex generator # 2 described by Joseph, [Ref. 10: p.76]. The vortex generator was located at a spanwise location of $z=4.79$ cm (note that the direction of $+z$ in [Ref. 10: p.75] is reversed). Figure 4.9 shows the streamwise velocity results, Figure 4.10 is a plot of the total velocity contours, Figure 4.11 is a contour plot of total pressure, and Figure 4.12 shows the secondary flow vectors. The contour plots for V_x , V , and P_0 show significant deficits caused by the generator wake which is rolled up with the vortex. The center of the wake is located at $y=3.3$ cm and $z=-3.05$ cm. Figure 4.12 shows that the vortex center is located near the same location, with overall characteristics similar to a Rankine vortex. Figure 4.13 shows the streamwise vorticity contours, where the vorticity is calculated using

$$\omega_f = (\partial V_z / \partial y) - (\partial V_y / \partial z) \quad (\text{eqn 4.1})$$

The vorticity is largest near the vortex center as expected. The circulation of the vortex is estimated to be $0.2708 \text{ m}^2/\text{s}$ using the equation

$$\Gamma = \int \omega_x dA. \quad (\text{eqn 4.2})$$

3. Boundary layer with vortex and film cooling

Figure 4.14 shows the streamwise velocity contours for this case, Figure 4.15 is the total velocity contour plots, Figure 4.16 shows the results for total pressure. Figure 4.17 shows the secondary flow vectors, and Figure 4.18 is a contour plot of

vorticity. Figure 4.15, 4-16, and 4-17 show that the deficits for V_x , V , and P_o from the film cooling are no longer present near the vortex. This result shows that the effects of film cooling are decimated by the vortex. The effect of the vortex is particularly pronounced near its downwash side. As for the previous case, Figure 4.18 shows that vorticity is again highest near the vortex center. Figure 4.19 from [Ref. 10: p.99] shows that the results of this case are consistent with previous work by Joseph which shows high heat transfer rates on the downwash side of the vortex and low heat transfer rates on the upwash side of the vortex. The circulation for this case is estimated to be $0.2708 \text{ m}^2/\text{s}$.

C. 20 M/S AND 10 M/S FREESTREAM VELOCITY RESULTS

Figure 4.20 is a plot of streamwise velocity for the case of an embedded vortex with no film cooling with a freestream velocity of 20 m/s. Figure 4.21 is a plot of the secondary flow vectors for the same case. Figure 4.22 and Figure 4.23 are for a boundary layer with embedded vortex and film cooling at 11 m/s freestream velocity. The blowing ratio for the 20 m/s case is 0.38, and the blowing ratio at 11 m/s was 0.68. The results for both cases show trends which are similar to those discussed above. The results at a freestream velocity of 11 m/s are believed to be less reliable because of disturbances at the inlet of the tunnel which propagated to the test section during the time period the data was acquired.

V. SUMMARY AND CONCLUSIONS

Measurements are presented of boundary layers with embedded vortices and with film cooling for freestream velocities of 15, and 11 m/s. Measurements of a boundary layer with embedded vortex and no film cooling, and of a boundary layer with film cooling but no vortex are presented for freestream velocity of 15 m/s. Plots of total velocity, V , streamwise velocity, V_x , secondary flow vectors, total pressure, P_o , and streamwise vorticity are presented for many of these test conditions.

The results show that the embedded vortices completely dominate the flow field in boundary layers with film cooling. This is indicated from the plots of V , V_x , and P_o which show the effects of film cooling to be completely decimated in the vicinity of the vortex. This result is consistent with the heat transfer results of Joseph, [Ref. 10: p.54], which shows a localized hot spot at the wall near the same location. Future film cooling injection-hole arrangements in turbine blades must be designed to compensate for hot spots due to the vortices.

In order to conduct this study, a five-hole pressure probe was calibrated for pitch and yaw. The probe was then used to measure five pressures associated with the flow. From these pressures, total velocity and the x , y , and z components of velocity were determined.

A boundary layer profile was conducted to verify the calibration of the pressure probe, measurement procedures, and velocity computations. The results show expected boundary layer behavior with a small V_y and V_z component.

It is recommended that flow visualization study of the interaction between the vortex and film cooling be conducted to enhance the understanding of this complex phenomena.

APPENDIX A
FIGURES

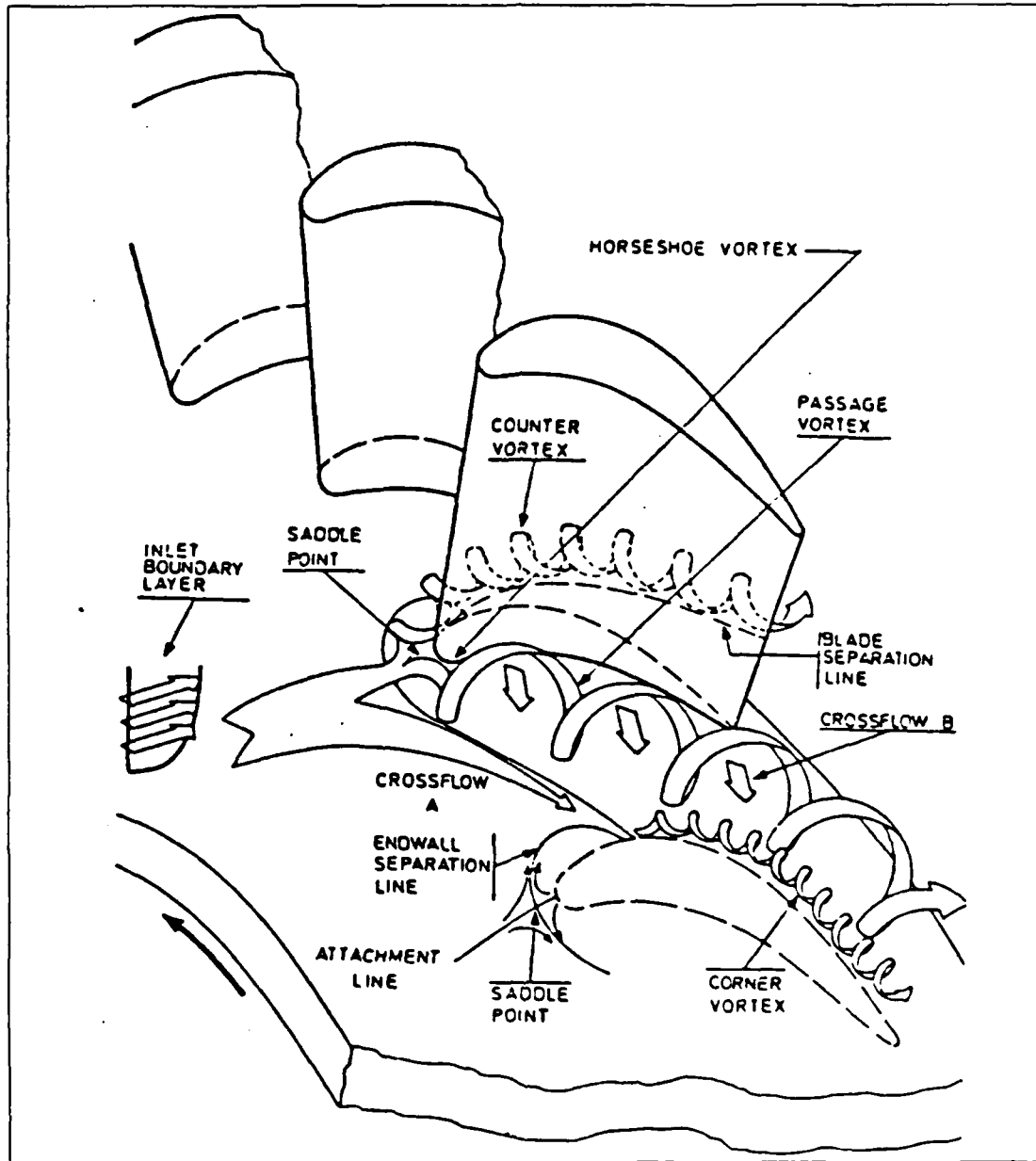


Figure 1.1 Endwall secondary flows.

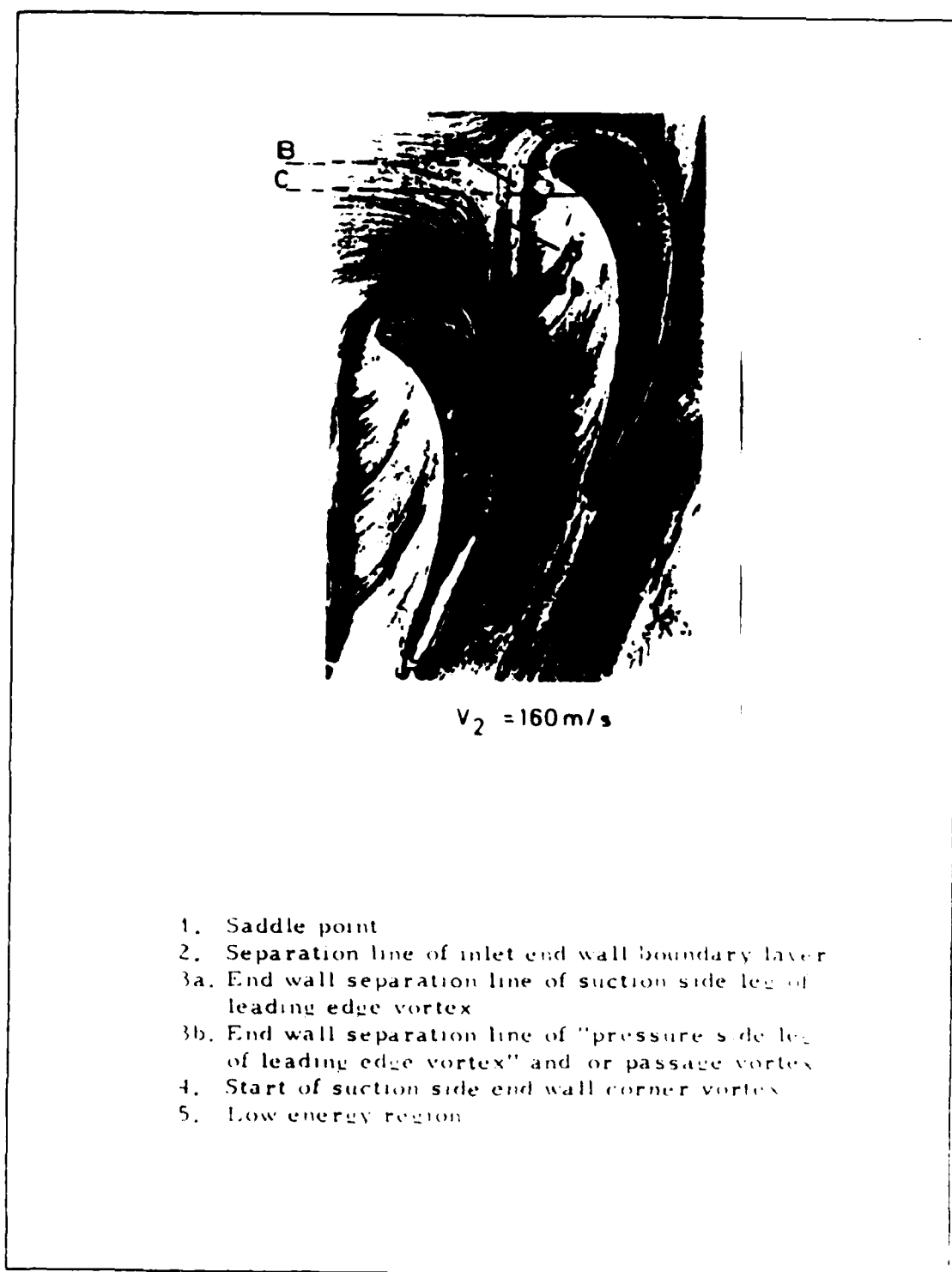


Figure 1.2 Smoke and oil visualization for rotor blade.

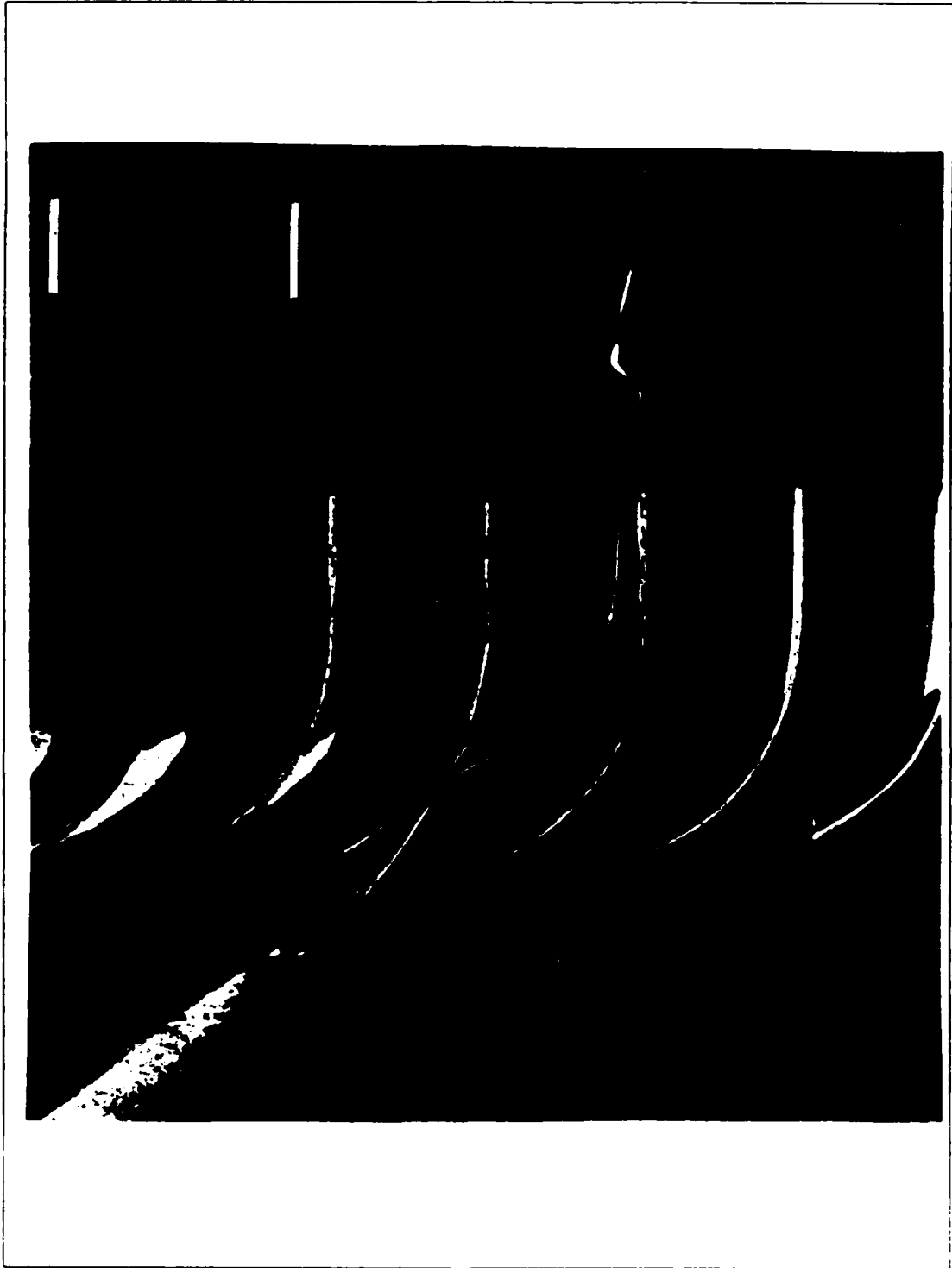


Figure 1.3 Secondary flow deflection.

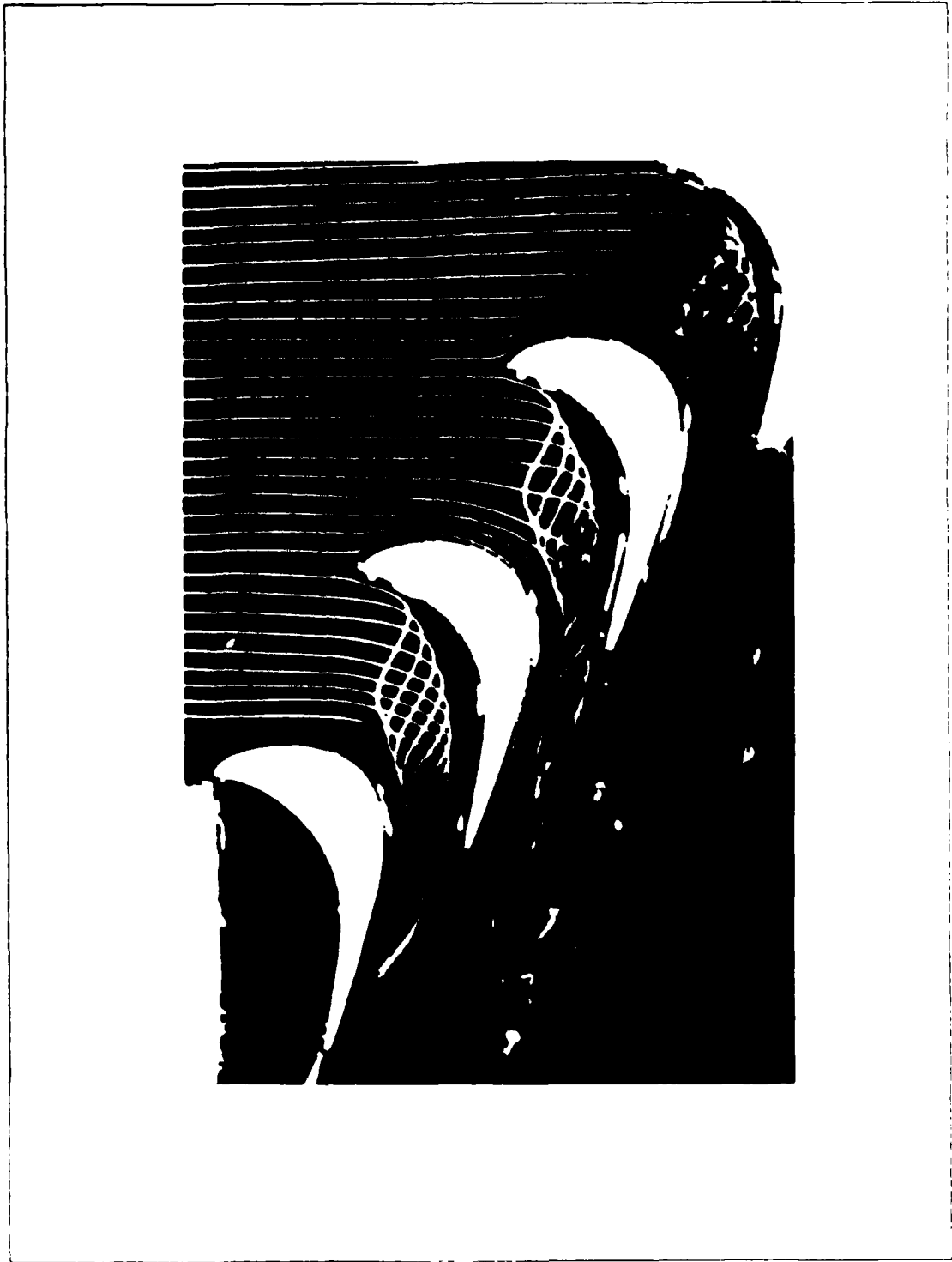


Figure 1.4 Rotation of passage and corner vortices in turbine cascade.



Figure 2.1 Photographs of wind tunnel

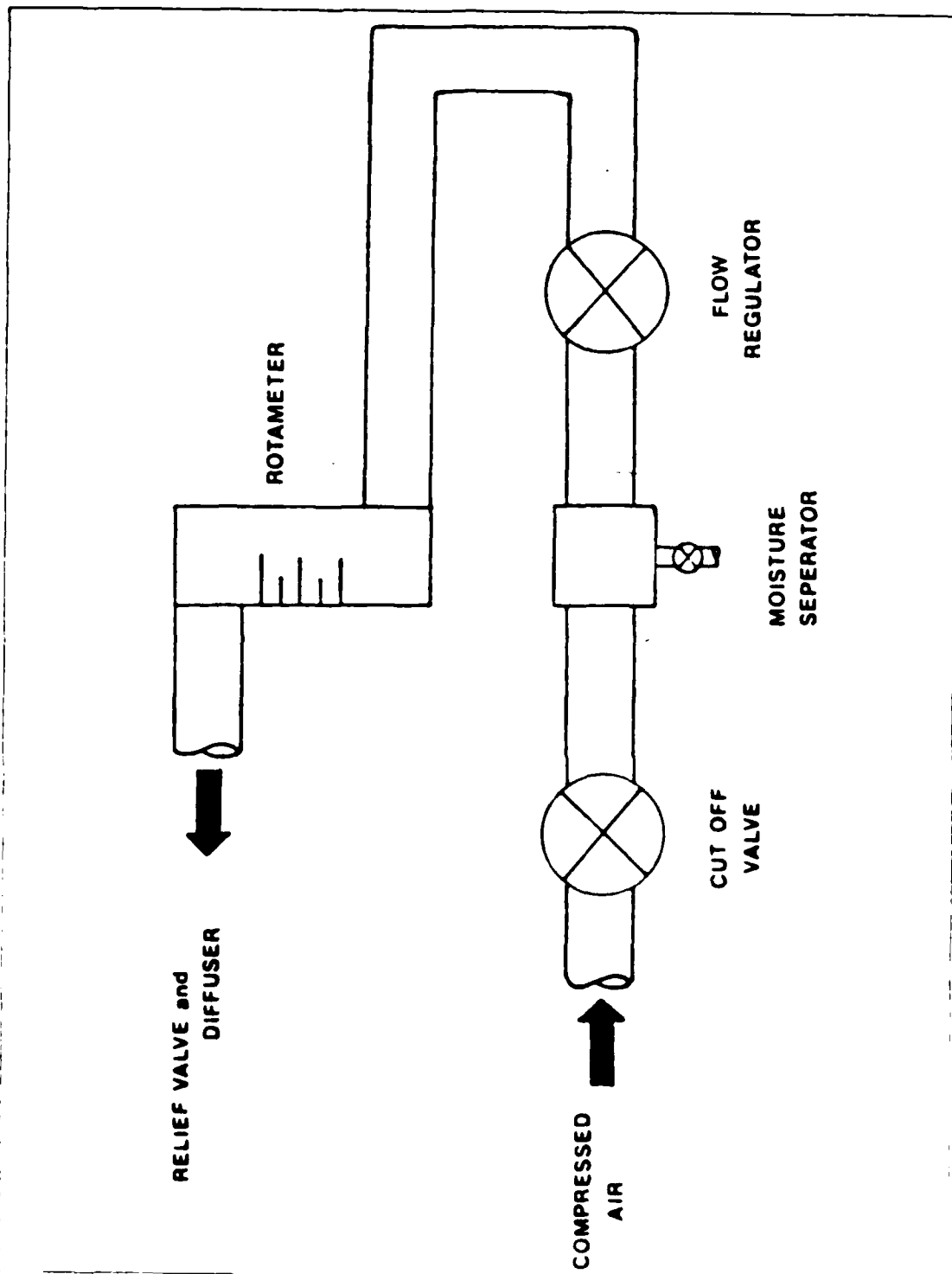


Figure 2.2 Schematic of injection air flow

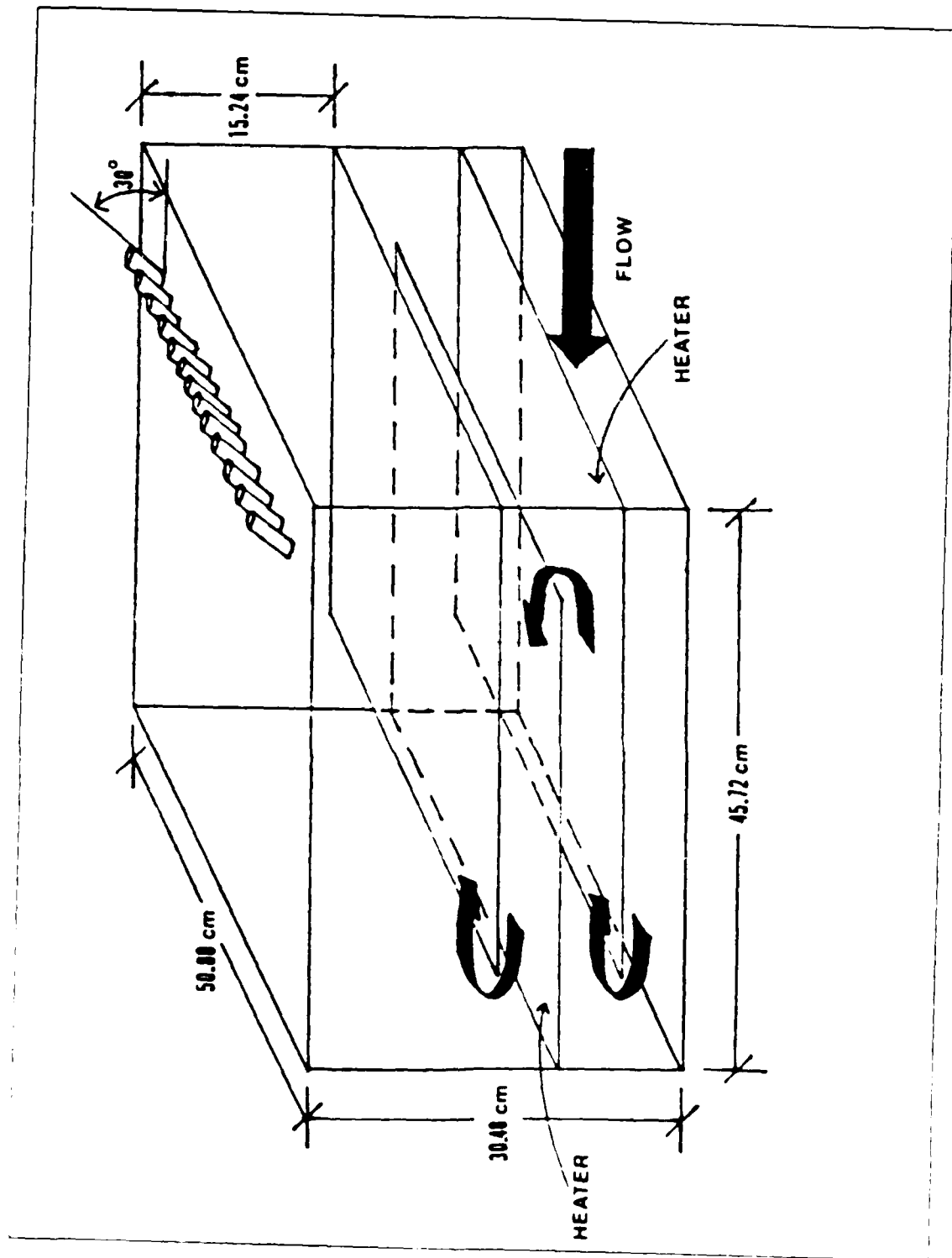


Figure 2.3 Schematic of injection plenum.

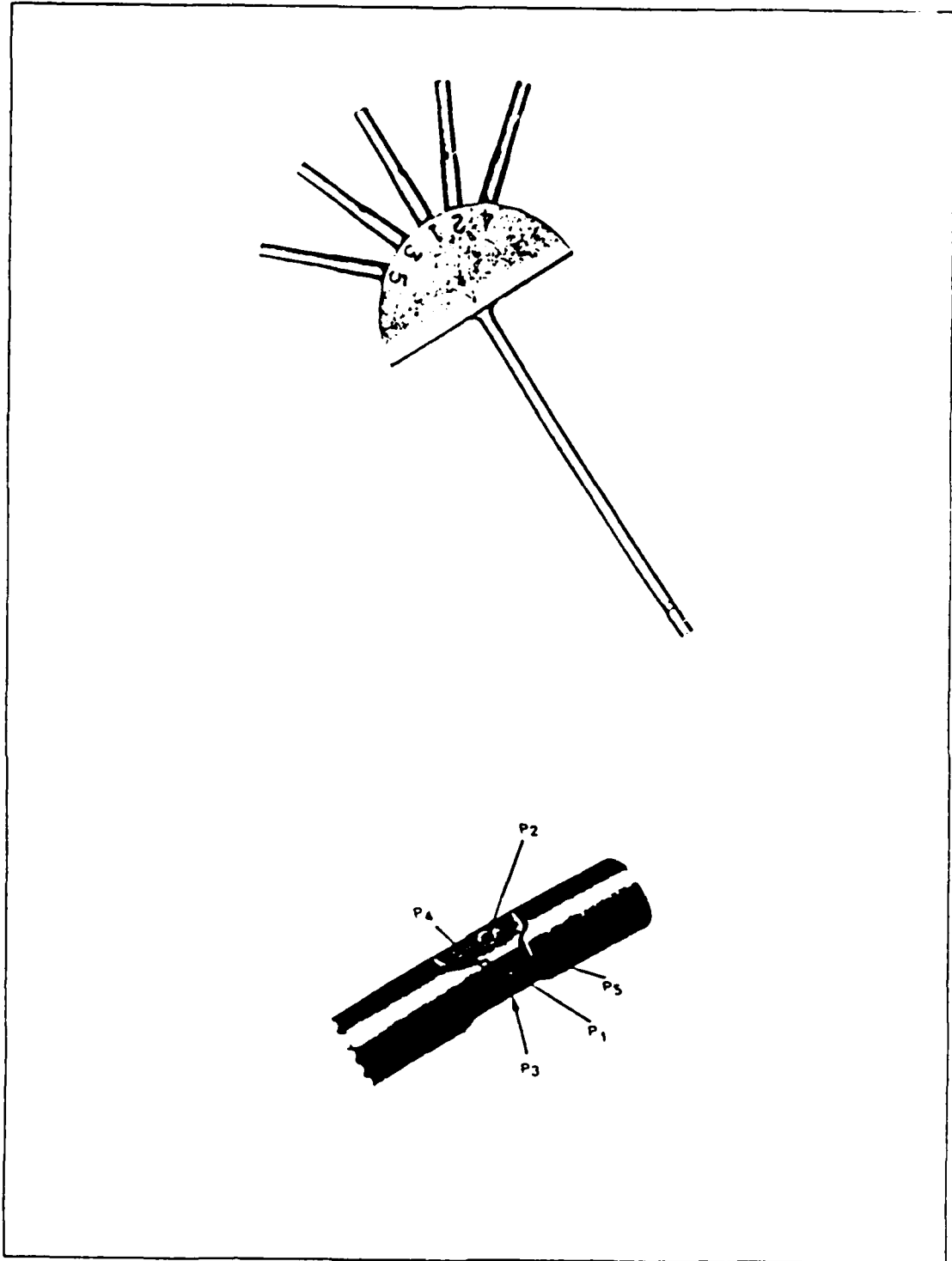


Figure 2.4 Photographs of pressure probe.

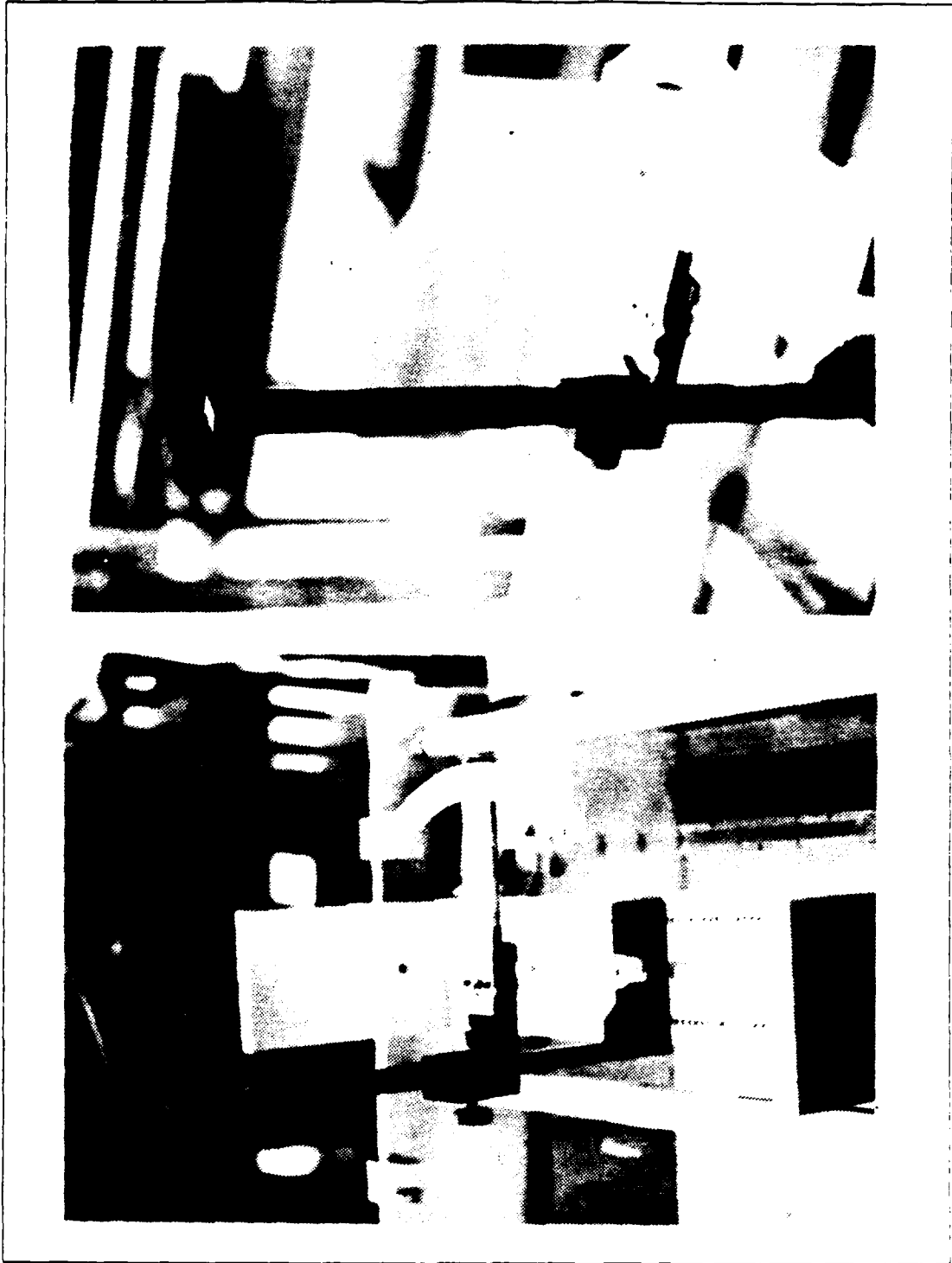


Figure 2.5 Manual traversing device.

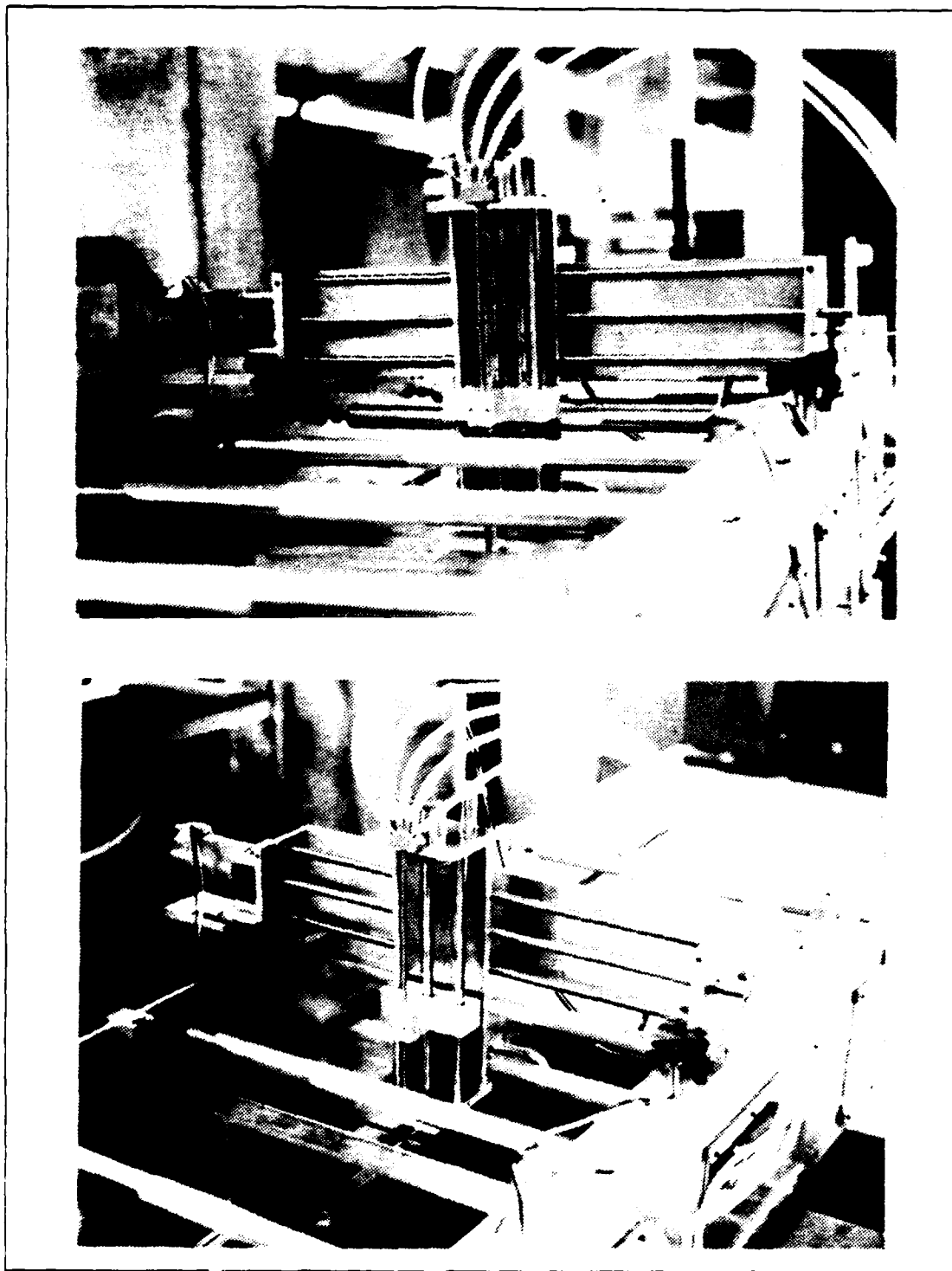


Figure 2.6 Automated traversing mechanism.

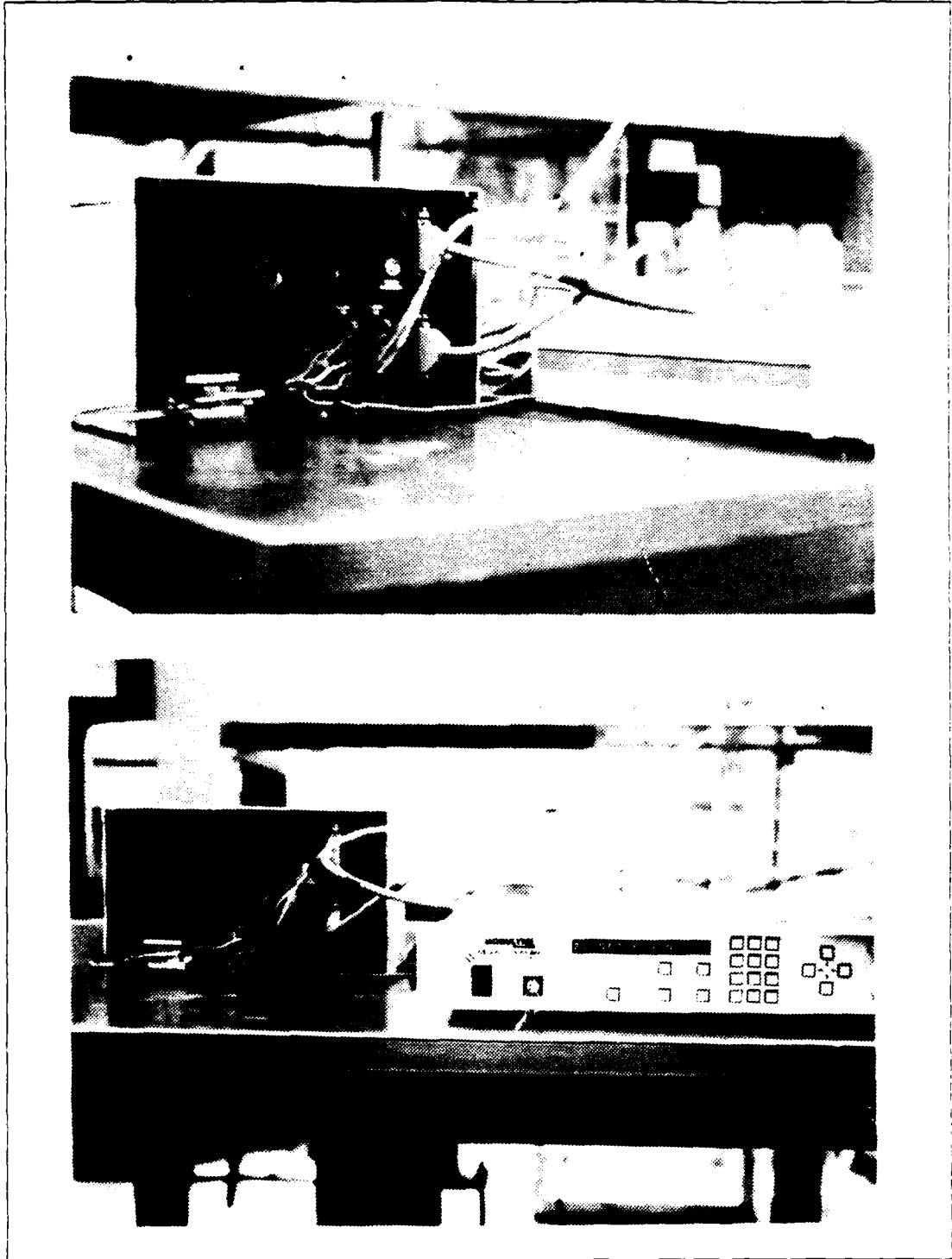


Figure 2.7 Photographs of Two-Axis Motion Controller.

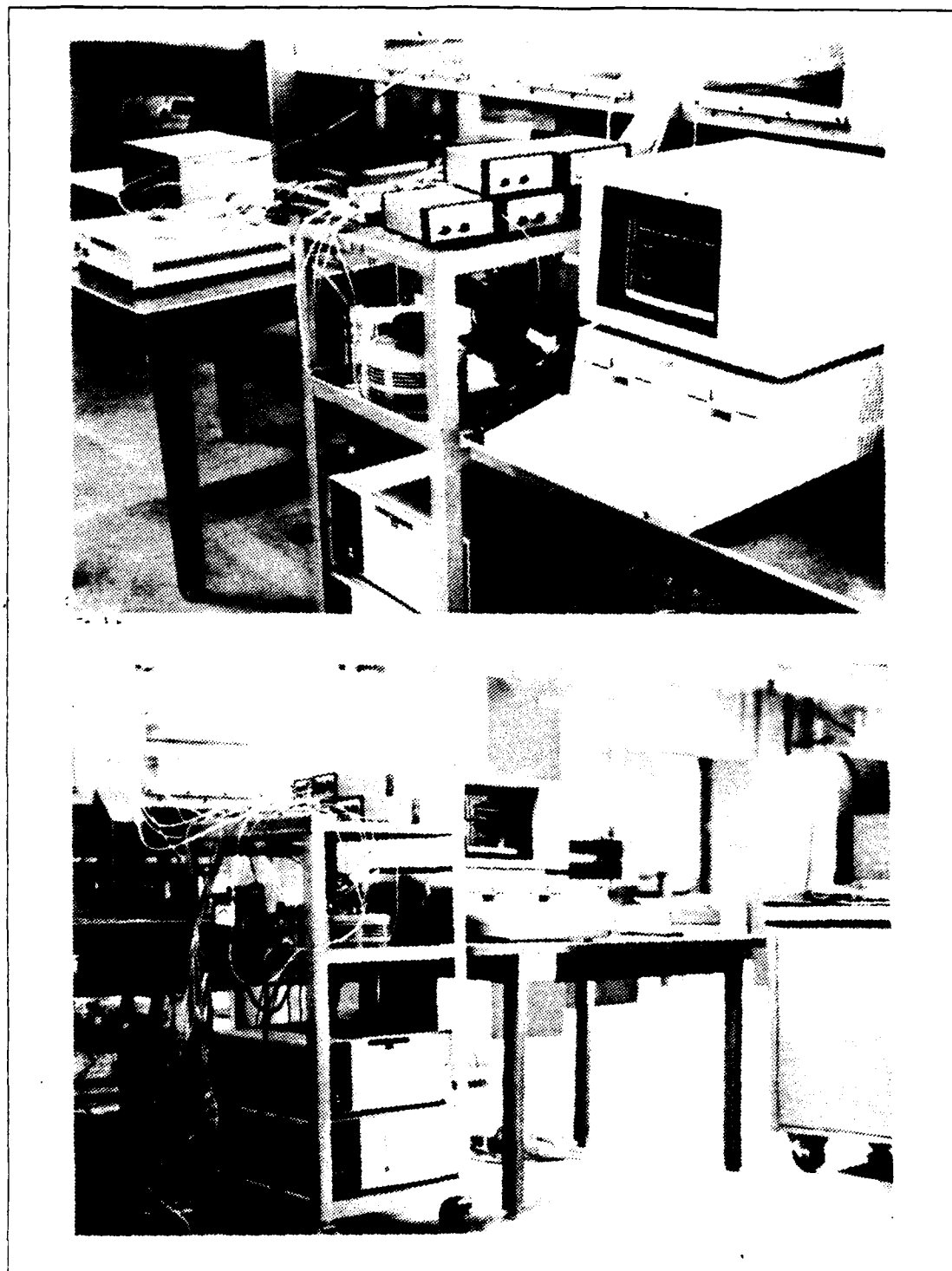


Figure 2.8 Photographs of data acquisition system.

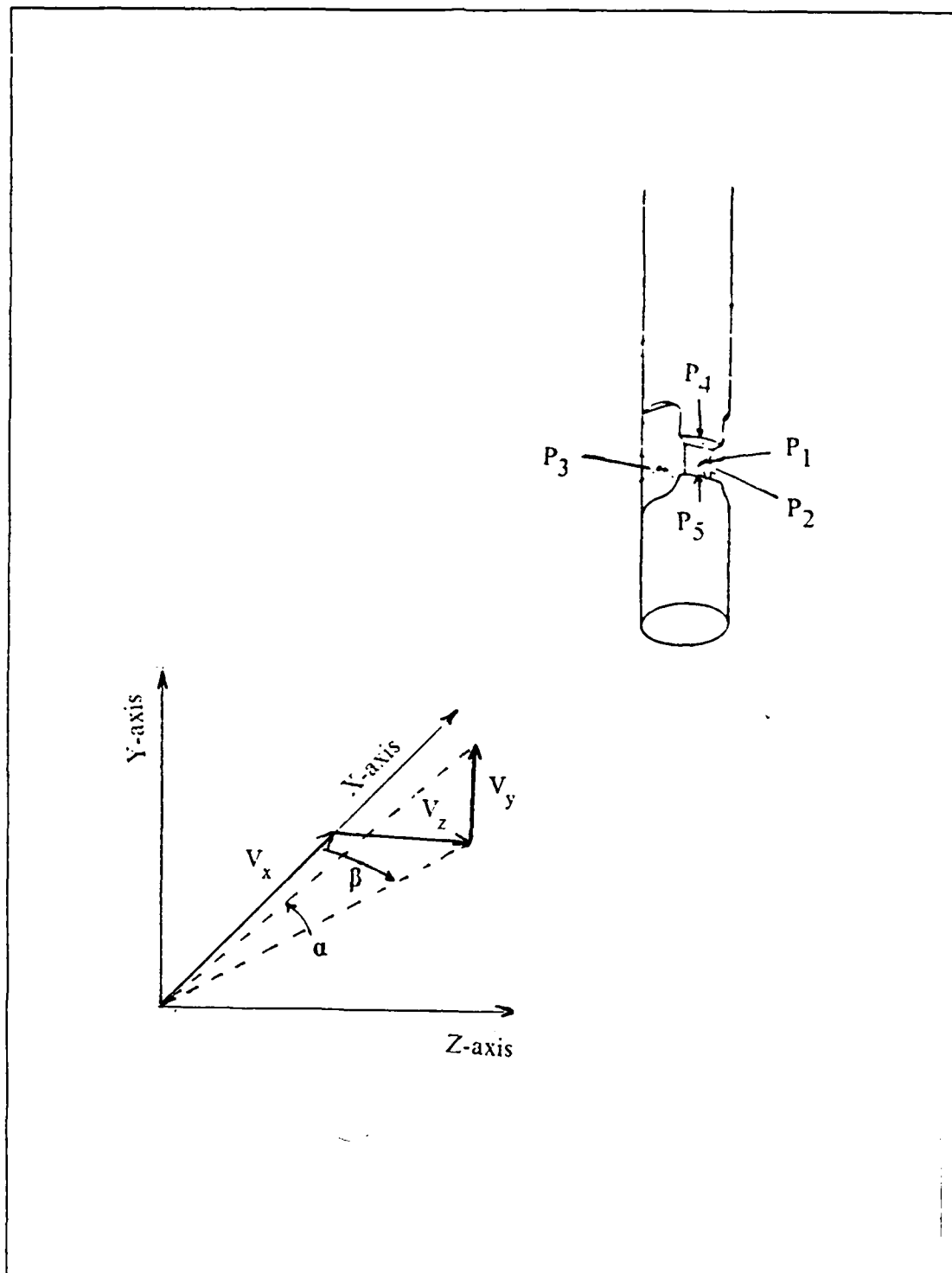


Figure 3.1 Coordinate system for flow measurement.

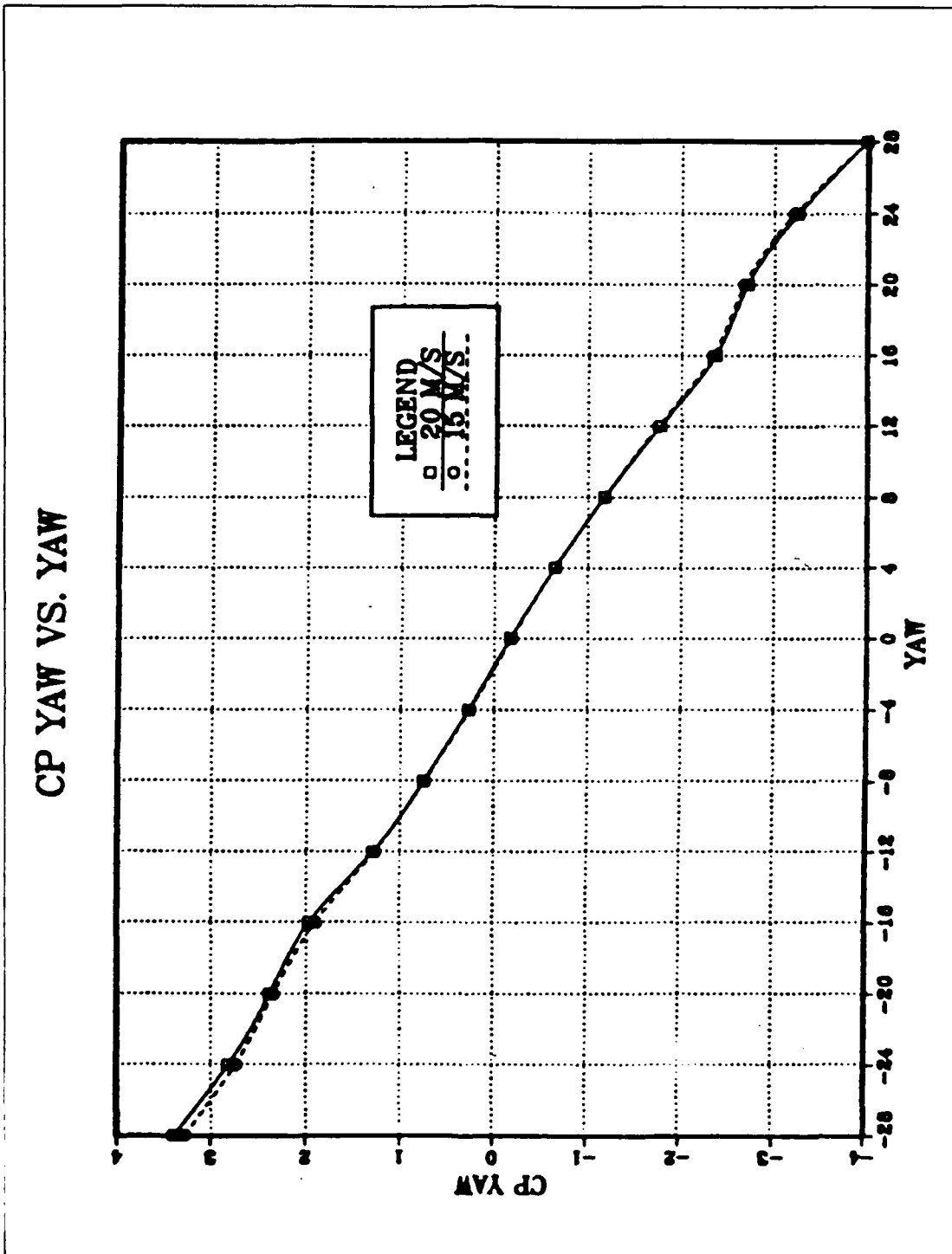


Figure 3.2 Repeatability of calibration results at different freestream velocities for C_{pyaw} vs. yaw angles.

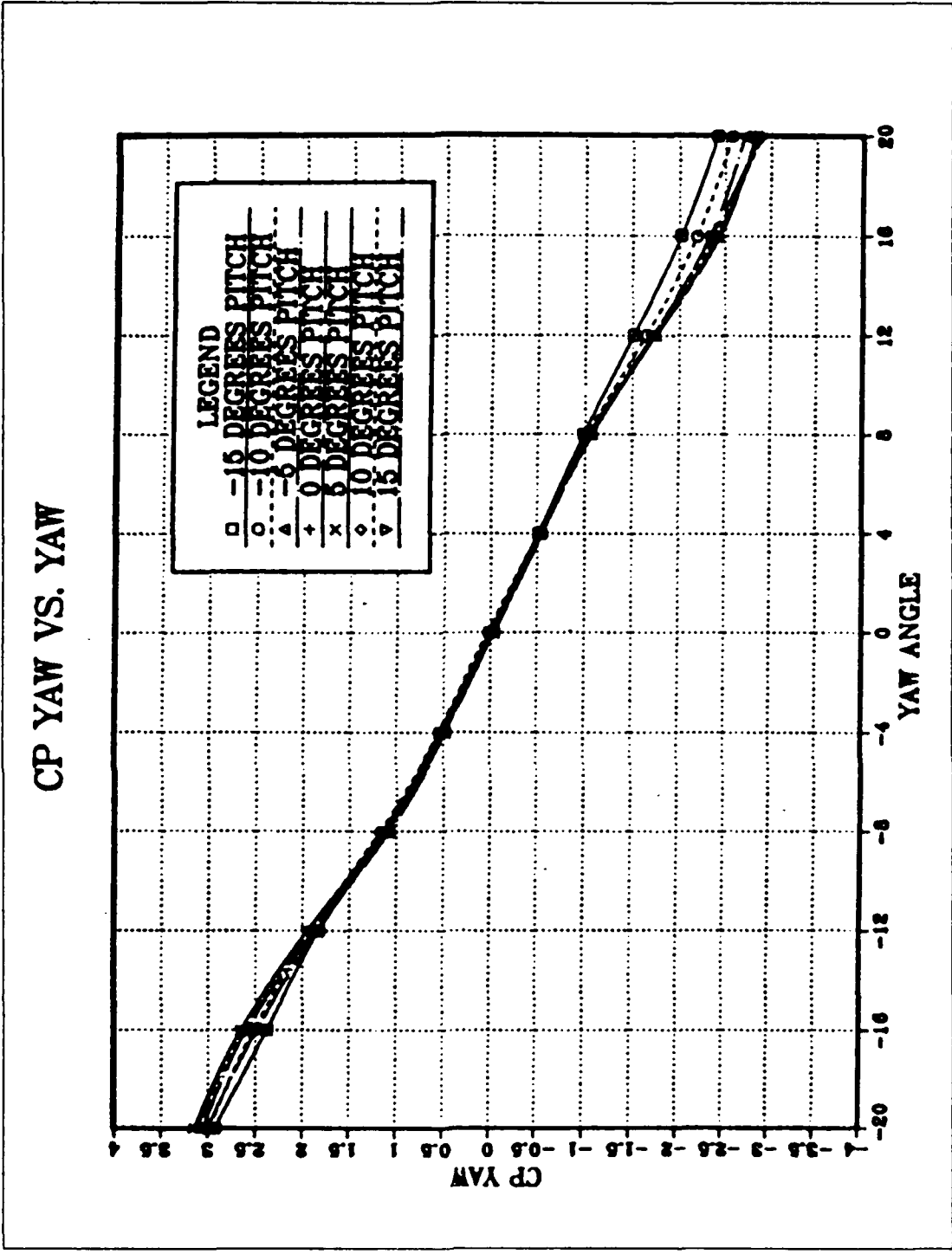


Figure 3.3 Probe calibration, $C_{p,yaw}$ vs. yaw angles, freestream velocity of 21 m/s.

CP PITCH VS. PITCH

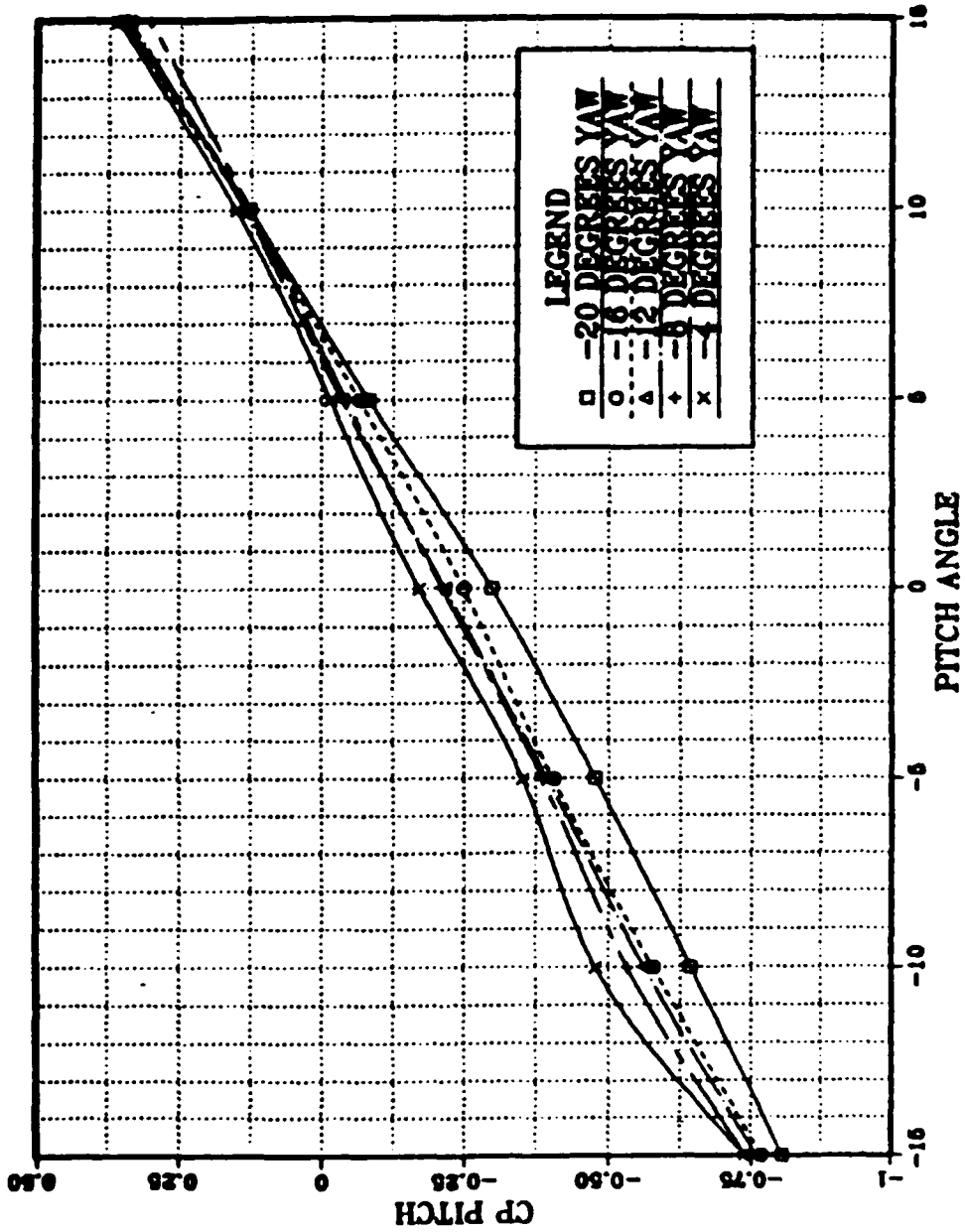


Figure 3.4 Probe calibration, $C_{p\text{pitch}}$ vs. pitch angle for -20° to -4° yaw, freestream velocity of 21 m/s.

CP PITCH VS. PITCH

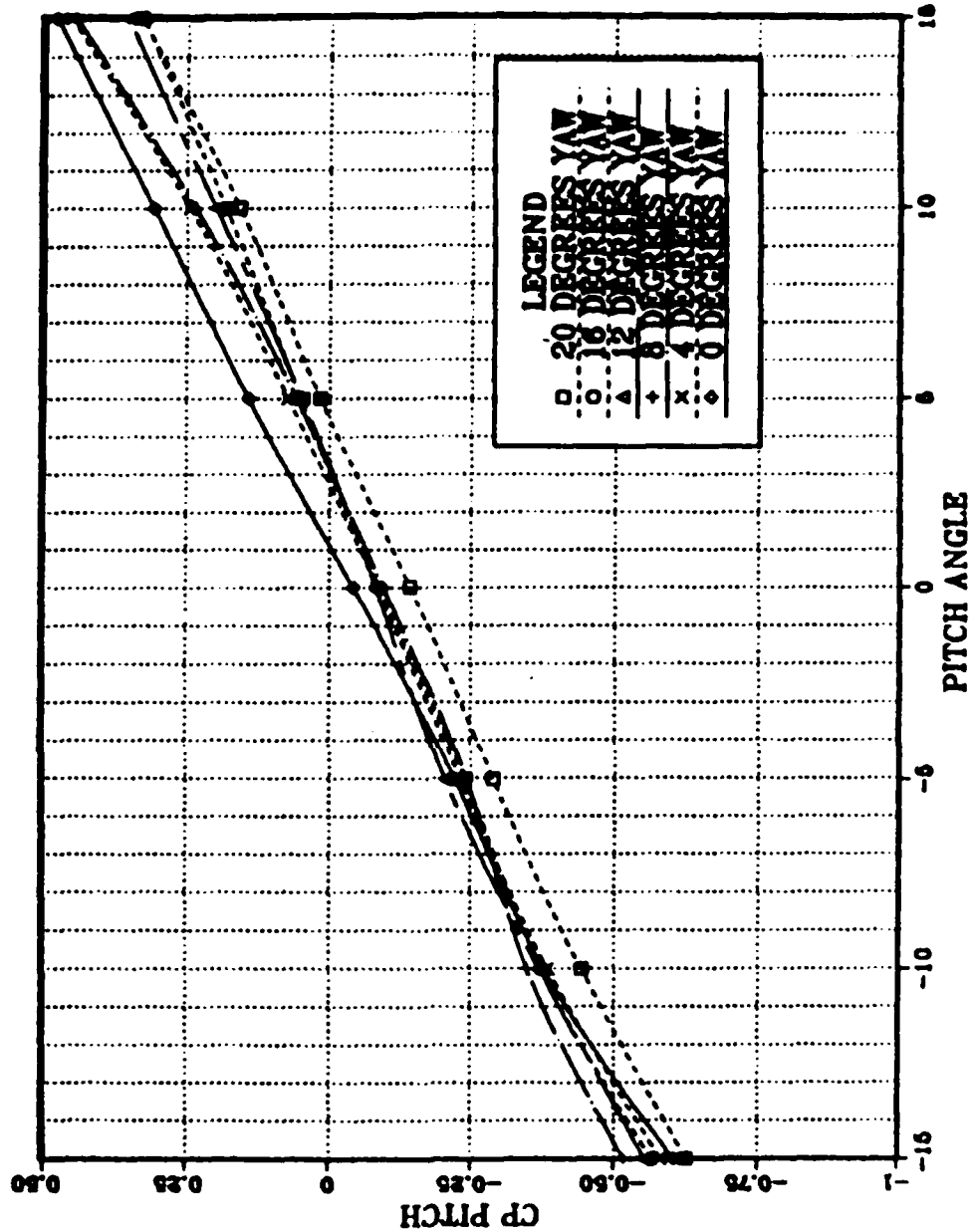


Figure 3.5 Probe calibration, $C_{p, \text{pitch}}$ vs. pitch angle for 0° to $+20^\circ$ yaw, freestream velocity of 21 m/s.

CP STATIC VS. PITCH

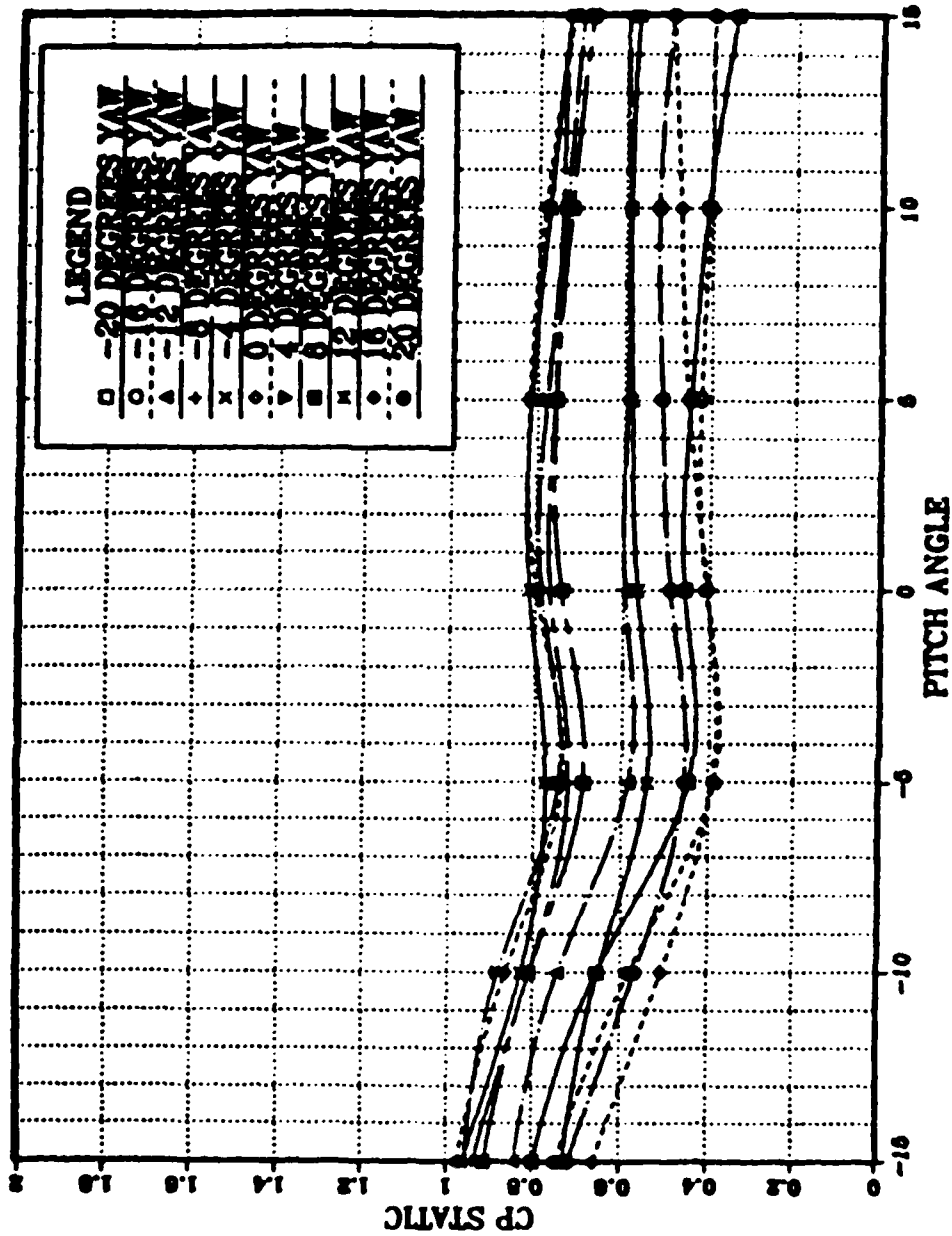


Figure 3.6 Probe calibration, $C_{p,static}$ vs. pitch angles, freestream velocity of 21 m/s.

CP TOTAL VS. PITCH

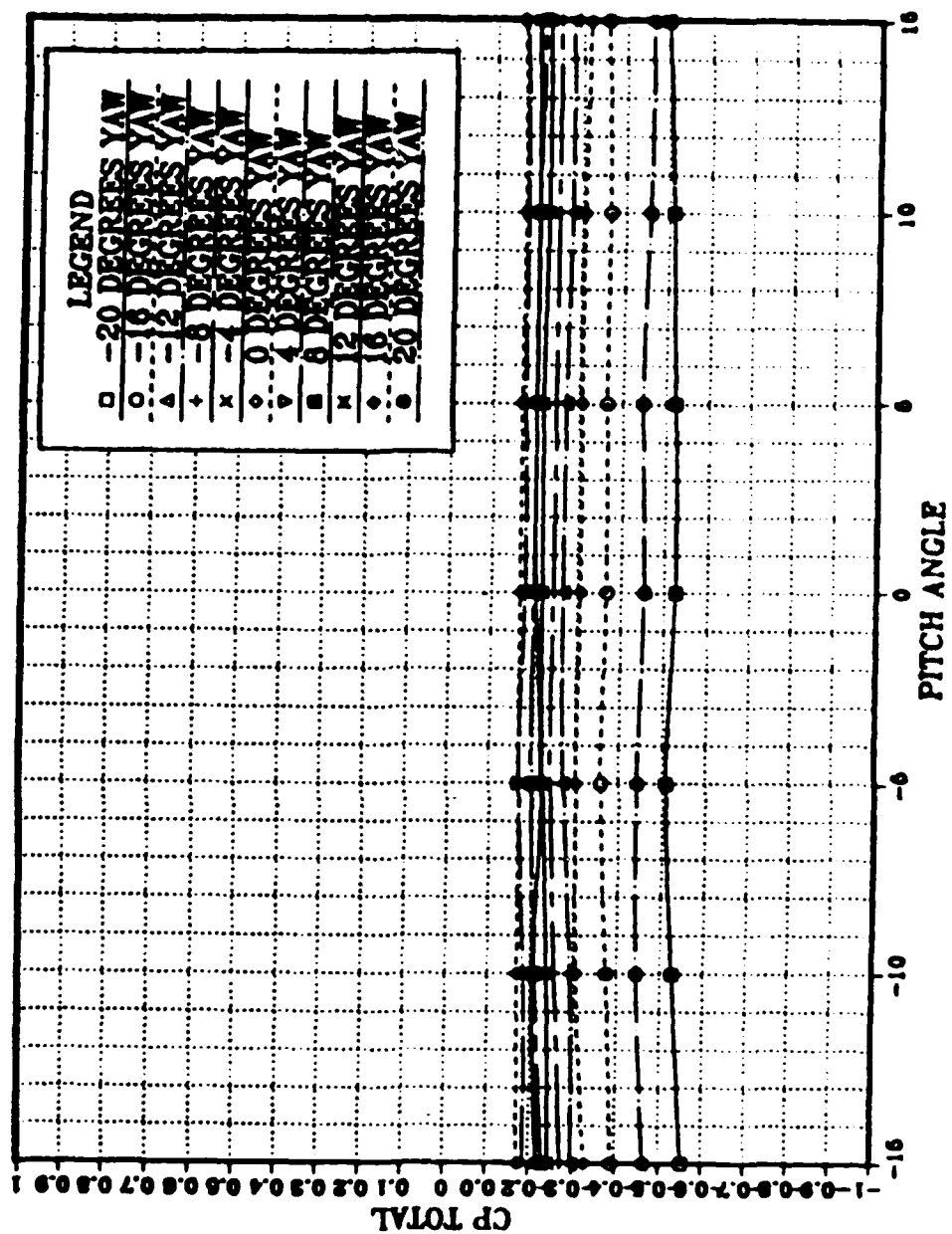


Figure 3.7 Probe calibration, $C_{p_{total}}$ vs. pitch angles, freestream velocity of 21 m/s.

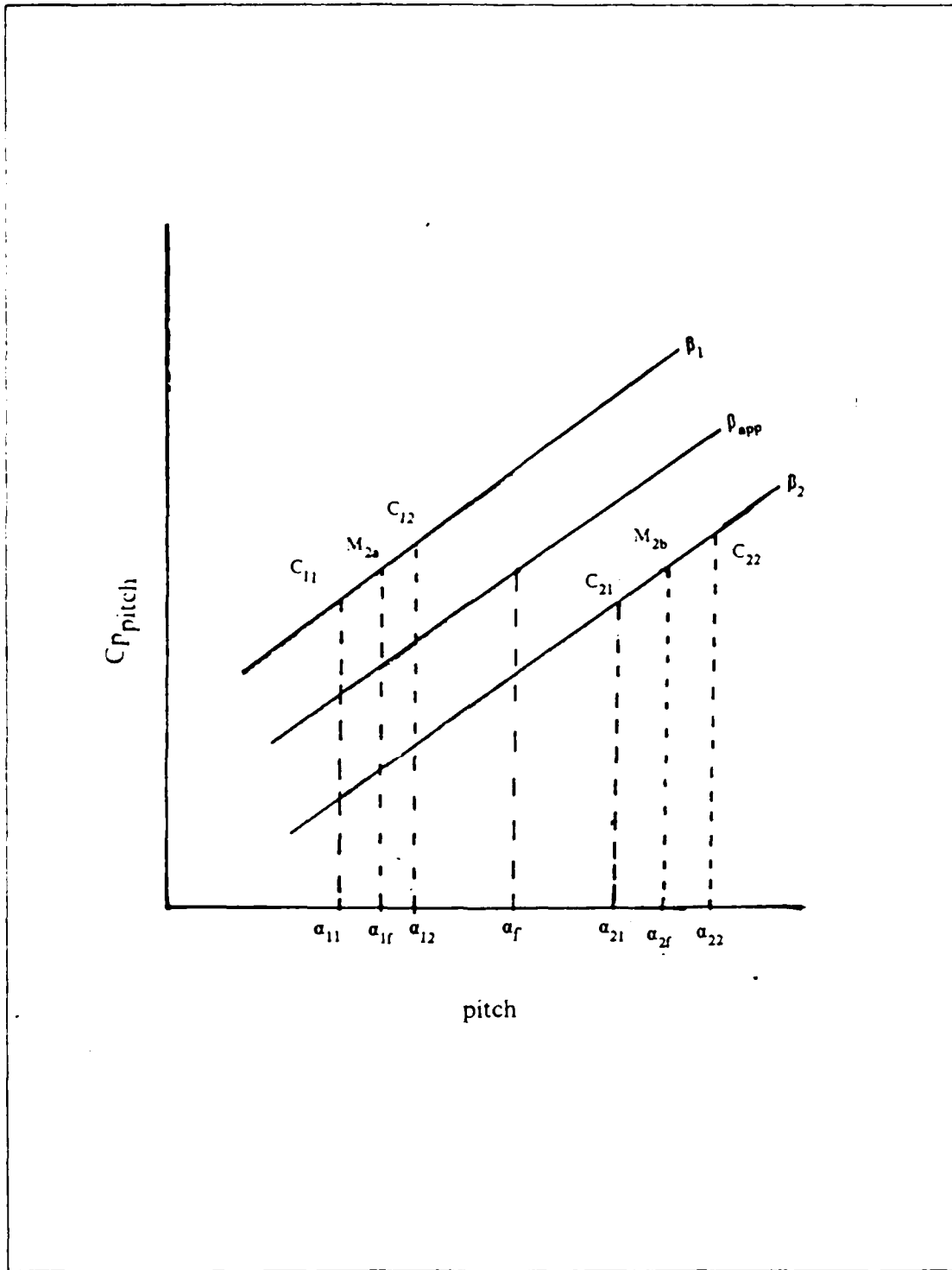


Figure 3.8 Interpolation for pitch angles.

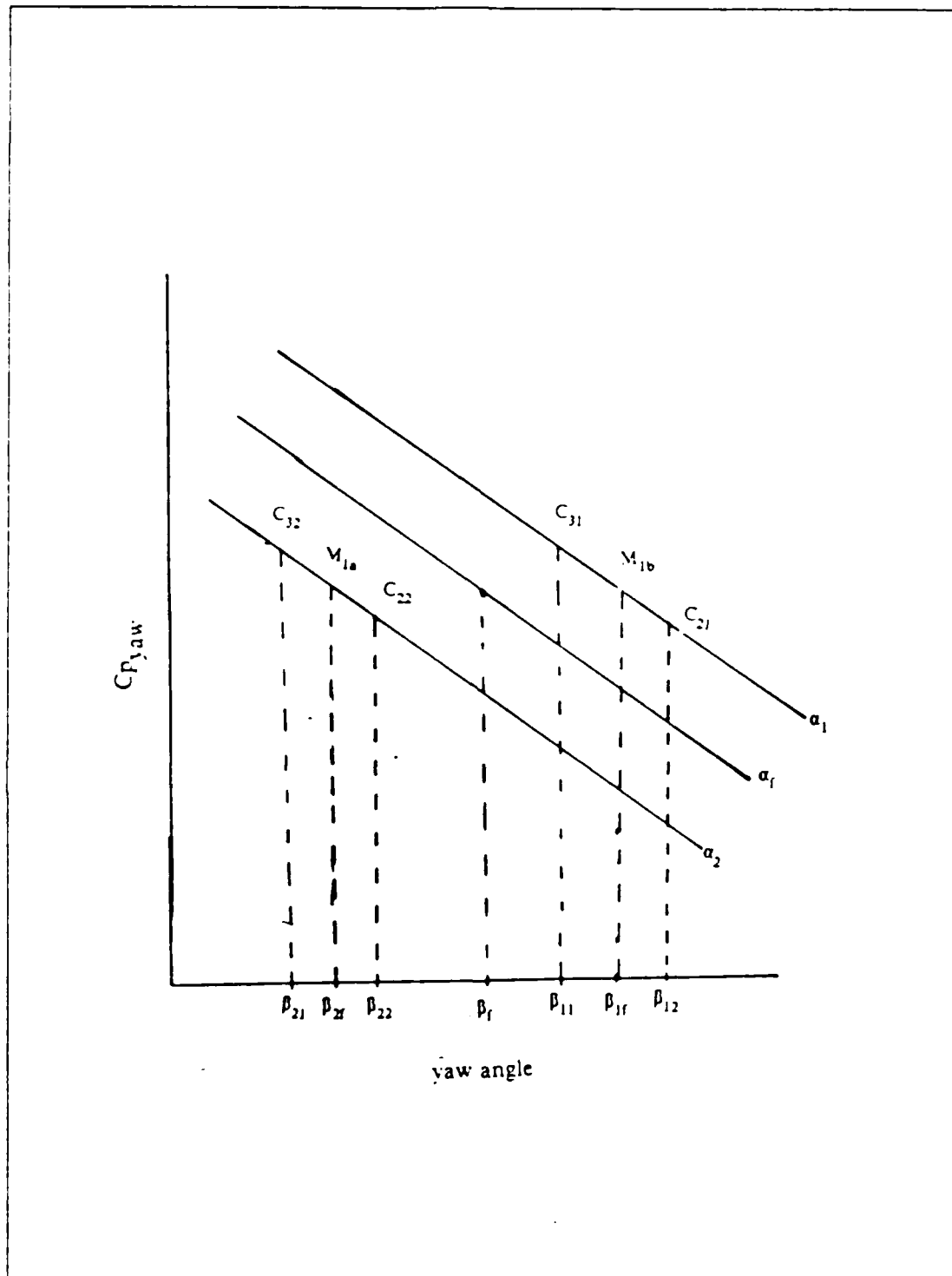


Figure 3.9 Interpolation for yaw angles.

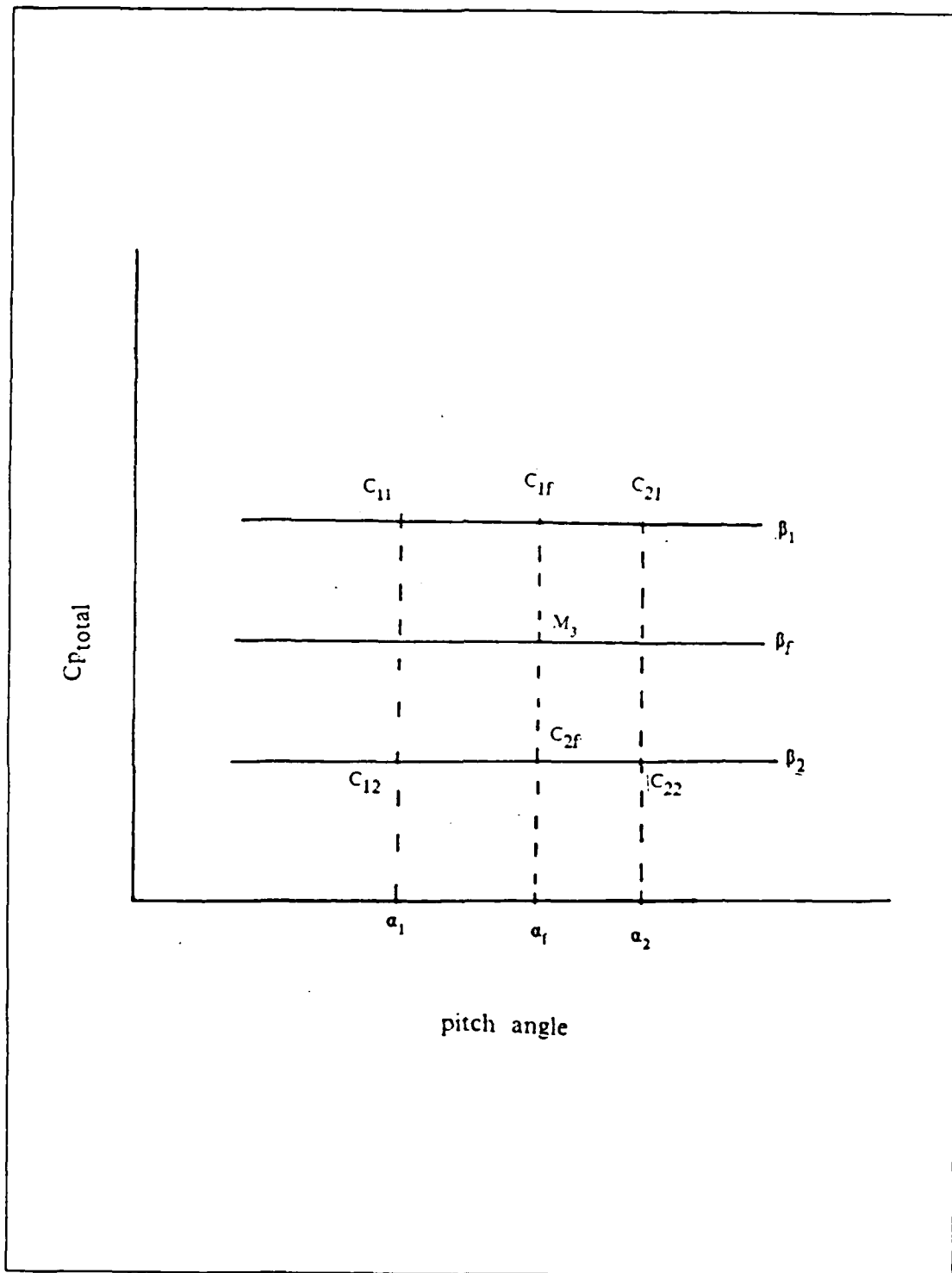


Figure 3.10 Interpolation for local $C_{p_{total}}$

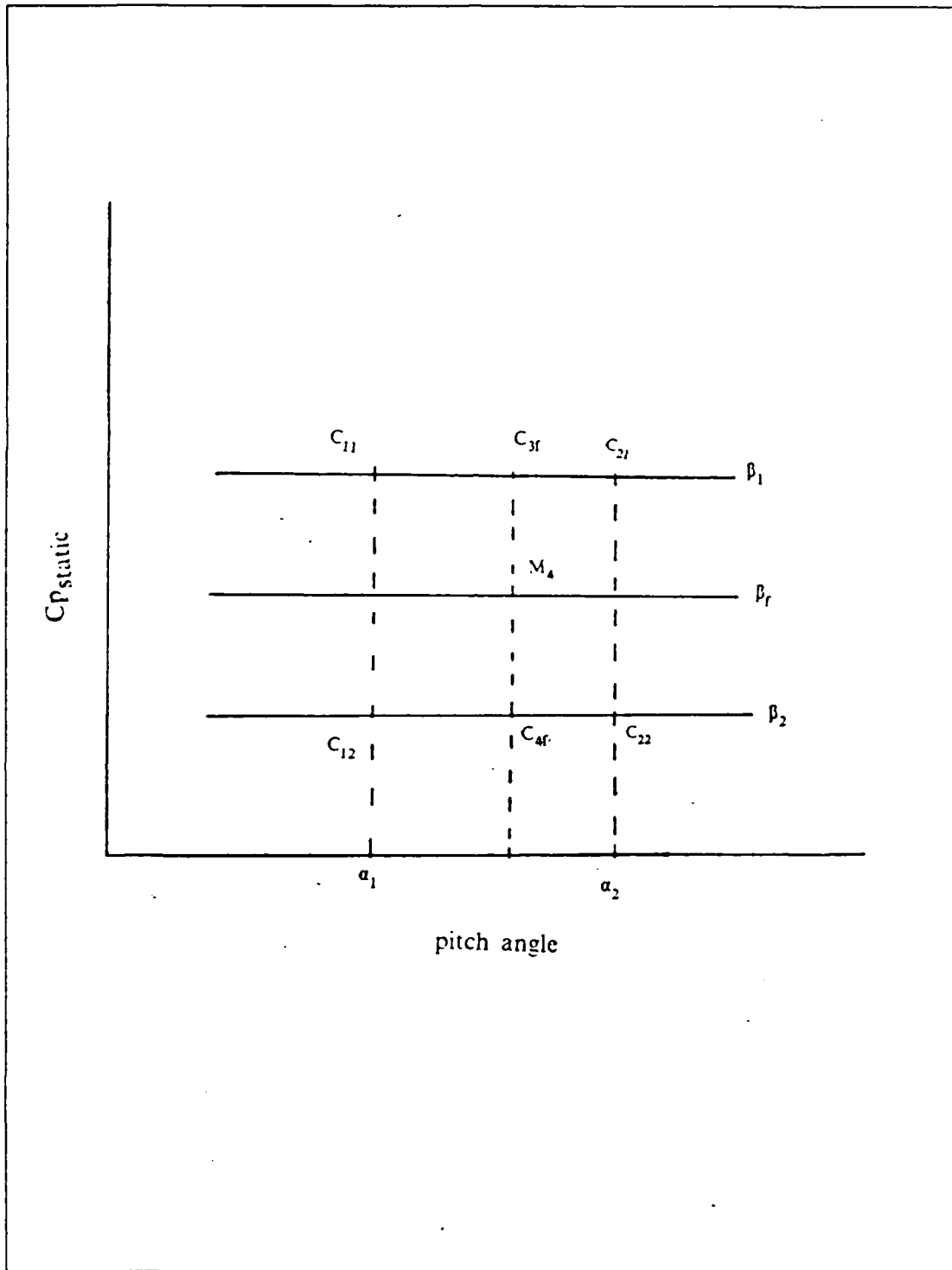


Figure 3.11 Interpolation for local $C_{p\text{static}}$

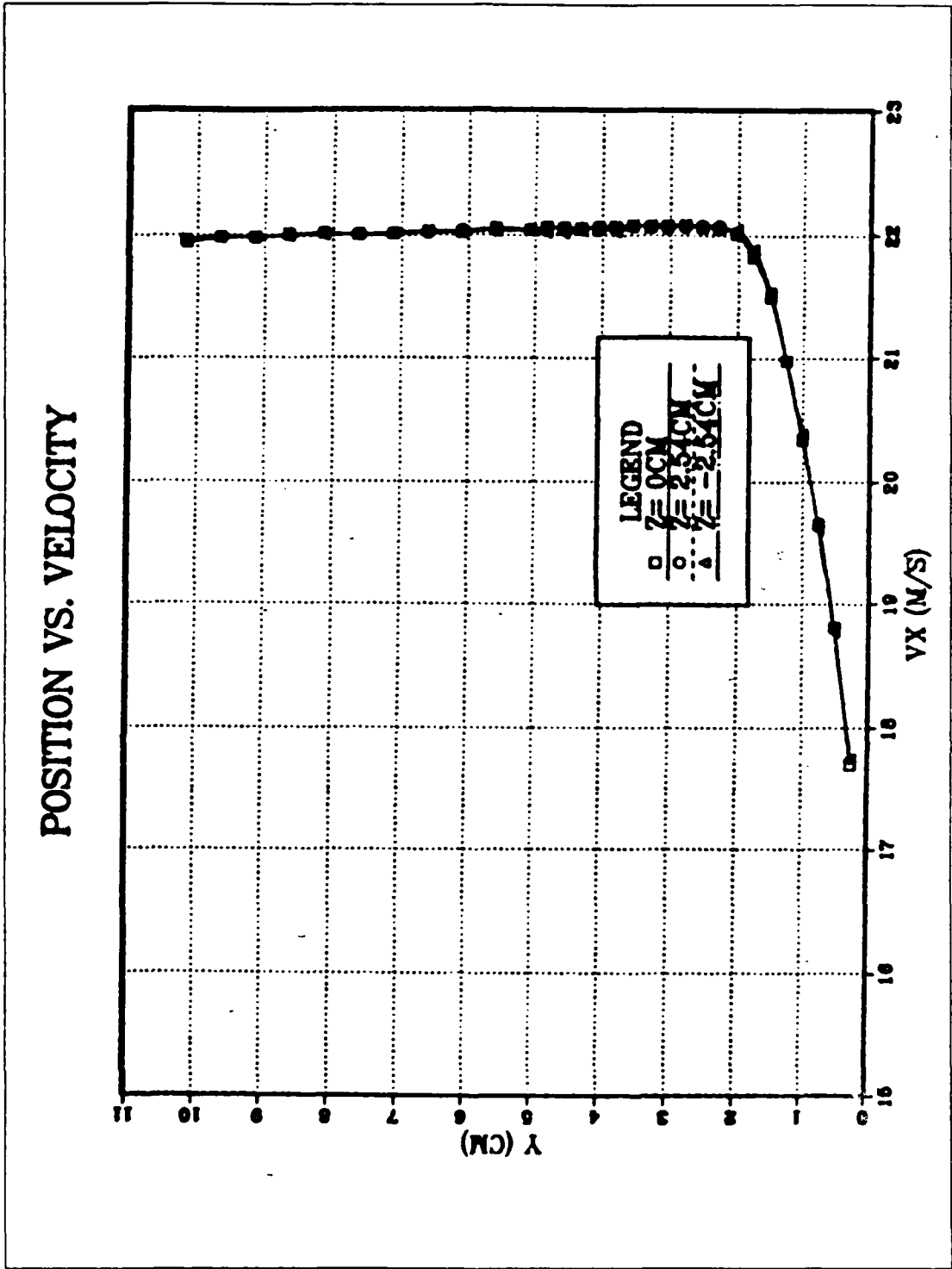


Figure 4.1 Baseline boundary layer results for streamwise velocity, V_x .

POSITION VS. VELOCITY

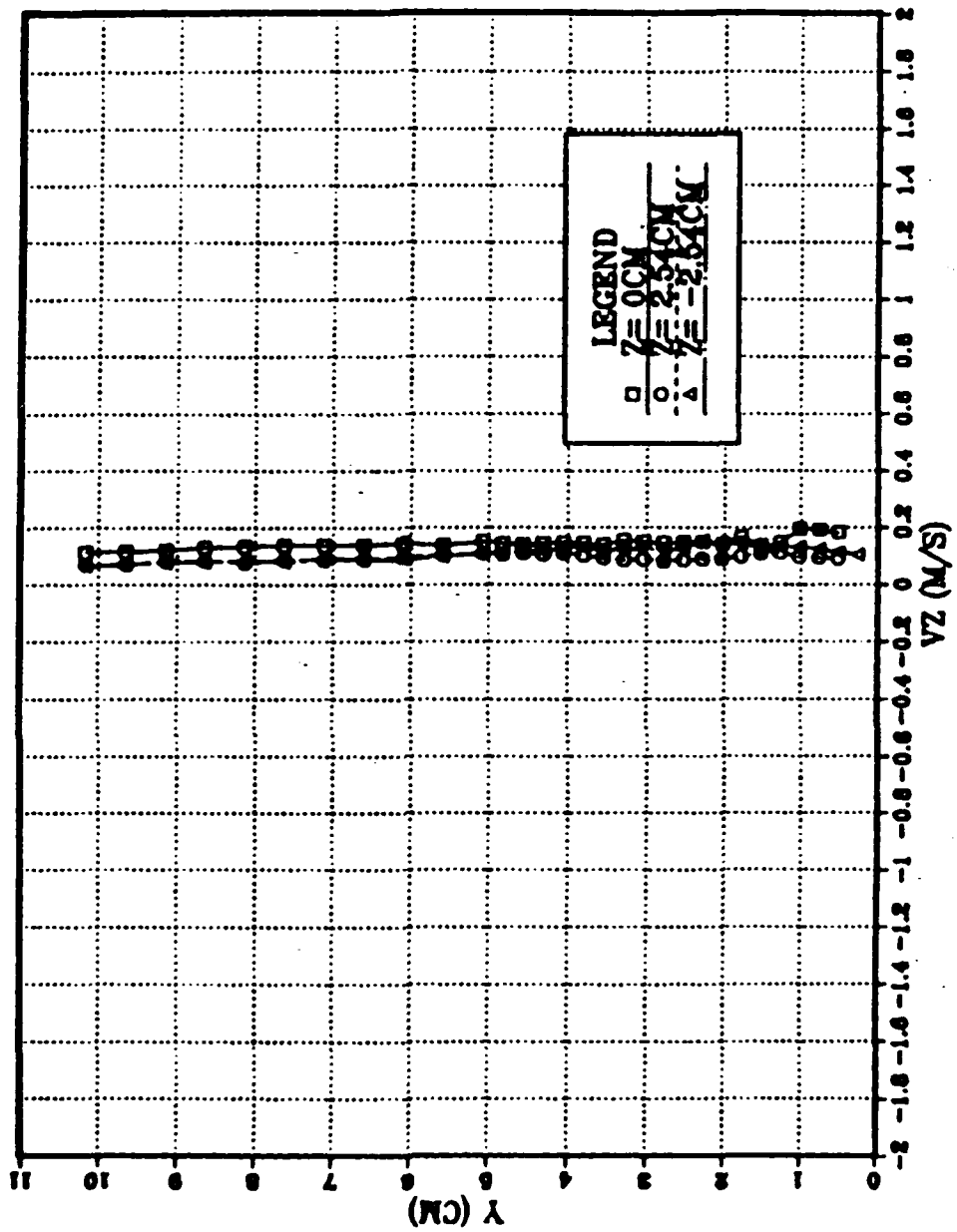
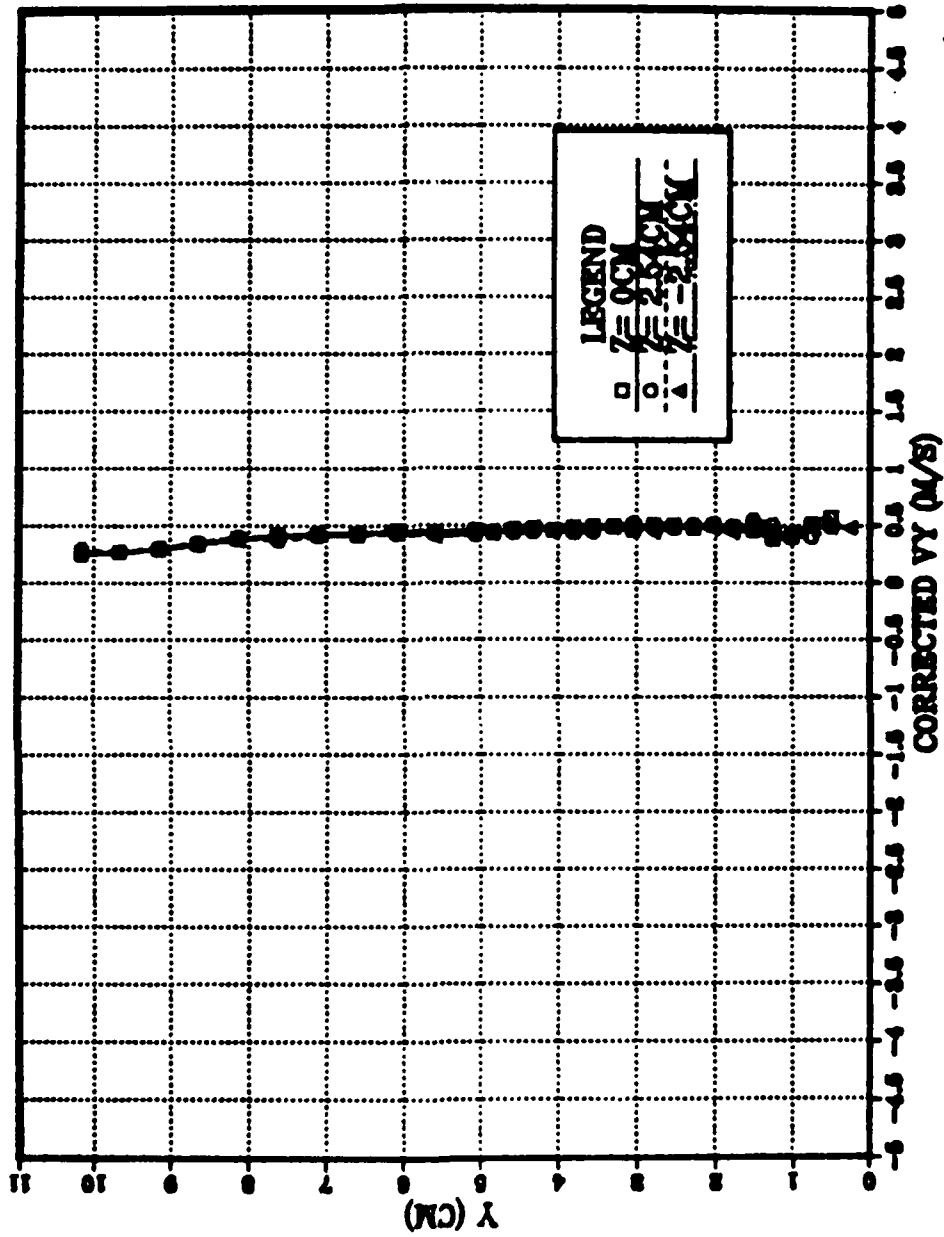


Figure 4.2 Baseline boundary layer results for spanwise velocity, V_z .

POSITION VS. VELOCITY



021057/2000

Figure 4.3 Baseline boundary layer results for corrected V_y .

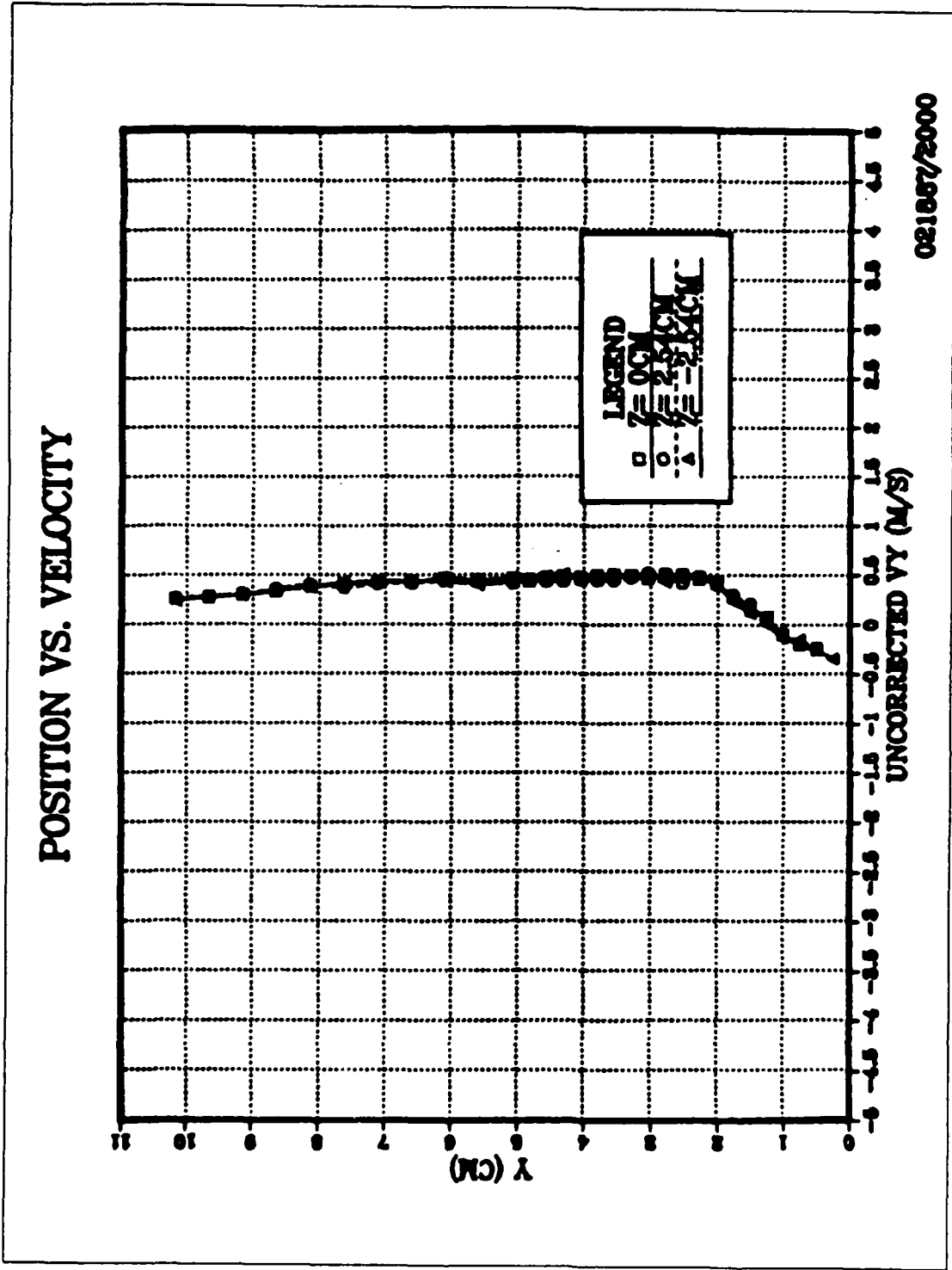


Figure 4.4 Baseline boundary layer results for uncorrected V_y .

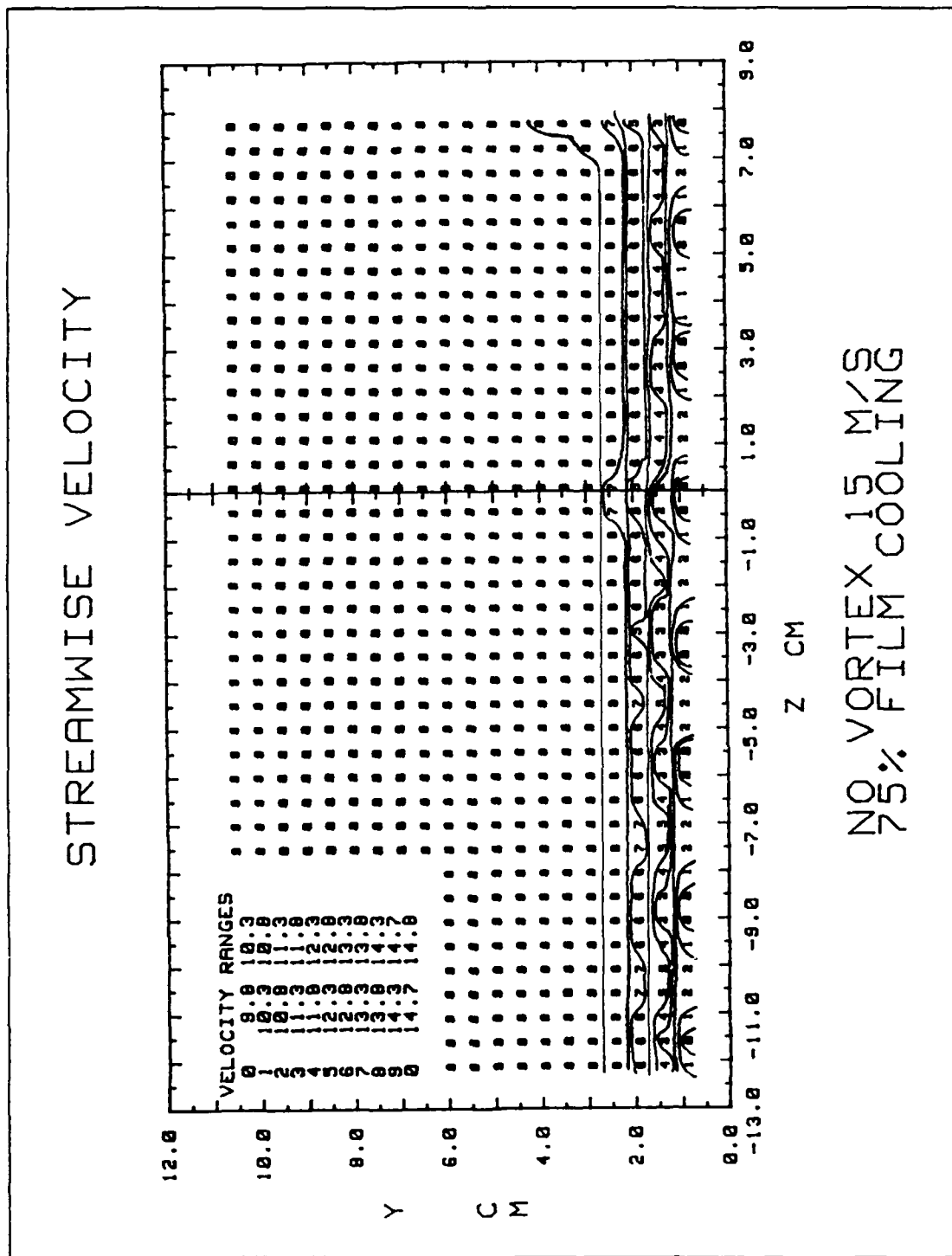


Figure 4.5 Streamwise velocity for boundary layer without embedded vortex, 75% film cooling, freestream velocity 15 m/s.

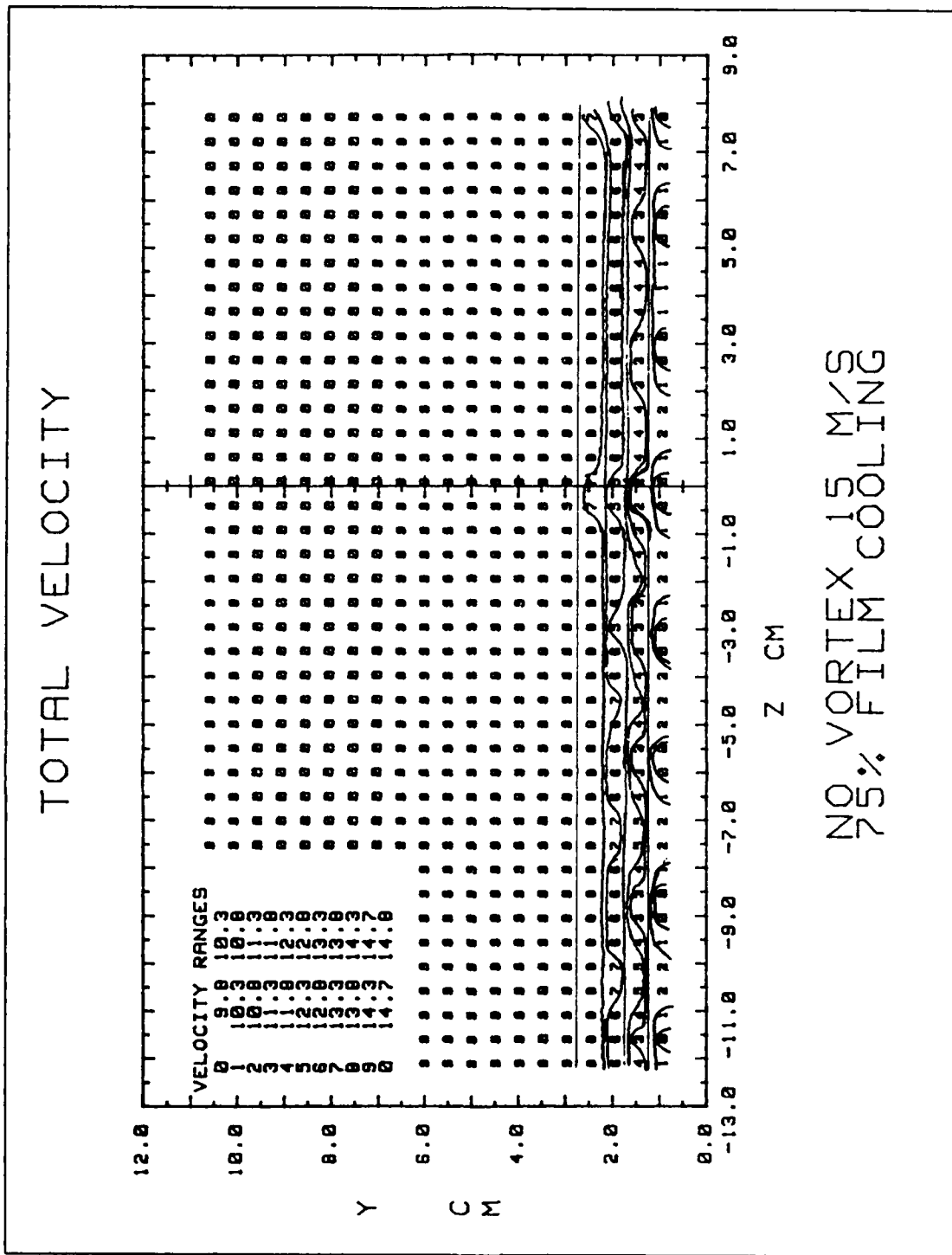


Figure 4.6 Total velocity for boundary layer without embedded vortex
75% film cooling, freestream velocity 15 m/s.

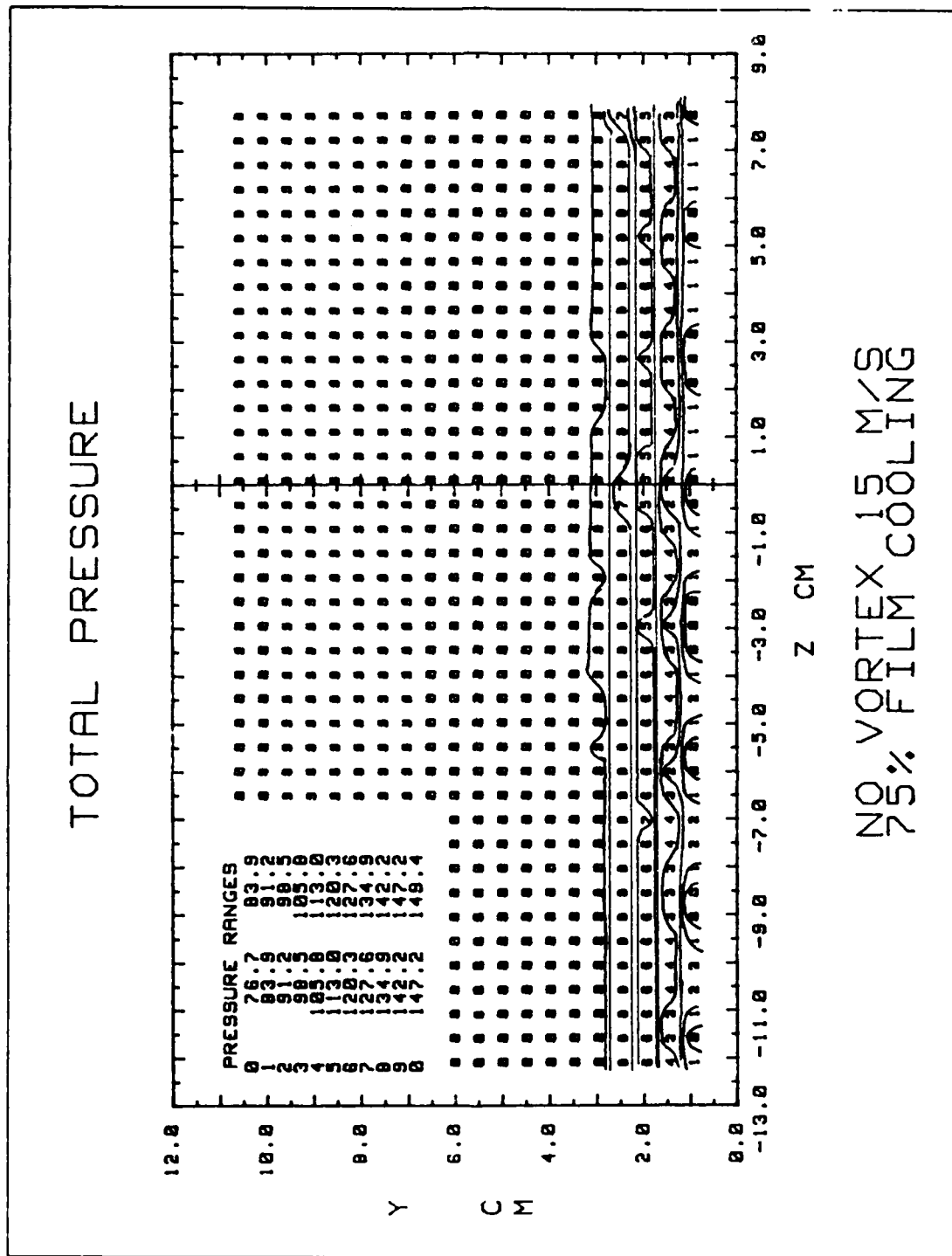


Figure 4.7 Total pressure for boundary layer without embedded vortex, 75% film cooling, freestream velocity 15 m/s.

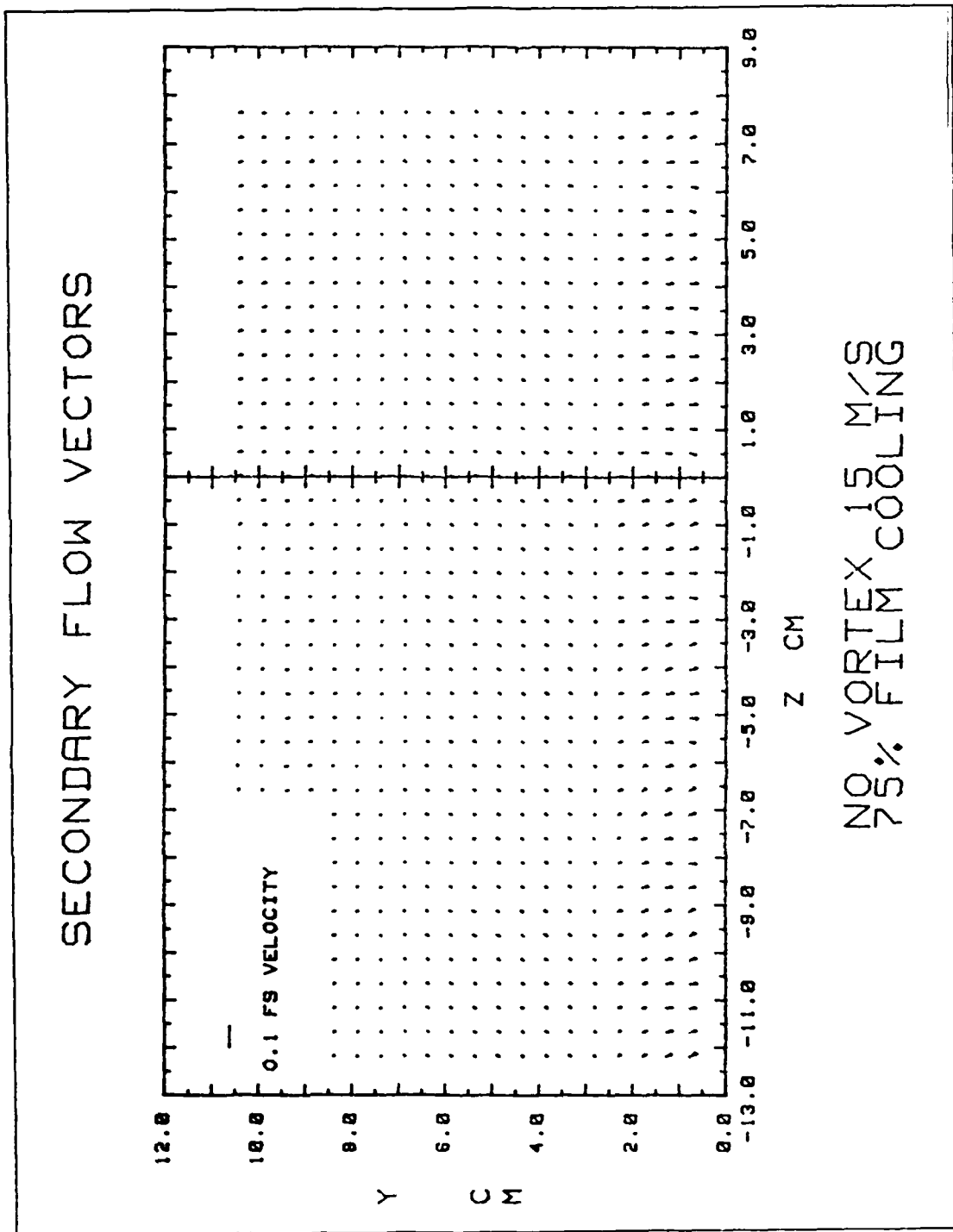


Figure 4.8 Secondary flow vectors for boundary layer without embedded vortex, 75% film cooling, freestream velocity 15 m/s.

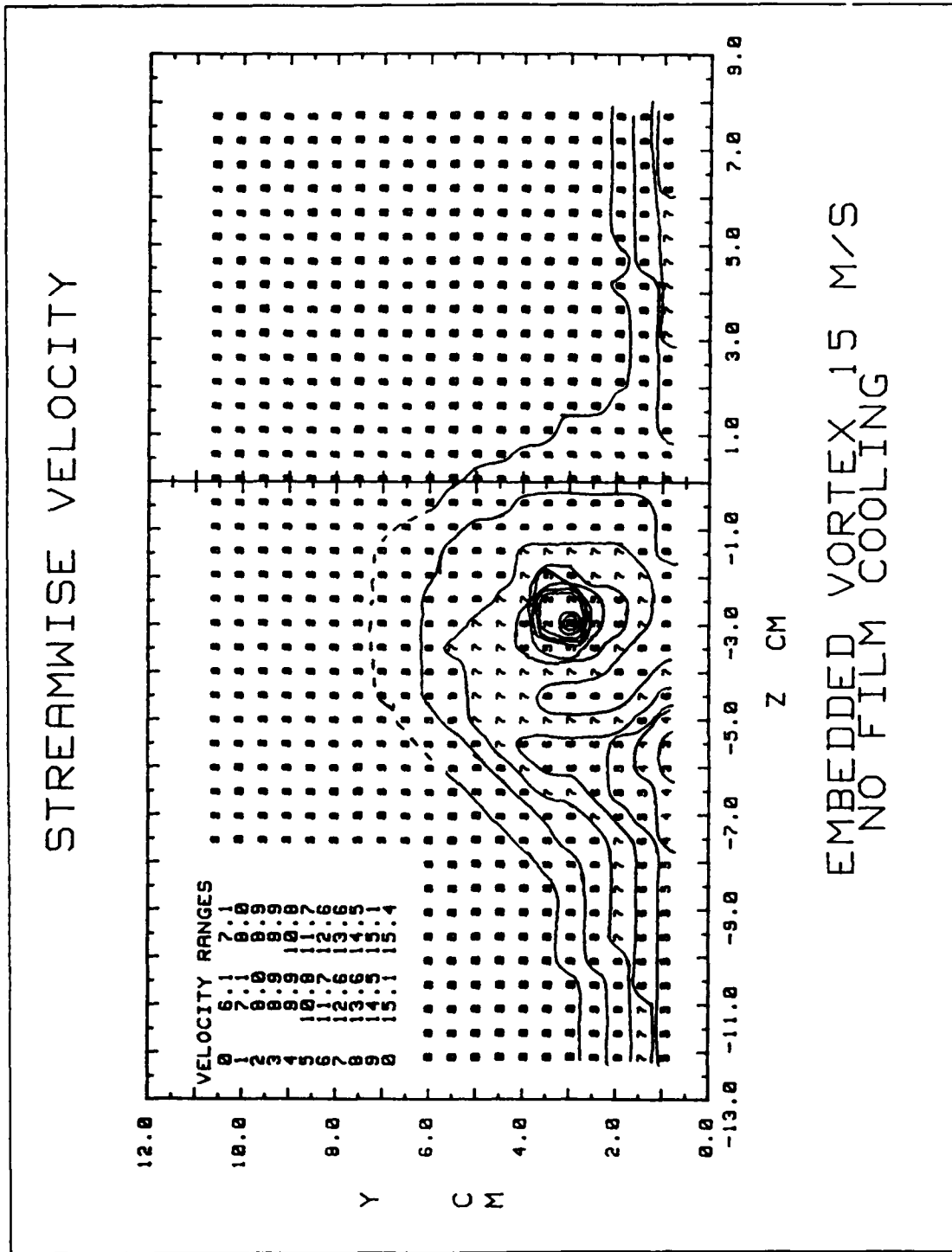


Figure 4.9 Streamwise velocity for boundary layer with embedded vortex, without film cooling, freestream velocity 15 m/s.

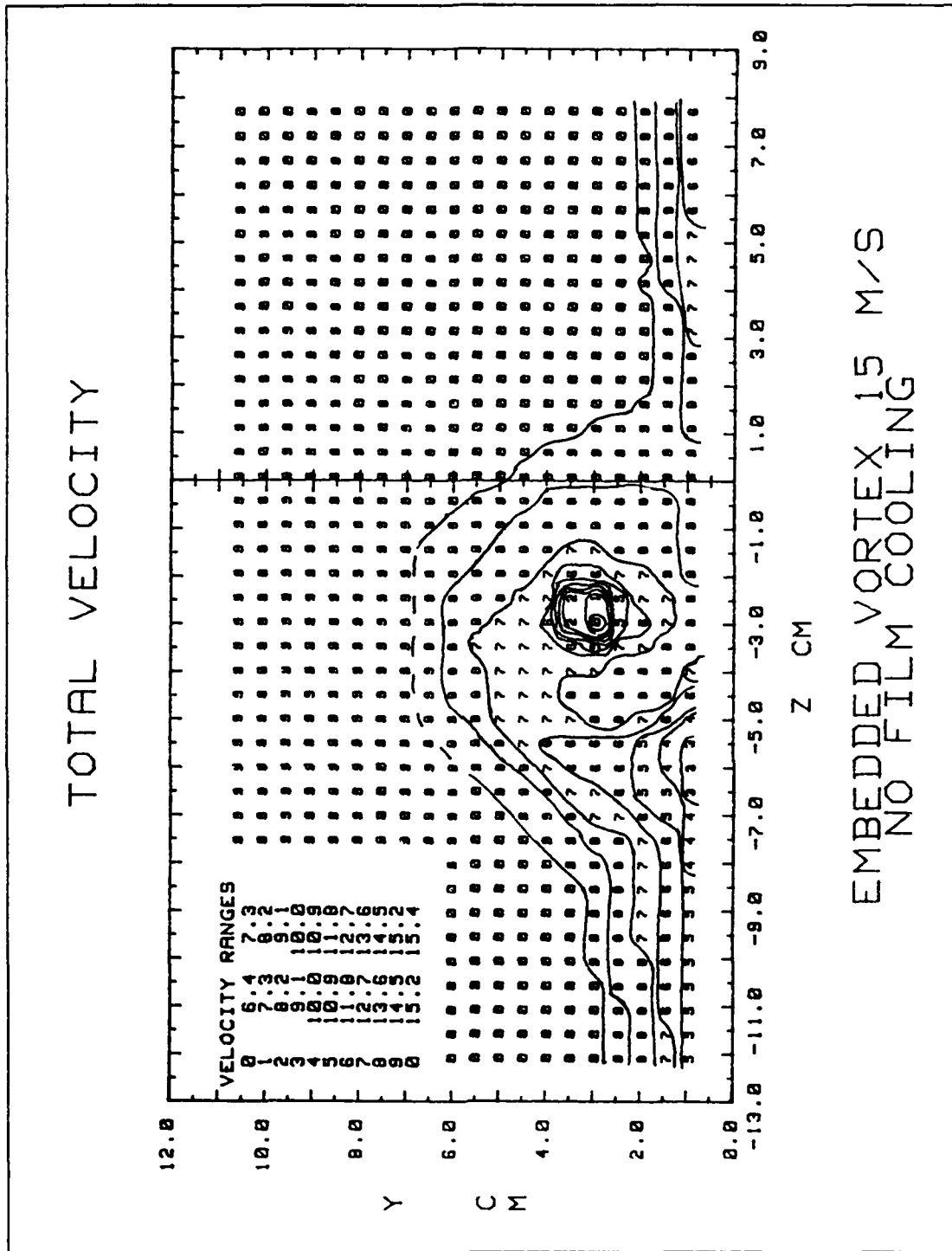


Figure 4.10 Total velocity for boundary layer with embedded vortex, without film cooling, freestream velocity 15 m/s.

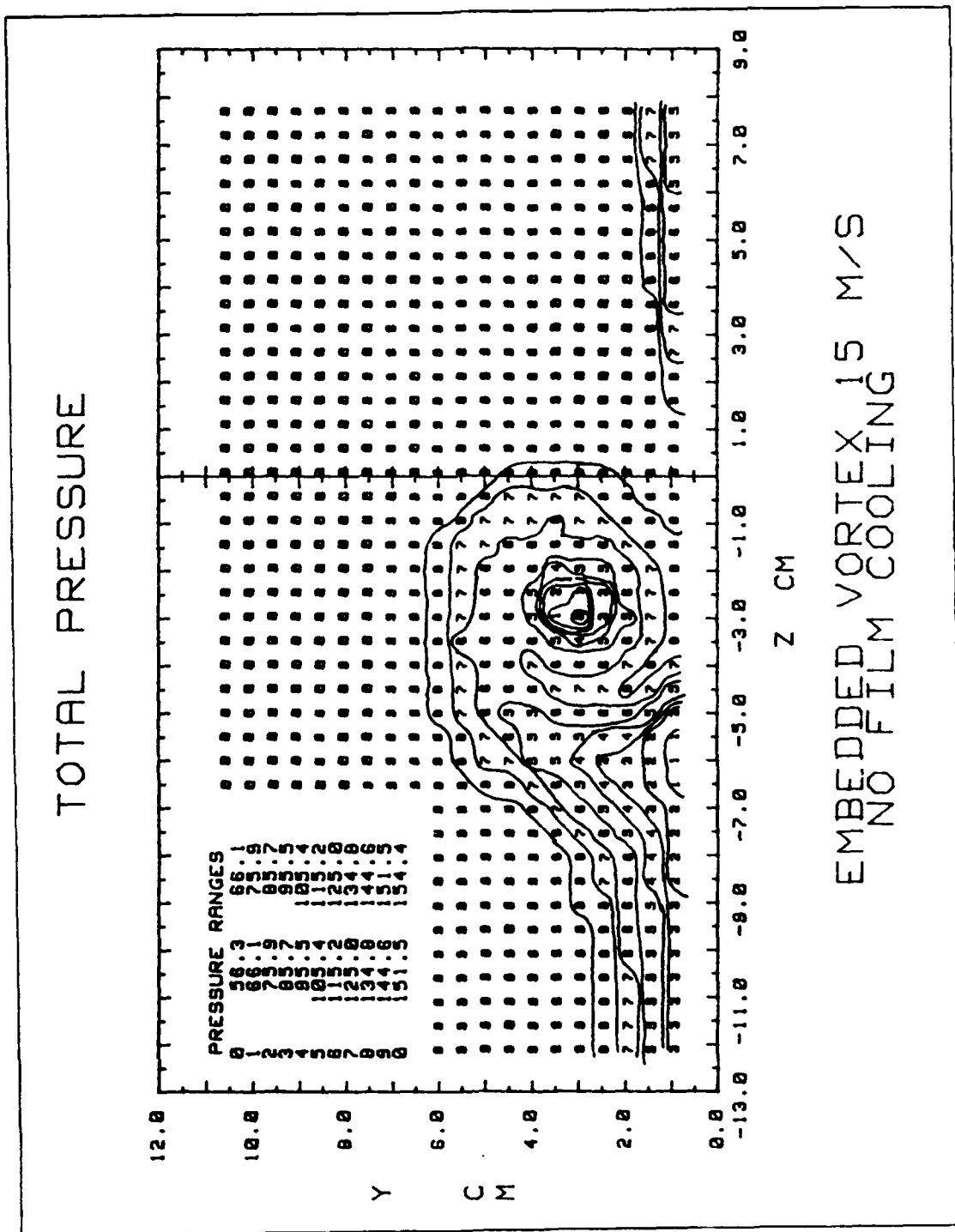


Figure 4.11 Total pressure for boundary layer with embedded vortex, without film cooling, freestream velocity 15 m. s.

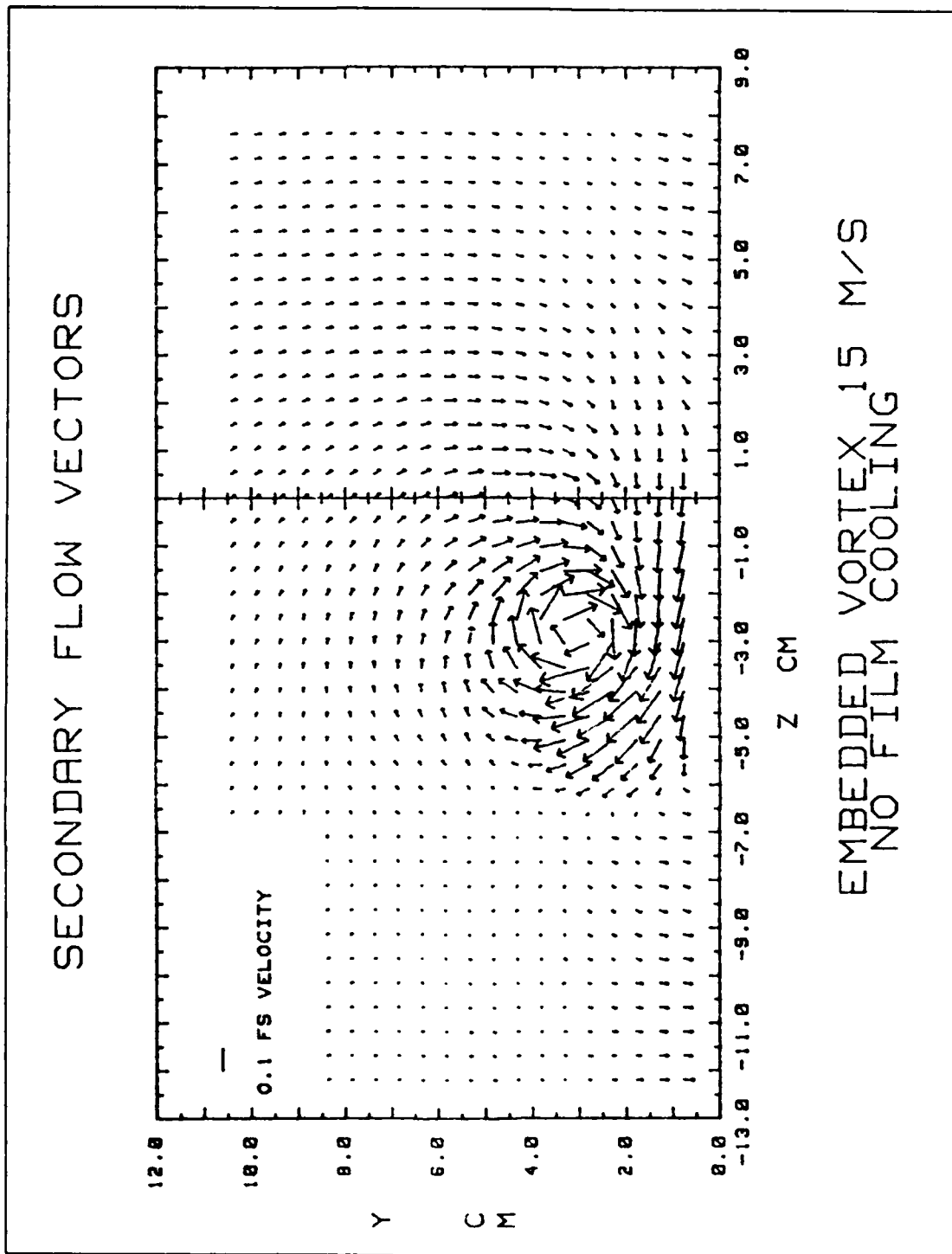


Figure 4.12 Secondary flow vectors for boundary layer with embedded vortex, without film cooling, freestream velocity 15 m. s.

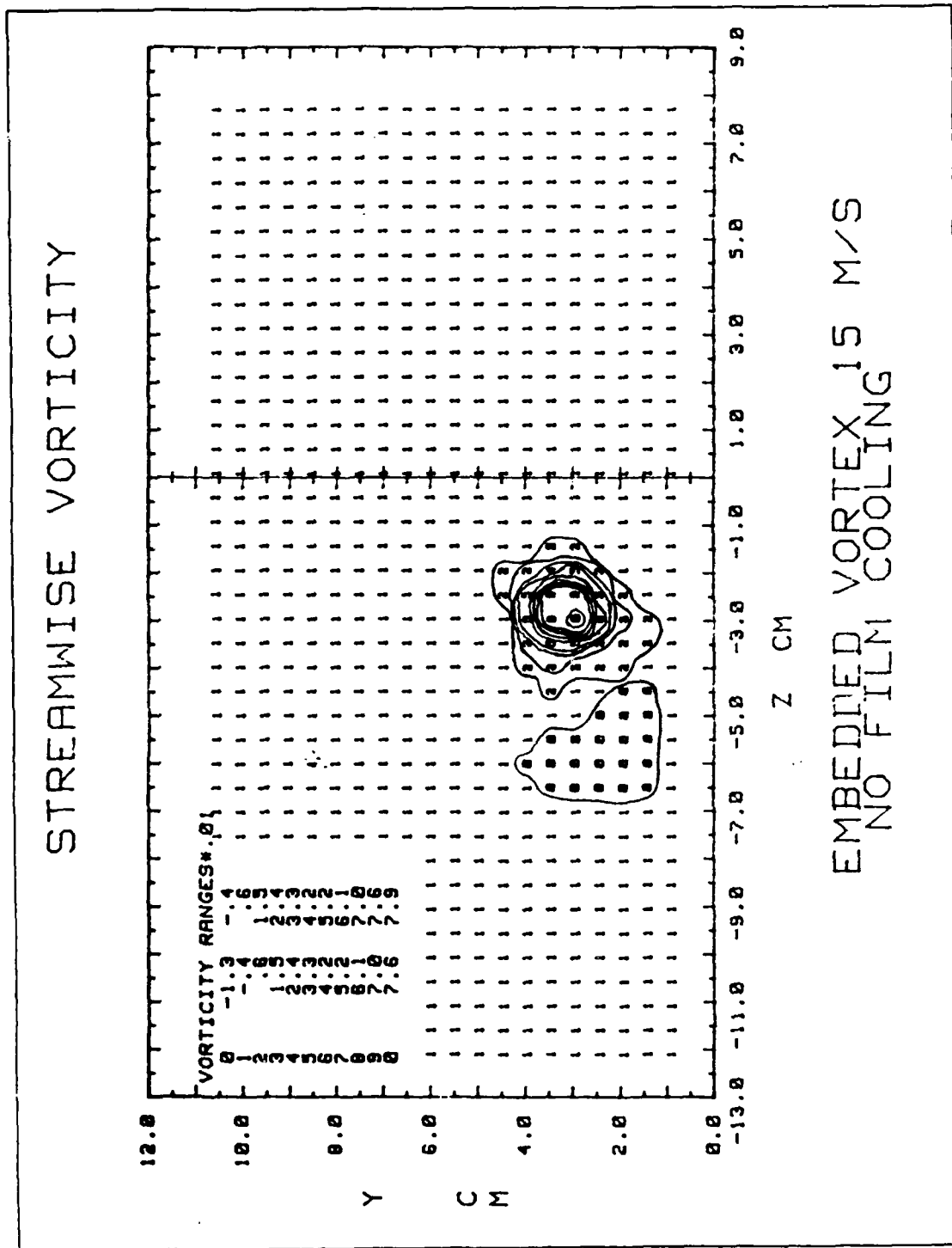


Figure 4.13 Vorticity contours for boundary layer with embedded vortex, without film cooling, freestream velocity 15 m. s.

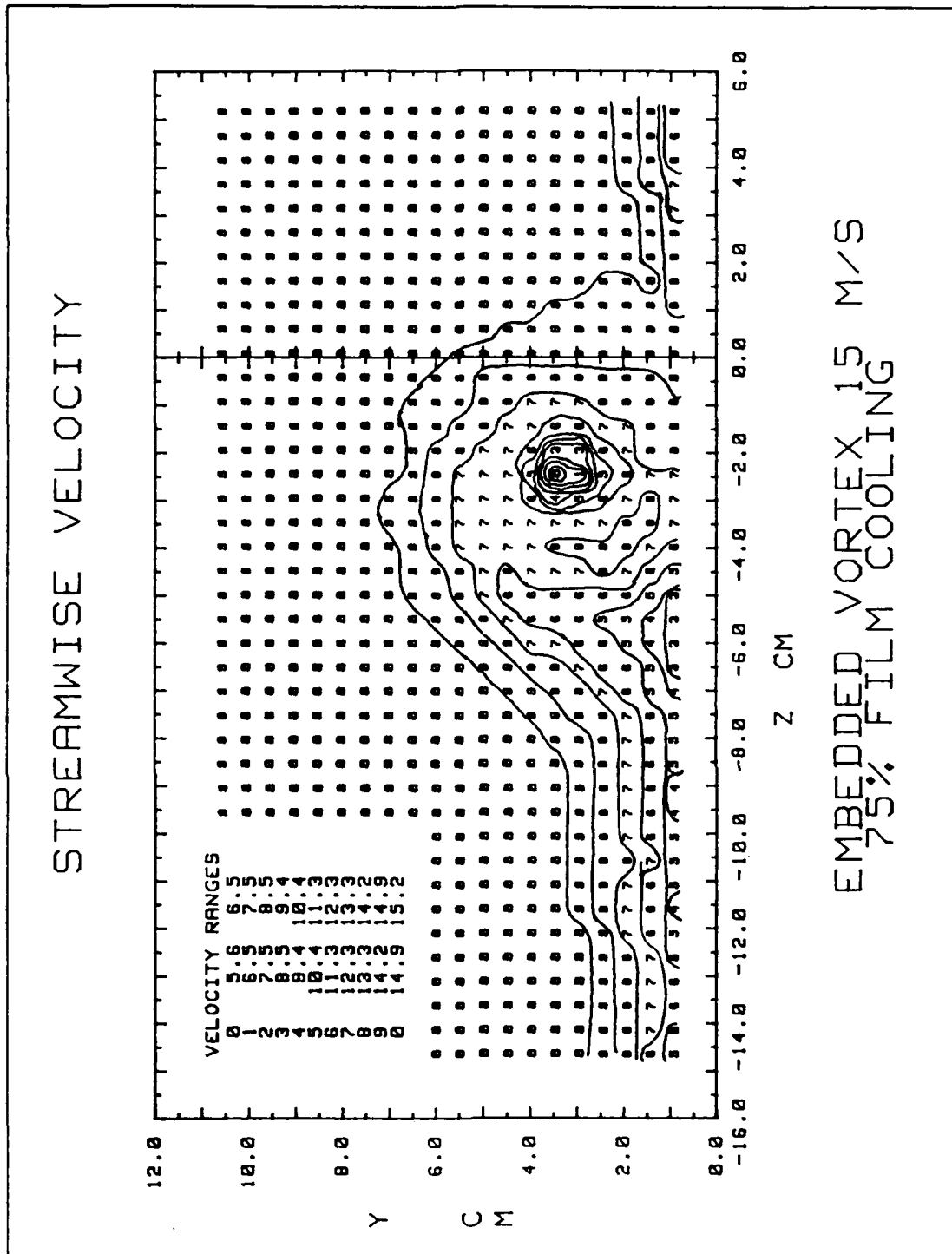


Figure 4.14 Streamwise velocity for boundary layer with embedded vortex and film cooling, freestream velocity 15 m/s.

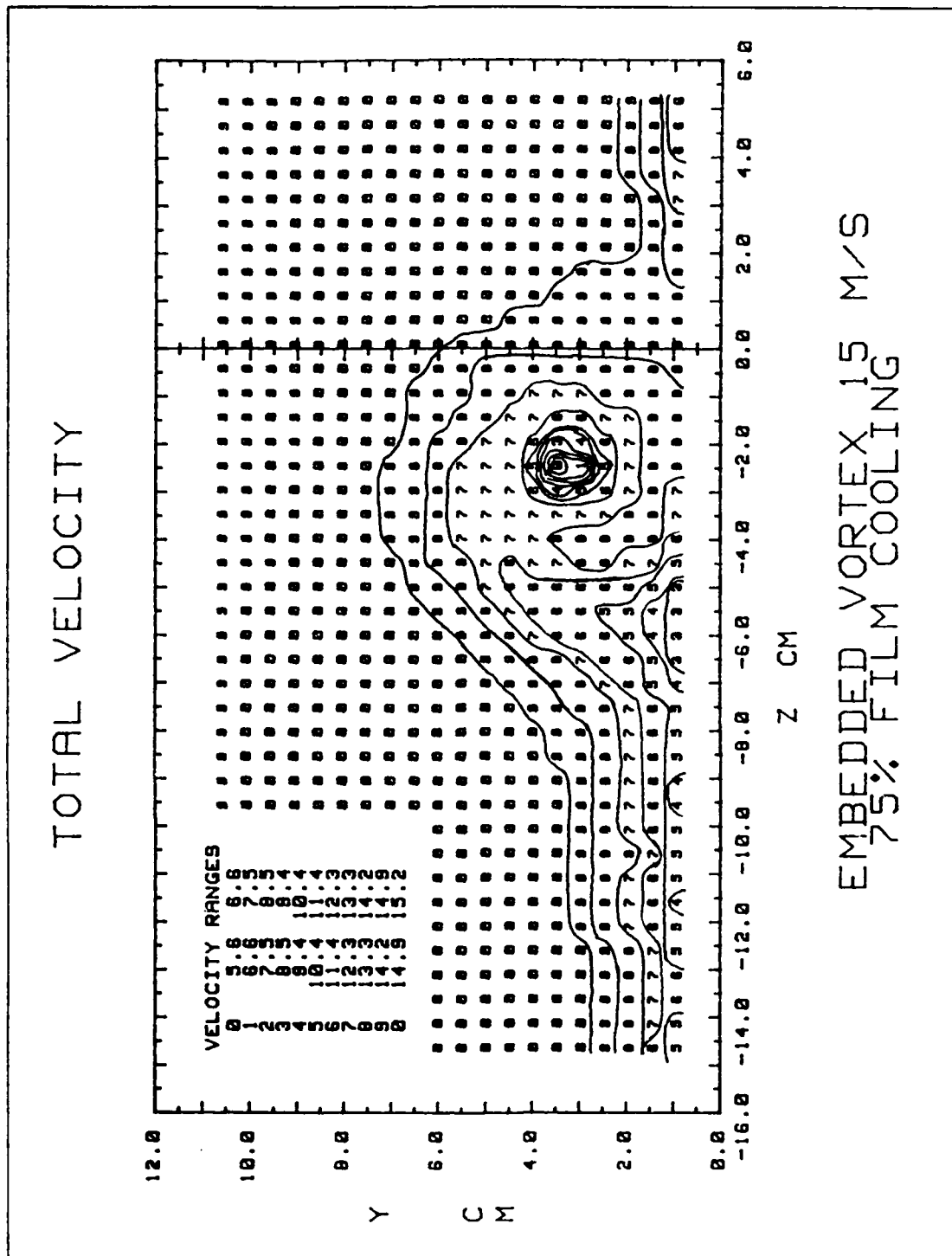


Figure 4.15 Total velocity for boundary layer with embedded vortex and film cooling, freestream velocity 15 m/s.

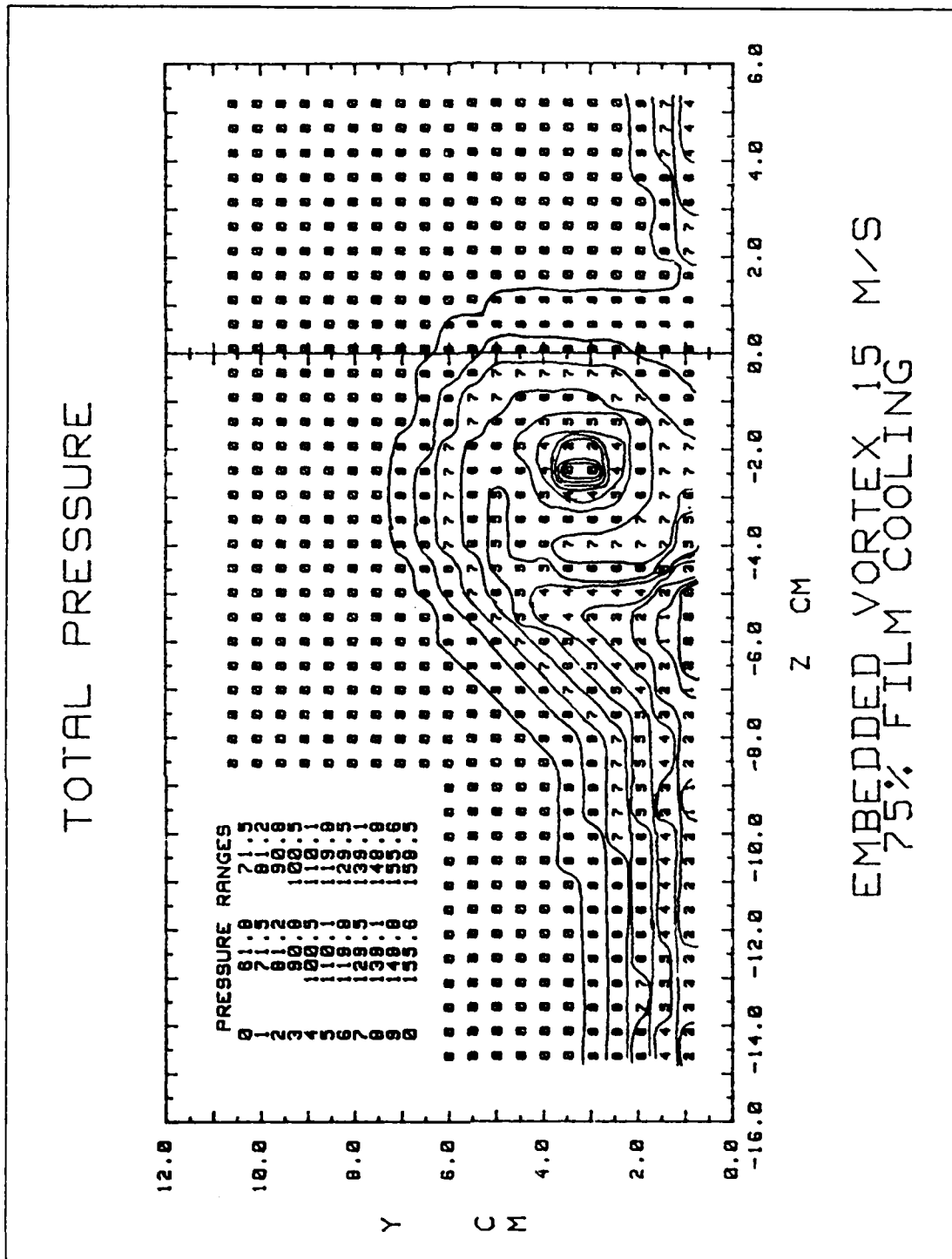


Figure 4.16 Total pressure for boundary layer with embedded vortex and film cooling, freestream velocity 15 m/s.

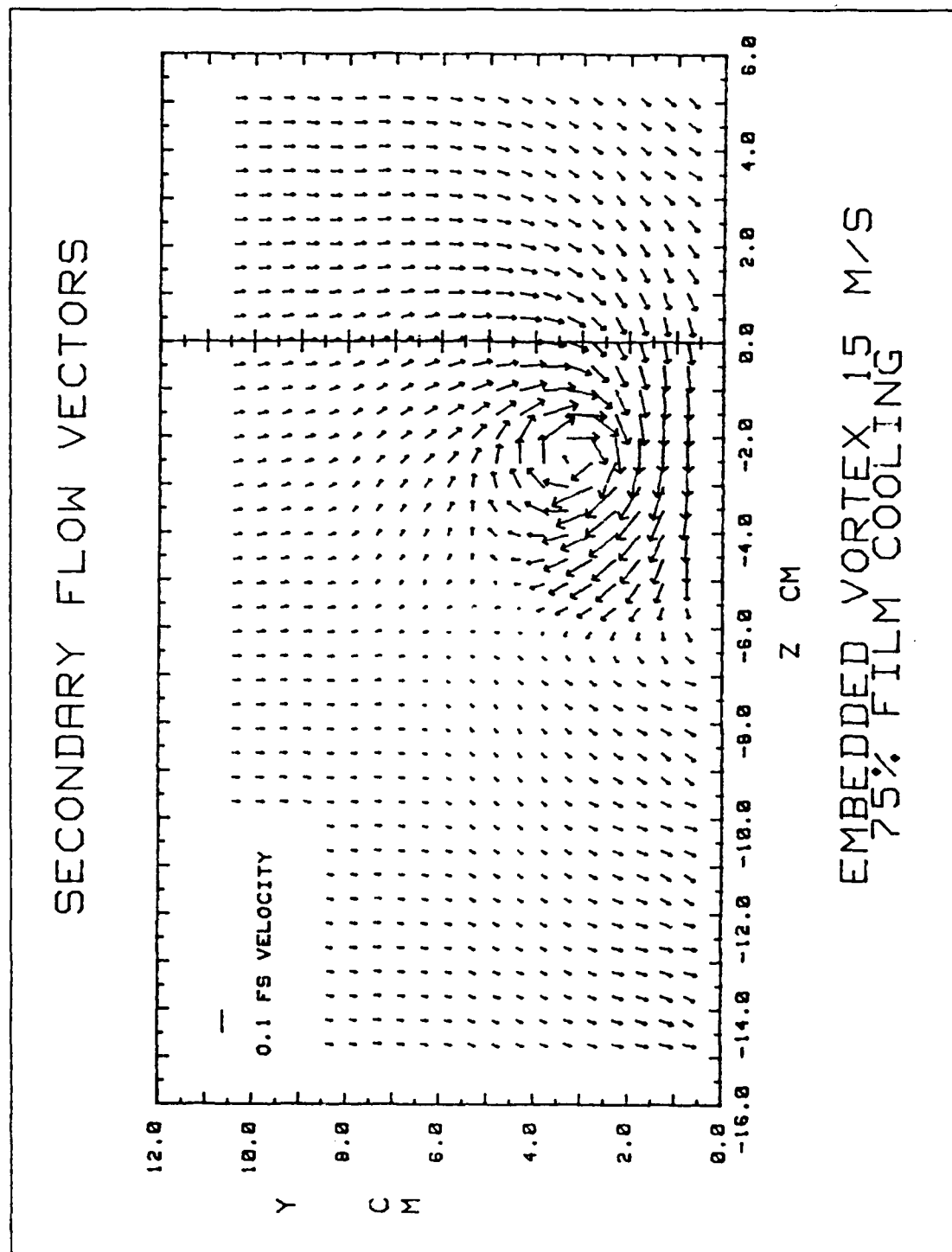


Figure 4.17 Secondary flow vectors for boundary layer with embedded vortex and film cooling, freestream velocity 15 m/s.

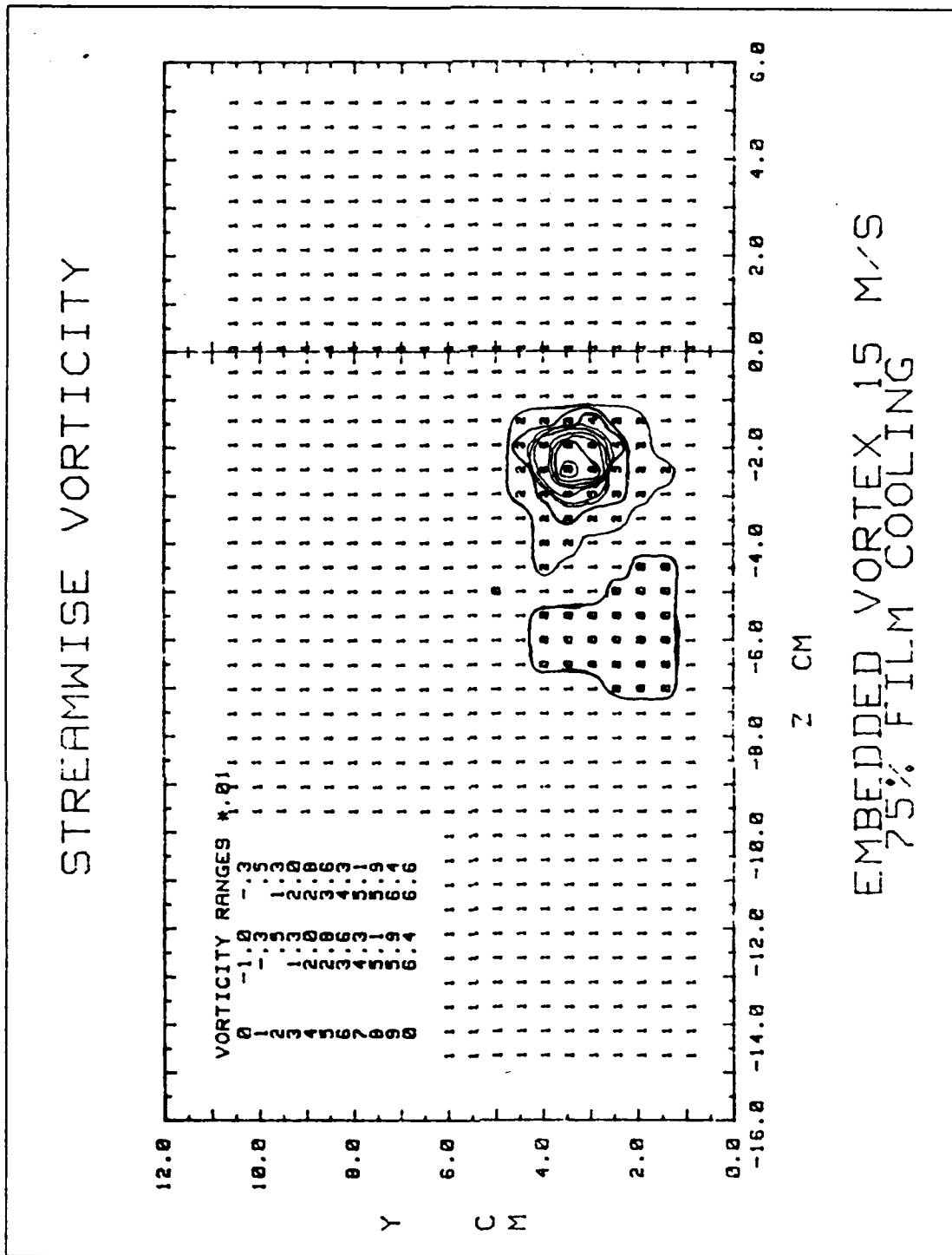


Figure 4.18 Vorticity contours for boundary layer with embedded vortex and film cooling, freestream velocity 15 m/s.

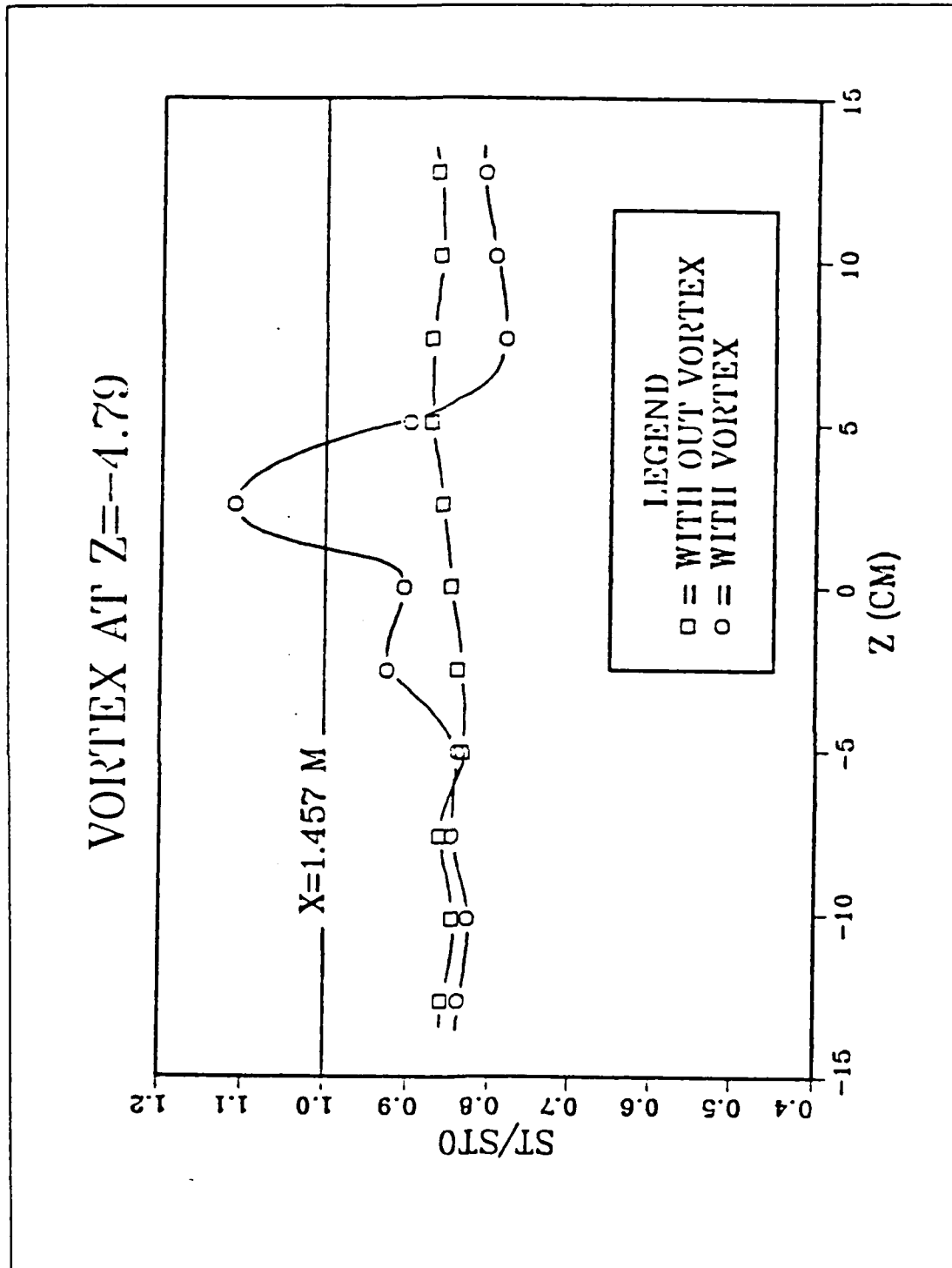


Figure 4.19 Stanton number ratio for vortex at $z = -4.79\text{cm}$ with film cooling.

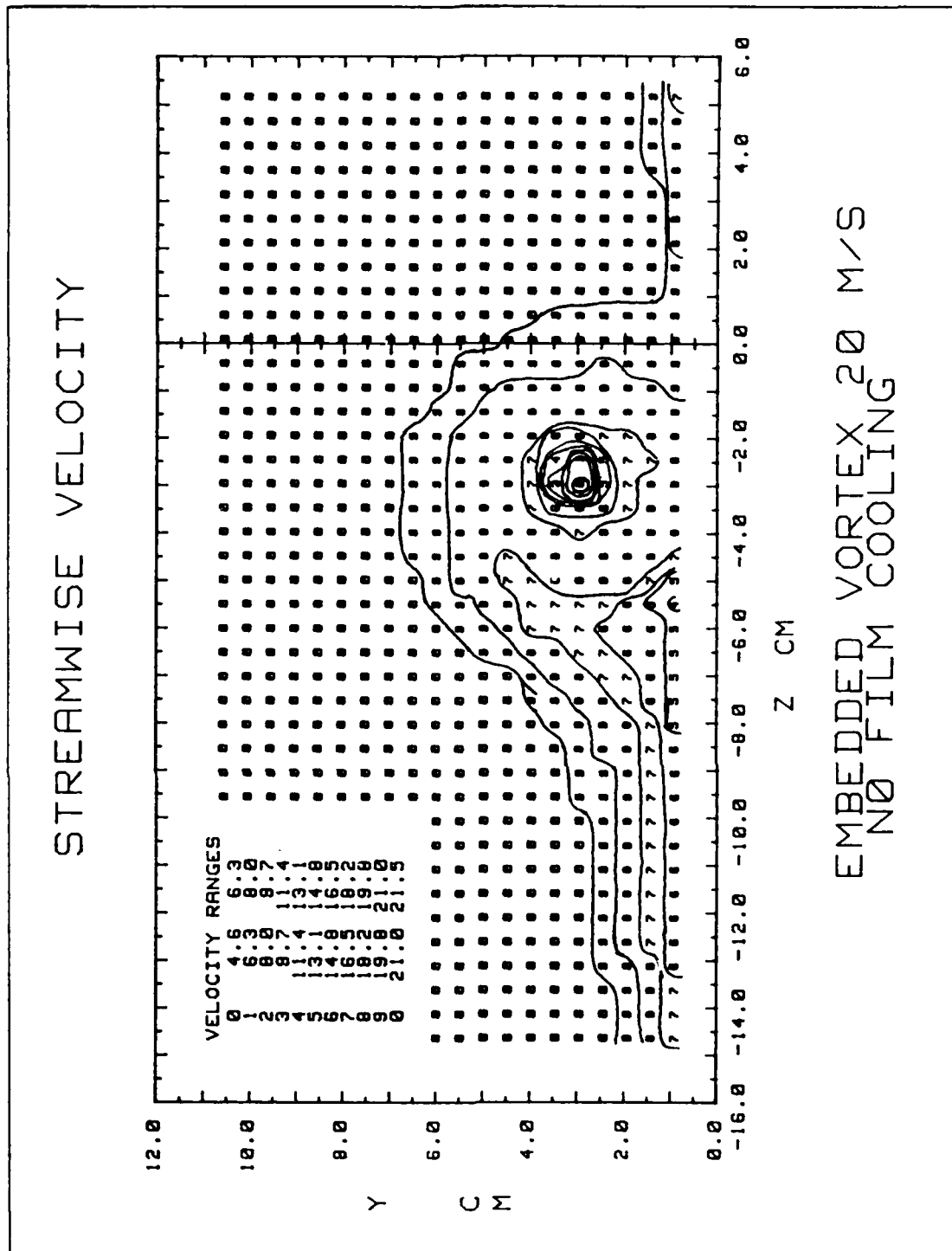


Figure 4.20 Streamwise velocity for embedded vortex without film cooling, freestream velocity 20 m/s.

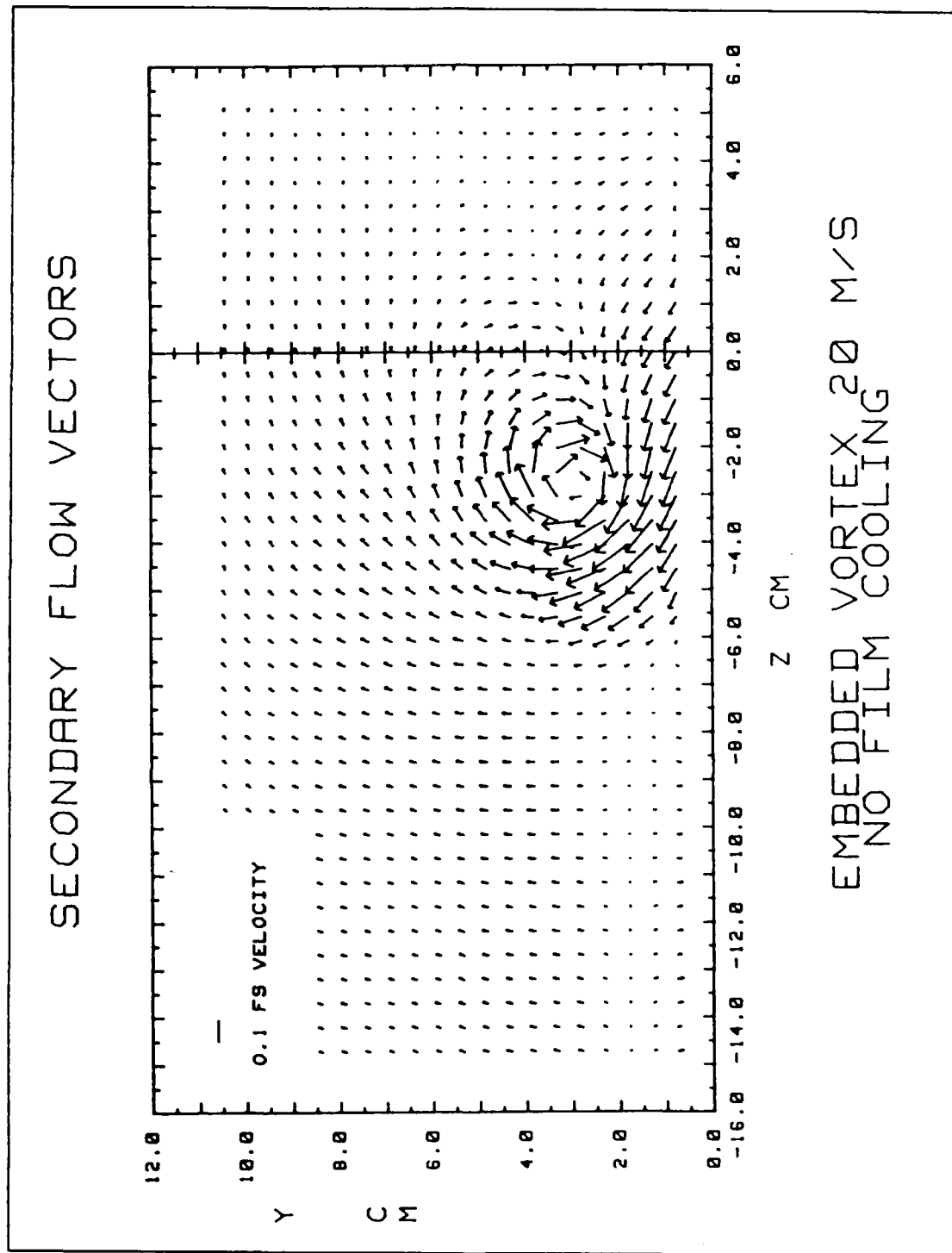


Figure 4.21 Secondary flow vectors for embedded vortex without filmcooling, freestream velocity 20 m. s.

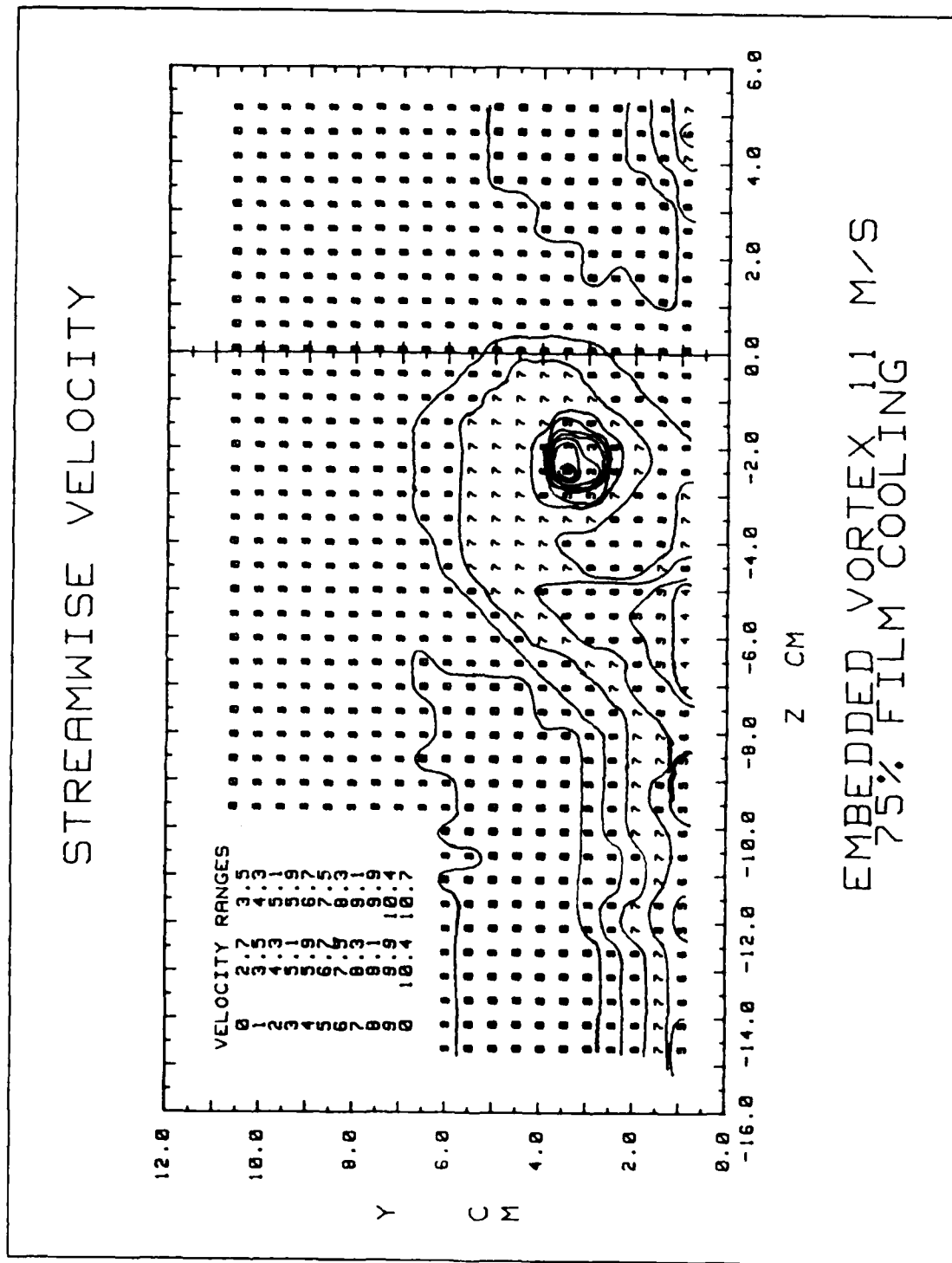


Figure 4.22 Streamwise velocity for embedded vortex with film cooling, freestream velocity 11 m/s.

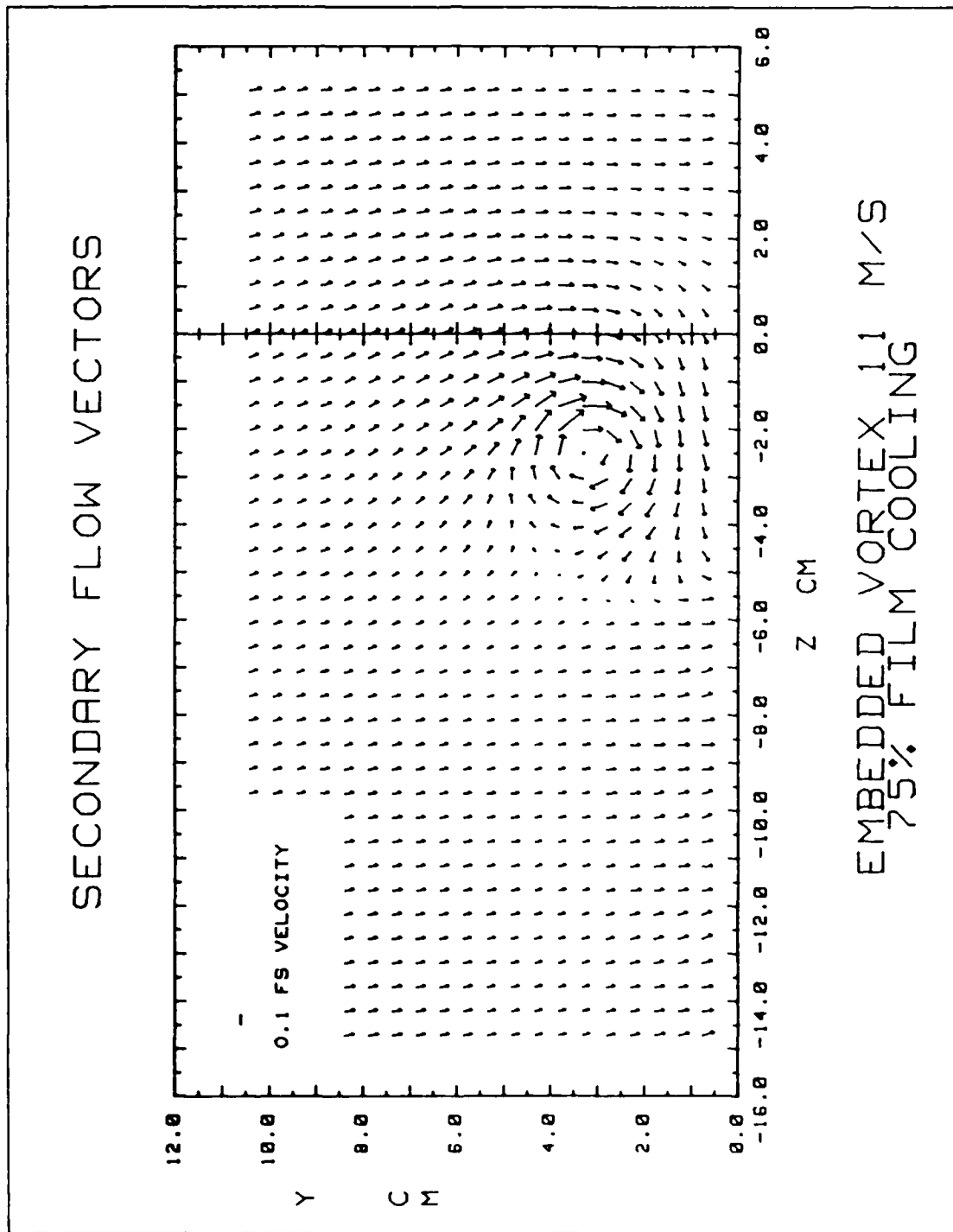


Figure 4.23 Secondary flow vectors for embedded vortex with film cooling, freestream velocity 11 m. s.

APPENDIX C SOFTWARE

```
10 REM PROGRAM PROCAL
20 REM THIS PROGRAM COMPUTES
30 REM THE COEFFICIENTS OF YAW
40 REM AND PITCH FOR THE FIVE
50 REM HOLE PRESSURE PROBE
60 REM
70 REM DAVID EVANS    NOV 1986
80 REM
90 REM VARIABLE NAMES
100 REM
110 REM E(I) IS THE VOLTAGE
120 REM READ FROM THE DATA
130 REM ACQUISITION SYSTEM
140 REM
150 REM A(I) IS THE CONVERSION
160 REM FROM VOLTAGE TO INCHES
155 REM OF WATER.
170 REM
180 REM P(I) WHERE I=1 TO 5
190 REM ARE THE PRESSURES
200 REM FROM THE 5 HOLES
210 REM OF THE PRESSURE PROBE
220 REM
230 REM P6=STATIC PRESSURE
240 REM P7=TOTAL PRESSURE
250 REM P(6)=AVERAGE PRESSURE
260 REM D1= P2-P3
270 REM D2=P4-P5
280 REM D3=P1-P(6)
290 REM C1= YAW COEFFICIENT
300 REM C2 = PITCH COEFFICIENT
310 REM C3=COEFFICIENT OF TOTAL
320 REM PRESSURE
330 REM C4=COEFFICIENT OF STATIC
PRESSURE
340 REM
350 DIM C1(100),C2(100),C3(100)
360 DIM C4(100),X1(100),Y(100)
370 REM
380 DISP "ENTER DATE,(MMDDYY)"
390 INPUT M1
400 DISP "ENTER TIME,(HHMM)"
410 INPUT M2
420 REM
430 PRINT M1,,M2
440 REM
450 CREATE "CALDA1",2
460 ASSIGN# 1 TO "CALDA1"
470 ! PRINT# 1 : M1,M2
480 REM
```

```

490 REM THIS SECTION COMPUTES
500 REM THE CONVERSION FACTOR
510 REM FOR VOLTAGE TO INCHES
520 REM OF WATER THE USER MUST
530 REM INPUT THE MANOMETER
540 REM
550 REM THIS SECTION COMPUTES
615 REM THE ZERO OFFSET COR
- 616 REM RECTION FOR THE
TRANS-
560 REM THE ZERO OFFSET COR-
622 REM RECTION FOR THE TRA
NS- 623 REM
570 REM
580 DISP "COMPUTE ZERO OFFSET "
590 DISP "CORRECTION "
600 DISP " !!! DISCONNECT ALL
TUBING TO THE TRA
NS
DUCERS!!!"
610 DISP " HIT CONT WHEN READY"
620 PAUSE
630 CLEAR
640 FOR I=200 TO 204
650 Z2=0
660 FOR J=1 TO 50
670 OUTPUT 709 ; "AI"; I; "VT1"
680 ENTER 709 ; X2
690 Z2=Z2+X2
700 NEXT J
710 Z3=Z2/50
720 Z4(I-199)=Z3
730 NEXT I
740 REM
750 REM
760 REM *****LOOP#1*****
770 REM
780 FOR I=200 TO 204
790 I1=I-199
800 DISP "TRANSDUCER CALIBRATION
ENTER THE MANOMETE
PRESSURE (IN
H2O)"
810 DISP "ENTER THE PRESSURE"
820 DISP "TRANSDUCER NP " . I1
830 INPUT H2
840 Z0=0
850 REM
860 REM *****LOOP#2*****
870 FOR J=1 TO 50
880 OUTPUT 709 ; "AI"; I; "VT1"
890 ENTER 709 ; X
900 Z0=Z0+X
910 NEXT J
920 REM *****

```

```

930 E1=20/50
940 A(I-199)=H2/(E1-24(I-199))
950 PRINT "A", I, "=", A(I-199)
960 DISP "IF A(I) IS UNSAT
      PRESS 8 "
970 INPUT N2
980 IF N2=8 THEN GOTO 800
990 NEXT I
1000 REM
1010 REM *****
1020 REM
1030 REM ENTER THE VALUES OF
1040 REM STATIC AND TOTAL
1050 REM PRESSURE.
1060 REM
1070 DISP "INPUT STATIC PRESSURE
      (INCHES OF H2O)"

```

```

1080 DISP "USE TRANSDUCER NR 1"
1090 DISP "AND CHANNEL NR. 200"
1100 REM
1110 DISP "HIT CONTINUE WHEN"
1120 DISP "P STATIC PROPERLY"
1130 DISP "HOOKED UP."
1140 PAUSE
1150 CLEAR
1160 B6=0
1170 FOR J=1 TO 50
1180 REM
1190 OUTPUT 709 : "AI", 200, "VT1"
1200 ENTER 709 : X6
1210 B6=B6+X6
1220 NEXT J
1230 P6=B6/50
1240 REM
1250 DISP "INPUT THE TOTAL PRES-
      SURE, (INCHES H2
      O)"
1260 DISP " AND CHANNEL NR 200"
1270 DISP " "
1280 DISP " HIT CONTINUE WHEN"
1290 DISP " P TOTAL PROPERLY"
1300 DISP " HOOKED UP "
1310 PAUSE
1320 CLEAR
1330 REM
1340 B7=0
1350 FOR J=1 TO 50
1360 OUTPUT 709 : "AI", 200, "VT1"
1370 ENTER 709 : X7

```



```

1380 B7=B7+X7
1390 NEXT J
1400 P7=B7/50
1410 REM
1420 REM
1430 REM ENTER AMBIENT CONDITION
      S
1440 REM
1450 DISP "ENTER PAMB(IN.HG)"
1460 INPUT A1
1470 REM
1480 T=0
1490 FOR J=1 TO 50
1500 OUTPUT 709 : "A1":109:"VT1"
1510 ENTER 709 : T1
1520 T=T+T1
1530 NEXT J
1540 T2=T/50
1550 GOSUB 3010
1560 REM
1570 REM DEL P COMPUTED FROM
1580 REM PTOTAL-PSTATIC
1590 REM
1600 C=P7-P6
1610 REM
1620 REM
1630 REM CONVERSION TO SI UNITS
1640 A1=A1*3385.92

```

```

1650 C=C*248.7
1660 T4=T2+273.15
1670 R1=A1/(.287*T4)
1680 U1=(2*C/R1)*.5
1690 REM
1700 REM
1710 REM ENTER THE BIG LOOP
1720 REM FOR READING PPRESSURES
1730 REM AND COMPUTING COEFF
1740 REM
1750 REM *****LOOP#3*****
1760 FOR K=1 TO 100
1770 K1=K
1780 REM ENTER THE VALUE OF THE
1790 REM PITCH ANGLE AND YAW
1800 REM
1810 DISP " ENTER THE VALUE OF
      THE PITCH ANGLE"
1820 INPUT X1(K1)
1830 REM
1840 DISP "ENTER THE VALUE OF"
1850 DISP "THE YAW ANGLE "

```

```

1850 INPUT Y(K)
1870 DISP " PITCH ANGLE ENTERED
        IS",X1(K)
1880 DISP "YAW ANGLE ENTERED IS
        ",Y(K)
1890 DISP " "
1900 DISP " DO YOU WANT TO CHANG
E        PITCH OR YAW IF
        SO PRE        SS 1"
1910 INPUT N4
1920 IF N4=1 THEN 1800
1930 REM THIS LOOP ACQUIRES EACH
1940 REM PRESSURE 50 TIMES AND
1950 REM TAKES THE AVERAGE.
1960 REM
1970 DISP "HIT 'CONTINUE' FOR"
1980 DISP "DATA ACQUISITION."
1990 PAUSE
2000 CLEAR
2010 REM
2020 REM *****LOOP#3*****
2030 FOR I=200 TO 204
2040 Z1=0
2050 REM *****LOOP#4*****
2060 FOR J=1 TO 50
2070 OUTPUT 709 ;"AI";I;"VT1"
2080 ENTER 709 ; X
2090 Z1=Z1+X
2100 NEXT J
2110 REM *****
2120 X=Z1/50
2130 E(I-199)=X
2140 P(I-199)=A(I-199)*E(I-199)-
        Z4*(I-199)
2150 NEXT I
2160 REM *****
2170 REM
2180 P(6)=0

```

```

2190 FOR I=2 TO 5
2200 P(6)=P(I)+P(6)
2210 NEXT I
2220 P(5)=P(6)/4
2230 O1=P(2)-P(3)
2240 O2=P(4)-P(5)
2250 O3=P(1)-P(6)
2260 C1(K)=O1/O3
2270 C2(K)=O2/O3
2280 C3(K)=(P(1)-P7)/O3
2290 C4(K)=(P(5)-P6)/O3

```

```

2300 REM
2310 PRINT# 1 : X1(K),Y(K),C1(K)
      ,C2(K),C3(K),C4(K)
2320 REM
2330 REM
2340 PRINT "PITCH ANGLE IS",X1(K)
      /
2350 PRINT "YAW ANGLE IS",Y(K)
2360 PRINT
2370 PRINT "P1=",P(1)
2380 PRINT "P2=",P(2)
2390 PRINT "P3=",P(3)
2400 PRINT "P4=",P(4)
2410 PRINT "P5=",P(5)
2420 PRINT
2430 PRINT
2440 DISP "LAST POINT?"
2450 DISP "IF SO PRESS 1"
2460 INPUT N1
2470 IF N1=1 THEN GOTO 2500
2480 NEXT K
2490 REM *****
      1705
2500 REM
2510 ASSIGN# 1 TO *
2520 REM
2530 PRINT
2540 PRINT "*****
      *****"
2550 PRINT
2560 PRINT
2570 PRINT "FIVE HOLE PRESSURE
      PROBE CALIBRAT
      ION."
2580 PRINT
2590 PRINT
2600 PRINT "DATE OF RUN IS",M1
2610 PRINT "TIME OF RUN IS",M2
2620 PRINT
2630 PRINT
2640 PRINT "DENSITY(KG/M3)"
2650 PRINT R1
2660 PRINT "VELOCITY(M/S)"
2670 PRINT U1
2680 PRINT "PAMB(N/M2)"
2690 PRINT A1
2700 PRINT "TAMB(C)"
2710 PRINT T3
2720 PRINT "P STATIC (IN. H2O)"
2730 PRINT P6
2740 PRINT "P TOTAL=(IN. H2O)"
2750 PRINT P7
2760 PRINT
2770 PRINT "PIT YAW    CP1      C
      P2"

```

```

2780 REM *****LOOP#5*****
2790 FOR I=1 TO K1
2800 PRINT USING 2810 ; X1(I),Y(
I),C1(I),C2(I)
2810 IMAGE MOD,2X,MOD,2X,MD,0000
,2 X,MD,0000
2820 NEXT I
2830 REM *****
2840 PRINT
2850 PRINT
2860 PRINT "PIT YAW CP3 CP
4"
2870 REM *****LOOP#6*****
2880 FOR I=1 TO K1
2890 PRINT USING 2900 ; X1(I),Y(
I),C3(I),C4(I)
2900 IMAGE MOD,2X,MOD,2X,MD,0000
,2 X,MD,0000
2910 NEXT I
2920 REM *****
*
2930 PRINT
2940 DISP " THANKS FOR USING ME"
2950 DISP " HOPE YOU FOUND WHAT"
2960 DISP "YOU WERE LOOKING FOR"
2970 DISP " REGARDS"
2980 DISP " HP-858"
2990 END
3000 REM
3010 REM VOLTAGE TO TEMPERATURE
3020 REM CONVERSION
3030 REM
3040 REM V(MV) TO T(C)
3050 REM
3060 E1=T2*1000
3070 T3=26.573*E1-1.936879*E1*E1
+.99785*E1*E1*E1-.261277*E1
*E1*E1*E1
3080 RETURN

```

```

20  REM PROGRAM PRSACQ
30  REM THIS PROGRAM ACQUIRES THE PRESSURES FROM
40  REM A FIVE HOLE PRESSURE PROBE AND COMPUTES CPMW AND
50  REM OBTAINED FROM THE PROGRAM "PROCAL"
60  REM
70  REM AUTHOR DAVE EVANS, JANUARY, FEBRUARY, 1977
80  REM
90  REM VARIABLE NAMES
100 REM
110 REM E(V) IS THE VOLTAGE READ FROM THE DATA ACQUISITION SYSTEM
120 REM A(I) IS THE CONVERSION FROM VOLTAGE TO INCHES OF WATER
130 REM P(I) IS THE PRESSURE READ FROM THE FIVE HOLE PRESSURE PROBE
140 REM I=1 TO 5 AND IN EACH OF THE ABOVE IS ASSOCIATED WITH THE
150 REM PRESSURES FROM THE FIVE HOLE PROBE
160 REM
170 REM P5=STATIC PRESSURE OF THE FREESTREAM
180 REM P7=TOTAL PRESSURE OF THE FREESTREAM
190 REM P(6)=AVERAGE PRESSURE
200 REM O1=P2-P3
210 REM O2=P4-P5
220 REM O3=P1-P(6)
230 REM
240 REM C1=CALIBRATED YAW COEFFICIENT
250 REM C2=CALIBRATED PITCH COEFFICIENT
260 REM C3=CALIBRATED TOTAL COEFFICIENT
270 REM C4=CALIBRATED STATIC COEFFICIENT
280 REM
290 REM M1=MEASURED YAW COEFFICIENT
300 REM M2=MEASURED PITCH COEFFICIENT
310 REM M3=MEASURED TOTAL COEFFICIENT
320 REM M4=MEASURED STATIC COEFFICIENT
330 REM
340 REM V=THE LOCAL TOTAL VELOCITY VECTOR
350 REM V1=THE X COMPONENT OF VELOCITY
360 REM V2=THE Y COMPONENT OF VELOCITY
370 REM VZ=THE Z COMPONENT OF VELOCITY
380 REM
390 REM X1=THE PITCH ANGLE FROM THE CALIBRATION DATA
400 REM Y=THE YAW ANGLE FROM THE CALIBRATION DATA
410 REM
420 REM X4=THE PITCH ANGLE OF THE FLOW
430 REM
440 REM Y1=THE VERTICAL LOCATION OF THE PROBE TIP
450 REM Z0=THE SPANWISE LOCATION OF THE PROBE TIP
460 REM Y3=THE YAW ANGLE OF THE FLOW
470 REM
480 REM P1=AMBIENT PRESSURE
490 REM T4=ABSOLUTE AMBIENT TEMP(KELVIN)
500 REM R1=DENSITY (KG/M3)
510 REM U8=VELOCITY OF THE FREESTREAM
520 REM

```

```

530 DIM Y(1000),Z(1000),M1(1000),M2(1000)
540 DIM P1(1000),P6(1000)
550 REM
560 REM
570 INPUT "ENTER DATE.(MMDDYY)",N8
580 INPUT "ENTER TIME.(HHMM)",N9
590 PRINT IS 701
600 PRINT "DATE OF RUN IS",N8
610 PRINT "TIME OF RUN IS",N9
620 REM
630 INPUT "ENTER PTS SPANWISE",M3
640 INPUT "ENTER PTS VERTICAL",M3
650 REM N3 MUST BE AN EVEN INTEGER
660 INPUT "ENTER SPANWISE RESOLUTION(IN)",Z4
670 INPUT "ENTER VERTICAL RESOLUTION(IN)",Y4
680 INPUT "INITIAL Z(IN)",Z3
690 INPUT "INITIAL Y(IN)",Y3
700 PRINT "PTS SPANWISE",M3
710 PRINT "PTS VERTICAL",M3
720 PRINT "SPANWISE RESOLUTION (IN)",Z4
730 PRINT "VERTICAL RESOLUTION (IN)",Y4
740 PRINT "INITIAL Z(IN)",Z3
750 PRINT "INITIAL Y(IN)",Y3
760 REM
770 Z(1)=Z3
780 Y(1)=Y3
790 N9=N3/2
800 FOR I7=1 TO N9
810 I6=I7-1
820 J1=2*I6*M3+2
830 J2=2*I6*M3+M3
840 FOR K=J1 TO J2
850 Z(K)=Z(K-1)+Z4
860 Y(K)=Y(K-1)
870 NEXT K
880 J3=2*I6*M3+M3+1
890 Z(J3)=Z(J3-1)
900 Y(J3)=Y(J3-1)+Y4
910 J4=J3+1
920 J5=2*I6*M3+2*M3
930 FOR K=J4 TO J5
940 Z(K)=Z(K-1)-Z4
950 Y(K)=Y(K-1)
960 NEXT K
961 IF I7=N9 THEN 1010
970 J6=J5+1
980 Z(J6)=Z(J6-1)
990 Y(J6)=Y(J6-1)+Y4
1000 NEXT I7
1010 REM

```

```

1030 ASSIGN @P@H2 TO "PRSD"
1031 INPUT "DO YOU WANT TO BE IN PRELIMINARY?,"N$
1032 IF N$="Y" THEN 2290
1040 REM
1050 REM THIS SECTION COMPUTES THE ZERO OFFSET CORRECTION
1060 REM FOR THE TRANSDUCERS.
1070 REM
1080 PRINTER IS 1
1090 PRINT "COMPUTE THE ZERO OFFSET CORRECTION"
1100 PRINT "!!! DISCONNECT ALL TUBING TO THE TRANSDUCER!!!!"
1110 PRINT " HIT CONTINUE WHEN READY"
1120 PAUSE
1130 FOR I=200 TO 204
1140 G2=0
1150 FOR J=1 TO 50
1160 OUTPUT 709;"A";I;"VT1"
1170 ENTER 709;X2
1180 G2=G2+X2
1190 NEXT J
1200 G3=G2/50
1210 G4(I-199)=G3
1220 NEXT I
1230 REM END OF LOOP FOR ZERO CORRECTION OF TRANSDUCERS
1240 REM
1250 REM THIS LOOP CALIBRATES THE TRANSDUCER AGAINST THE MANOMETER
1260 REM
1270 FOR I=200 TO 204
1280 I1=I-199
1290 PRINT " TRANSDUCER CALIBRATION, ENTER THE MANOMETER PRESSURE IN INCHES OF
      WATER"
1300 PRINT
1310 PRINT
1320 PRINT "ENTER THE PRESSURE FOR TRANSDUCER NR.",I1
1330 INPUT H2
1340 G0=0
1350 FOR J=1 TO 50
1360 OUTPUT 709;"A";I;"VT1"
1370 ENTER 709;X
1380 G0=G0+X
1390 NEXT J
1400 E1=G0/50
1410 A(I-199)=H2/(E1-G4(I-199))
1420 PRINTER IS 701
1430 PRINT "A",I,"=",A(I-199)
1431 PRINTER IS 1
1432 PRINT "A",I,"=",A(I-199)
1440 INPUT "IS A(I-199) SATISFACTORY (Y/N)?"N$
1450 IF N$="N" THEN 1390
1460 PRINT
1470 PRINT
1490 NEXT I

```

```

1500 REM END OF LOOP FOR CALIBRATING TRANSDUCERS
1510 REM
1520 REM ENTER THE VALUES OF STATIC AND TOTAL PRESSURE OF THE FREESTREAM
1530 PRINT "INPUT STATIC PRESSURE OF FREESTREAM (IN.HG)"
1540 PRINT "USE TRANSDUCER NR.1 AND CHANNEL NR.200"
1550 PRINT
1560 PRINT "HIT CONTINUE WHEN P STATIC IS PROPERLY SET UP"
1570 PAUSE
1580 B6=0
1590 FOR J=1 TO 50
1600 OUTPUT 709;"AI";200;"UT1"
1610 ENTER 709;X6
1620 B6=B6+X6
1630 NEXT J
1540 REM END LOOP FOR ACQUIRING STATIC PRESS. OF FREESTREAM
1650 P6=B6/50
1660 PRINT
1670 PRINT
1680 REM
1690 PRINT "INPUT TOTAL PRESSURE OF THE FREESTREAM (IN.HG)"
1700 PRINT "USE TRANSDUCER NR.1 AND CHANNEL NR.200"
1710 PRINT "HIT CONTINUE WHEN P TOTAL PROPERLY SETUP"
1720 PAUSE
1730 B7=0
1740 FOR J=1 TO 50
1750 OUTPUT 709;"AI";200;"UT1"
1760 ENTER 709;X7
1770 B7=B7+X7
1780 NEXT J
1790 REM END OF LOOP FOR ACQUIRING TOTAL PRESSURE OF FREESTREAM
1800 P7=B7/50
1810 REM
1820 REM ENTER AMBIENT CONDITIONS
1830 INPUT "ENTER PAMB (IN.OF HG)",A1
1840 REM
1850 REM LOOP FOR ACQUIRING TEMP OF FREESTREAM VIA THERMOCOUPLE
1860 T=0
1870 FOR J=1 TO 50
1880 OUTPUT 709;"AI";109;"UT1"
1890 ENTER 709;T1
1900 T=T+T1
1910 NEXT J
1920 REM END OF LOOP
1930 T2=T/50
1940 REM CONVERT VOLTAGE TO TEMPERATURE
1950 E1=T2*1000
1960 T3=26.573*E1-1.936879+E1**2*.58795+E1**3-.051277*E1**4
1970 REM
1980 REM CONVERSION TO SI UNIT.
1990 T4=T3+273.15
2000 A1=A1*3385.82

```



```

2010 R1=A1/(287*T4)
2020 C=(P7-P9)*248.7
2030 REM FREESTREAM VELOCITY
2040 U9=(2*C/R1)**.5
2050 REM
2060 REM BEFORE EACH DATA RUN ENSURE THAT P2=P3 I.E. THE PROBE IS BALANCED
2070 PRINT "BALANCE P2 AND P3. "
2080 PRINT "HIT CONTINUE WHEN ALL TUBING HAS BEEN CONNECTED"
2090 PAUSE
2100 REM LOOP FOR BALANCING PROBE
2110 FOR I=201 TO 202
2120 G1=0
2130 FOR J=1 TO 50
2140 OUTPUT 709;"A1";I;"VT1"
2150 ENTER 709;X
2160 G1=G1+X
2170 NEXT J
2180 X=G1/50
2190 E=(I-199)*X
2200 P(I-199)=A(I-199)+E*(I-199)-64(I-199)
2210 NEXT I
2220 PRINT
2230 PRINT
2240 PRINT "P2=";P(2)
2250 PRINT "P3=";P(3)
2260 INPUT "DOES P2=P3 (Y/N)";N$
2270 IF N$="N" THEN 2100
2280 REM
2290 REM ENTER THE LOOP FOR ACQUIRING EACH PRESSURE COMPUTING COEFFICIENTS
2300 REM AND COMPUTING TWO PRESSURE COEFFICIENTS AND TWO PRESSURES
2301 PRINTER IS 701
2302 PRINT "Y      Z      M1      M2      P1      P2"
2303 PRINTER IS 1
2310 REM
2320 K9=0
2321 K2=M3*N3
2330 FOR K=1 TO K2
2331 K9=K
2340 REM
2390 WAIT 10
2400 REM LOOP FOR ACQUIRING EACH PRESSURE
2410 FOR I=200 TO 204
2420 G1=0
2430 REM
2440 FOR J=1 TO 10  REM ENTER THE DAS AND SAMPLE EACH PRESSURE 10 TIMES
2450 OUTPUT 709;"A1";I;"VT1"
2460 ENTER 709;X
2470 G1=G1+X
2480 NEXT J
2490 REM
2500 X=G1/10  REM AVERAGE THE VALUES

```

```

2510 E(I-199)=X
2520 P(I-199)=A(I-199)+E(I-199)+64 I-199  CORRECTION FOR ZERO AND TRANS. CH
2521 IF I=200 THEN
2522     P(I)=P(I-199)
2523 END IF
2530 NEXT I
2540 REM END OF LOOP FOR ACQUIRING PRESSURES
2550 REM
2560 REM COMPUTE THE AVERAGE OF P1,P3,P4,P5
2570 Q5=0
2580 FOR I=0 TO 5
2590 Q5=P(I)+Q5
2600 NEXT I
2610 P5(K)=Q5/4
2620 REM END LOOP
2630 REM
2640 REM COMPUTE THE COEFFICIENTS OF YAW AND PITCH
2650 REM
2660 Q1=P(2)-P(3)
2670 Q2=P(4)-P(5)
2680 Q3=P(1)-P6(K)
2710 M1(K)=Q1/Q3      LOCAL YAW COEFFICIENT
2720 M2(K)=Q2/Q3      LOCAL PITCH COEFFICIENT
2730 PRINTER IS 701
2740 PRINT USING 2750:(Y(K),Z(K),M1(K),M2(K),P1(K),P5(K))
2750 IMAGE MOD.00,2X,MOD.00,2X,MOD.0000,2X,MOD.0000,2X,MOD.0000,2X,MOD.0000
2760 REM
2770 NEXT K
2780 REM
2790 FOR I=1 TO K9
2800 OUTPUT @Path2:(I),Z(I),M1(I),M2(I),P1(I),P5(I)
2810 NEXT I
2820 ASSIGN @Path1 TO *
2830 ASSIGN @Path2 TO *
2840 PRINT "*****"
2850 PRINT
2860 PRINT "VELOCITY COMPUTATION AND VELOCITY COMPONENTS"
2870 PRINT
2880 PRINT
2890 PRINT "DATE OF RUN IS",NB
2900 PRINT "TIME OF RUN IS",NB
2910 PRINT
2920 PRINT "DENSITY(KG/M3)",R1
2930 PRINT "FREESTREAM VELOCITY (M/S)",U9
2940 PRINT "R AMBIENT(N/M2)",A1
2950 PRINT "T AMBIENT(C)",T3
2960 END

```

```

10 REM PROGRAM VEL
20 REM THIS PROGRAM COMPUTES THE COMPONENTS OF VELOCITY FROM
30 REM THE RAW DATA COLLECTED VIA THE PROGRAM PRS2
40 REM
50 REM AUTHOR GAVE ENVAL, SANDIA, WEDNESDAY, 11/11/77
60 REM
70 REM VARIABLE NAMES
80 REM
90 REM KE=AVERAGE PRESSURE
100 REM
110 REM M1=MEASURED YAW COEFFICIENT
120 REM M2=MEASURED PITCH COEFFICIENT
130 REM M3=MEASURED TOTAL COEFFICIENT
140 REM M4=MEASURED STATIC COEFFICIENT
150 REM
160 REM U=THE TOTAL VELOCITY AT THE PROBE TIP
170 REM U1=THE X COMPONENT OF VELOCITY
180 REM U2=THE Y COMPONENT OF VELOCITY
190 REM U3=THE Z COMPONENT OF VELOCITY
200 REM
210 REM X1=THE PITCH ANGLE FROM THE CALIBRATION DATA
220 REM Y1=THE YAW ANGLE FROM THE CALIBRATION DATA
230 REM
240 REM X4=THE PITCH ANGLE OF THE FLOW
250 REM
260 REM Y=THE VERTICAL LOCATION OF THE PROBE TIP
270 REM Z=THE SPANWISE LOCATION OF THE PROBE TIP
280 REM Y3=THE YAW ANGLE OF THE FLOW
290 REM
300 DIM C1(77),C2(77),C3(77),C4(77),M1(800),M2(800)
310 DIM X1(77),Y1(77),Y1(800),P1(800),P6(800),P8(800)
320 DIM Z(800),U(800),U1(800),U2(800),U3(800)
330 DIM Z1(800),F(800),U4(800),U5(800),U6(800),U7(800)
340 REM
350 INPUT "WHAT IS THE DENSITY FOR THIS RUN(RHO)?" ,R1
360 REM
370 REM READ CALIBRATION DATA INTO COMPUTER MEMORY
380 REM
390 ASSIGN @Path1 TO "CAL"
400 FOR I=1 TO 77
410 ENTER @Path1:X1(I),Y1(I),C1(I),C2(I),C3(I),C4(I)
420 NEXT I
430 REM READ RAW DATA INTO COMPUTER MEMORY
440 ASSIGN @Path2 TO "PRS2"
450 FOR I=1 TO 800
460 ENTER @Path2:Y1(I),Z(I),M1(I),M2(I),P1(I),P6(I)
470 NEXT I
480 REM
490 CREATE BDAT "VEL2",215
500 ASSIGN @Path3 TO "VEL2"

```

```

510 FOR I=1 TO 40
520 I9=K
530 X1(K)=Y1(K)*2.154
540 Z1(K)=Z1(K)*0.154
550 REM
560 REM COMPUTE THE FIRST APPROXIMATION OF YAW ANGLE
570 B3=-.15205904
580 B4=-7.26986712      ! COEFFICIENTS AND POLYNOMIAL ARE
590 C5=.10580689        ! FROM FOREIGN PROGRAM -SLEWT- AND
600 C6=.004015935       ! ARE COMPUTED FROM THE P-YAW AND
610 C7=.009000029       ! YAW DATA FROM THE CALIBRATION
620 C8=-.126008887
630 P3=B3+B4*M1(K)+C5*M1(K)^2+C6*M1(K)^3+C7*M1(K)^4+C8*M1(K)^5
640 REM
650 REM GO TO THE SUB-ROUTINE FOR PITCH ANGLE INTERPOLATION
660 GOSUB 1400
670 REM
680 REM GO TO THE SUB-ROUTINE FOR YAW ANGLE INTERPOLATION
690 GOSUB 1000
700 REM
710 REM GO TO THE SUB-ROUTINE FOR CP TOTAL AND CP STATIC INTERPOLATION
720 GOSUB 1350
730 REM
740 REM THIS SECTION COMPUTES THE MAGNITUDE OF THE LOCAL VELOCITY
750 REM VECTOR AT THE PROBE TIP
760 REM
770 P1(K)=P1(K)*248.2     ! CONVERT P1 TO N/M^2
780 P6(K)=P6(K)*248.2     ! CONVERT P6 TO N/M^2
790 REM CALCULATE STATIC AND TOTAL PRESSURE
800 P1(K)=P6(K)+.5*P1(K)-P6(K)
810 P6=P6      ! MORE BECAUSE INTERPOLATION RESULTS IN NEGATIVE VALUE FOR PSTAT
820 P1(K)=P1(K)+.5*(P1(K)-P6(K))
830 U4(K)=(2*(P1(K)-P6(K)))**.5
840 REM
850 REM COMPUTE THE COMPONENTS OF VELOCITY
860 REM
870 U5(K)=U4(K)*COS(X4)*COS(Y3)
880 U6(K)=U4(K)*SIN(X4)
890 U7(K)=U4(K)*COS(X4)*SIN(Y3)
900 NEXT K
910 REM END OF DATA REDUCTION LOOP
920 REM RE-ORDER DATA
930 I1=1
940 I2=40
950 FOR I=1 TO 721 STEP 80
960 J1=I1
970 J2=I2
980 FOR K=1 TO 40
990 Z0(J1)=Z(J2)
1000 P3(J1)=P(J2)
1010 U4(J1)=U4(J2)

```

```

1020 V1(J1)=V5(K1)
1030 V2(J1)=V6(K1)
1040 V3(J1)=V7(K1)
1050 J1=J1+1
1060 J2=J2+1
1070 NEXT J
1080 I1=I1+30
1090 I2=I2+30
1100 NEXT I
1110 I3=41
1120 FOR I=41 TO 803 STEP 30
1130 K=I3
1140 FOR J=1 TO 32
1150 I0(K)=I(K)
1160 P0(K)=P(K)
1170 Q0(K)=Q(K)
1180 V1(K)=V5(K)
1190 V2(K)=V6(K)
1200 V3(K)=V7(K)
1210 K=K+1
1220 NEXT J
1230 I3=I3+60
1240 NEXT I
1250 FOR K=1 TO 89
1260 OUTPUT @Path3:Y1(I),Z0(I),P0(I),Q0(I),V1(I),V2(I),V3(I)
1270 NEXT K
1280 ASSIGN @Path1 TO *
1290 ASSIGN @Path2 TO *
1300 ASSIGN @Path3 TO *
1310 PRINTER IS 1
1320 PRINT "Y:CM)      Z:CM)      P:LT)  Q:RT)      V1:M/S)      V2:M/S)      V3:M/S)"
1330 FOR I=1 TO 89
1340 PRINT USING 1350:Y1(I),Z0(I),P0(I),Q0(I),V1(I),V2(I),V3(I)
1350 IMAGE MOD.00,2X,MOD.00,2X,MOD00.000,2X,MOD.000,2X,MOD000.000,2X,MOD.000,2X,MOD000.000,2X,MOD.000,2X,MOD000.000
1360 NEXT I
1370 REM
1380 STOP
1390 REM
1400 REM PITCH ANGLE INTERPOLATION
1410 REM
1420 FOR I=1 TO 77
1430 IF Y3-Y(I) THEN 1450      SEARCH THRU CALIBRATION DATA TO FIND
1440 NEXT I                  YAW ANGLES WHICH BRACKET THE APPROX YAW
1450 K1=I                    ANGLE
1460 K2=I-7
1470 K3=I-1
1480 I4=I+5
1490 FOR J=K2 TO K3          FIND THE PITCH ANGLE WHICH CORRESPONDS TO
1500 IF MD K1-02(3) THEN 1520 THE MEASURED PITCH ANGLE

```

```

1510 NEXT J
1520 C1=C2/J -R2/(X1-X2)/(C1-C2)
1530 X2=X1/J -C1*(X1/J-X1)/(C1-C2) (BRACKETED TERM SAME AS IN 1510)
1540 FOR J=1 TO 14
1550 IF MOD(C2/J) THEN 1510
1560 NEXT J
1570 C2=C2/J -R2/(X1-X2)/(C2-C1)
1580 X1=X2/C2 -C1*(X1/C2-X1)/(C2-C1) (BRACKETED TERM SAME AS IN 1570)
1590 C3=X2/C2 -R2/(X1-X2)/(C3-C2) (BRACKETED TERM SAME AS IN 1570)
1610 X3=X1
1620 REM
1630 REM NEW MODEL INTERPOLATION
1640 REM
1650 FOR I=1 TO 7
1660 IF C1=C2 THEN 1680
1670 NEXT I
1680 REM
1690 REM
1700 FOR I=2 TO M3 (FIND YAW ANGLES WHICH
1710 IF X4 X1(I) THEN 1730 (CORRESPOND TO THE MEMBERS)
1720 NEXT I (FOR YAW ON PITCH ANGLES WHICH
1730 F1=1 (BRACKET X4)
1740 C1=X1
1750 F2=I+6
1750 F3=I+7
1760 Z4=C1*(F1-R1)/(C1(F1)-C1(F4))
1770 X4=X1(F1)-Z4*(Y1-F1)-Y(F4))
1780 Z5=C1*(F2-R1)/(C1(F2)-C1(F3))
1800 Y5=X1(F2)-Z5*(Y(F2)-Y(F3))
1810 Z6=X1*(F1-X4)/(X1(F1)-X1(F2))
1820 Y2=Y4-Z6*(Y4-Y5)
1830 RETURN
1840 REM
1850 REM INTERPOLATION FOR LOCAL COEFFICIENTS OF STATIC AND TOTAL PRESSURE
1860 Z=0
1870 D=0
1880 FOR I=1 TO 77
1890 IF Y3 Y(I) THEN 1910
1900 NEXT I
1910 F1=I
1920 F2=I-7
1930 F3=I-1
1940 F4=I+6
1950 FOR J=F2 TO F3
1960 IF X4 X1(J) THEN 1980
1970 NEXT J
1980 F5=J
1990 F6=I+1
2000 F7=J+7

```

```

2010  F6=J+6
2020  Z3=X1(F6)+X4*(X1(F6)-X1(F5))
2030  N4=C4(F6)+Z3*(C4(F6)+C4(F5))
2040  N3=C3(F6)+L3*(C3(F6)+C3(F5))
2050  L4=C4(F6)+Z3*(C4(F6)+C4(F5))
2060  L3=C3(F6)+L3*(C3(F6)+C3(F5))
2070  Z2=X1(F6)+N3*(X1(F6)+X1(F5))
2080  M4=N4+Z2*(M4+L4)      LOCAL STATIC COEFFICIENT
2090  M3=N3+Z2*(M3+L3)      LOCAL TOTAL COEFFICIENT
2100  RETURN
2110  STOP
2120  END

```

```

1  REM PROGRAM PLOT
2  REM THIS PROGRAM MAKES CONTOUR PLOTS FOR STREAMWISE
3  REM VELOCITY AND CAN BE MODIFIED TO MAKE CONTOUR PLOTS
4  REM FOR TOTAL PRESSURE
10  DIM X(300),Z(400),P(300),V(300),T(300),C(300)
20  DIM X(300)
30  ASSIGN EPROM TO "PLOT1"
40  FOR I=1 TO 300
50  ENTER EPROM:V(I),Z(0),P(I),V(I),T(I),C(I)
60  NEXT I
70  V=V(I)
80  V3=V(I)
90  FOR J=1 TO 300
100  IF V(I) > V3 THEN V3=V(I)
110  IF V(I) < V3 THEN V3=V(I)
120  NEXT J
130  C=V3-V(I)
140  FOR J=1 TO 300
150  Z=V3+J
160  IF V(I) > Z THEN V3=V(I)
170  FOR J=1 TO 3
180  Z1=V3+J+10*0
190  Z2=V3+J
200  IF V(I) > Z1 AND V(I) > Z2 THEN X(J)=0
210  NEXT J
220  NEXT I
230  FOR I=1 TO 300
240  IF X(I) > 9 THEN GOTO 226
250  Z1=V3+10*0
260  Z2=V3+9.7*0
270  IF V(I) > Z1 AND V(I) > Z2 THEN X(I)=0
280  NEXT I
290  GINIT
300  (PLOTTER IS 705,"HPGL"
310  PLOTTER IS CRT,"INTERNAL"
320  GRAPHICS ON
330  CSIZE 4.5,.85
340  MOVE 39,10
350  LABEL "EMBEDDED VORTEX 20 M/S "
360  MOVE 43.5,7
370  LABEL "75% FILM COOLING"
380  MOVE 41,85
390  LABEL "STREAMWISE VELOCITY"
400  MOVE 56.17
410  CSIZE 3.0
420  LABEL "Z CM "
430  MOVE 5,56
440  CSIZE 3.0
450  LABEL "Y CM "
460  FOR I=1 TO 6
470  GOTO 300

```



```

380 NEXT I
390 VIEWPORT 15,114,15,13
400 SHADE 10,5,0,10
410 FRAME
420 XYES 15,15,0,0,2,0
430 XYES 15,15,-16,12,0,0
440 XYES 10,15,5,12,0,0
450 ZSIZE 2,0,1,55
460 MOVE 14,0,10,95
470 LABEL "VELOCITY RANGES"
480 A=10.1
490 FOR K=0 TO 9
500 S=A-K*.35
510 MOVE 14,3,0
520 ZI=VS+(0+I)*D
530 IF K=9 THEN ZI=VS+(0+I)*D
540 LABEL USING "D,2X,00.0,X,00.0",A,12,ZI
550 NEXT K
560 MOVE 14,3,0-.35
570 LABEL USING "0,2X,00.0,X,00.0",0,11,93
580 CSIZE 1,3,1,72
590 FOR I=1 TO 800
600 MOVE (0+I),Y1+I)
610 IF Y1+I>5.0 AND Z0+I>=10. THEN GOTO 491
620 LABEL USING "0",X+I)
630 NEXT I
640 CLIP OFF
650 CSIZE 2,0,1,55
660 FOR I=1.0 TO 11.0 STEP 2
670 MOVE 17.5,I
680 I1=14.2
690 LABEL USING "#,00.0",I1
700 NEXT I
710 FOR J=17.0 TO 5.0 STEP 2
720 MOVE J,-.7
730 J1=J+1.0
740 LABEL USING "#,MOD.0",J1
750 NEXT J
760 END

```

```

10  REM PROGRAM VECTOR
20  REM THIS PROGRAM USE DATA FROM VELO DATA FILES
30  REM TO PLOT SECONDARY FLOW VECTORS
40  DIM Y(100),Z(100),P(100),U(100),V(100),W(100),X(100)
50  DIM X(100),Y(5),Z(5)
60  ASSIGN @PathJ TO "VELOC1A"
70  FOR I=1 TO 100
80  ENTER @PathJ(1),Z(1),P(1),U(1),V(1),W(1)
90  NEXT I
100 GINIT
110 PLOTTER IS 705,"HABL"
120 !PLOTTER IS CRT,"INTERNAL"
130 GRAPHICS ON
140 CSIZE 4.5, 55
150 MOVE 39,10
160 LABEL "EMBEDDED NUMBER 11"
170 MOVE 43.5,7
180 LABEL "75% FIRM 10/100"
190 MOVE 55.4,85
200 LABEL "SECONDARY FLOW ONLY"
210 MOVE 62,17
220 CSIZE 3.0
230 LABEL "ON"
240 MOVE 5,65
250 CSIZE 3.0
260 Label="Y ON"
270 FOR J=1 TO 5
280   LABEL Label(1),J
290   NEXT J
300 VIEWPORT 15,114,25,70
310 SHOW -15.5,0,12
320 FRAME
330 AXES .5,.5,0,0,2,2
340 AXES .5,.5,-15,12,2,2
350 AXES .5,.5,8,12,2,2
360 CSIZE 1.3,.72
370 S1=.21
380 A1=0.
390 FOR K=751 TO 800
400   A1=A1+V1(K)
410   NEXT K
420   A1=A1*S1/40.
430   MOVE -14.5,10.5
440   Y(1)=10.5
450   Y(2)=10.6
460   Z(1)=-14.5
470   Z(2)=-14.5+A1*.1
480   FOR J=1 TO 2
490     PLOT Z(J),Y(J)
500   NEXT J
510 PENDING

```

AD-A183 428

STUDY OF VORTICES EMBEDDED IN BOUNDARY LAYERS WITH FILM 2/2
COOLING(U) NAVAL POSTGRADUATE SCHOOL MONTEREY CA
D L EVANS MAR 87 NIPR-FY-1455-86-N0616

UNCLASSIFIED

F/G 20/4

NL





MICROCOPY RESOLUTION TEST CHART

```

520 MOVE -15.,9.5
530 CSIZE 2.0,.65
540 LABEL "0.1 FS VELOCITY"
550 FOR I=1 TO 900
560 Y(1)=Y1(I)
570 Z(1)=Z0(I)
580 Y(2)=Y1(I)+S1*V2(I)
590 Z(2)=Z0(I)+S1*V3(I)
600 I
610 I BUSINESS TO MAKE ARROWS
620 I
630 D1=(Y(2)-Y(1))
640 D2=(Z(2)-Z(1))
650 DEG
660 A3=ATN(D2/D1)
670 A4=45-A3
680 E3=0.
690 IF D1<0 AND D2<0 THEN E3=1.0
700 IF E3=1.0 AND A3<-45. THEN A4=A3+135
710 D4=((Z(2)-Z(1))^2+(Y(2)-Y(1))^2)^(.5)
720 D4=.20*D4
730 D8=1.0
740 D9=1.0
750 IF A4<45 THEN D9=-1.0
760 E1=0.
770 E2=0.
780 IF D1<0 AND D2<0 THEN D9=-1.0
790 IF D1>0 AND D2<0 THEN D8=-1.0
800 IF D1<0 AND D2<0 THEN D8=-1.0
810 IF D1<0 AND D2<0 THEN D9=-1.0
820 IF D1<0 AND D2>0 THEN D8=-1.0
830 IF D1<0 AND A3>45 THEN D8=1.0
840 IF A3<-45. AND A3<0. THEN D8=1.0
850 IF D1>0 AND D2<0 THEN E1=1.0
860 IF E1=1.0 AND A3<-45. THEN D8=1.0
870 IF D1<0 AND D2<0 THEN E2=1.0
880 IF E2=1.0 AND A3<45. THEN D9=1.0
890 Y(3)=Y(2)-D4*COS(A4)*D8
900 Z(3)=Z(2)-D4*SIN(A4)*D9
910 Y(4)=Y(2)+
920 Z(4)=Z(2)+
930 A5=A4-90
940 IF D1>0 AND D2<0 THEN D8=1.0
950 IF D1<0 AND D2<0 THEN D9=1.0
960 Y(5)=Y(2)+D4*COS(A5)*D9
970 Z(5)=Z(2)+D4*SIN(A5)*D8
980 I
990 I END OF BUSINESS TO MAKE ARROWS
1000 I
1010 MOVE Z0(I),Y1(I)

```

```
1020 IF Y(I)>8.5 AND Z(I)>10. THEN GOTO 1070
1030 FOR J=1 TO 5
1040 PLOT Z(J),Y(J)
1050 NEXT J
1060 PENUP
1070 NEXT I
1080 CLIP OFF
1090 CSIZE 2.0,.55
1100 FOR I=-1.2 TO 11.0 STEP 2
1110 MOVE -17.5,I
1120 I1=I+.2
1130 LABEL USING "I,DD.D":I1
1140 NEXT I
1150 FOR J=-17.0 TO 5.0 STEP 2
1160 MOVE J,-.7
1170 J1=J+1.0
1180 LABEL USING "J,DD.D":J1
1190 NEXT J
1200 END
```

APPENDIX C UNCERTAINTY ANALYSIS

Uncertainty analysis was performed using the method originally attributed to Kline and McCormick, [Ref. 13]. Let δ_r be the uncertainty in the result and $\delta_1, \delta_2, \dots, \delta_n$ be the uncertainties associated with each independent variable. The uncertainty in the result can be expressed as

$$\delta_r = [\sum((\partial R/\partial x_i) \times (\delta_i))]^{1/2} \quad (\text{eqn C.1})$$

To determine the uncertainty of the pitch angle, α , a straight line approximation was made for α

$$\alpha = m + b(C_{p_{\text{pitch}}}) \quad (\text{eqn C.2})$$

The following independent variables were determined: $\delta_m = \pm 1.97^\circ$, $\delta_b = \pm 2.32^\circ$, and $\delta_{C_{p_{\text{pitch}}}} = \pm 0.04637$. The uncertainty of α , was determined to be $\pm 2.36^\circ$. The high uncertainty of the pitch angle is caused by the probe being highly sensitive in the pitch plane.

The uncertainty of the yaw angle, β , is determined in a similar manner. Once again, a straight line approximation is made.

$$\beta = m + b(C_{p_{\text{yaw}}}) \quad (\text{eqn C.3})$$

In this case, the uncertainties of the independent variables were found to be $\delta_m = \pm 0.954$, $\delta_b = 0.5924$, and $\delta_{C_{p_{\text{yaw}}}} = \pm 0.058$. From these values the uncertainty of β was calculated to be $\pm 1.29^\circ$.

LIST OF REFERENCES

1. Horlock, J. H., "Recent Developments in Secondary Flow," *AGARD Conference Proceeding No. 214*, March 1977.
2. Herzig, H. Z., Hansen, A. G., and Costello, G. R., *A Visualization Study of Secondary Flows in Cascades*, NACA Report 1163, 1953.
3. Langston, L. S., Nice, M. L., and Hooper, R. M., "Three Dimensional Flow Within a Turbine Cascade Passage," *Journal of Engineering for Power*, v. 99, pp. 21-28, January 1977.
4. Marchal Ph. and Sieverding, C. H., "Secondary Flows Within Turbomachinery Bladings," *AGARD Conference Proceedings No. 214*, March 1977.
5. Sieverding, C. H. and Van Den Bosche, P., "The Use of Coloured Smoke to Visualize Secondary Flows in Turbine-Blade Cascade," *Journal of Fluid Mechanics*, v. 134, pp. 85-89, September 1983.
6. Ongoren, A., *Heat Transfer on Endwalls of a Turbine Cascade with Film Cooling*, Project Report 1981-19, Von Karmen Institute for Fluid Dynamics, Rhode Saint Genese, Belgium, June 1981.
7. Langston, L. S., "Crossflow in a Turbine Cascade Passage," *Journal of Engineering for Power*, v. 102, pp. 866-874, October 1980.
8. Gostelow, J. P., *Cascade Aerodynamics*, p. 49, Pergamon Press, 1984.
9. Aerolab, *Operating Instructions for Aerolab 8"x24" Laminar Turbulent Shear Layer Facility with Variable Height Test Section for U.S. Naval Postgraduate School*, November 1985.
10. Joseph, S. J., *The Effects of an Embedded Vortex on a Film Cooled Turbulent Boundary Layer*, ME Thesis, U.S. Naval Postgraduate School, Monterey, Ca., December 1986.
11. Ligrani, P. M., *Qualification and Performance of NPS Shear Layer Research Facility*, NPS Report, Department of Mechanical Engineering, U.S. Naval Postgraduate School, Monterey, Ca., in preparation to appear in 1987.
12. Treaster, A. L. and Yocum, A. M., "The Calibration and Application of Five Hole Probes," *ISA Transactions*, v.18, pp. 23-34.
13. Kline, S. J. and McClintock, F. A., "Describing Uncertainties in Single-Space Experiments," *Mechanical Engineering*, pp.3-8, January 1953.

INITIAL DISTRIBUTION LIST

		No. Copies
1.	Defense Technical Information Center Cameron Station Alexandria, VA 22304-6145	2
2.	Library, Code 0142 Naval Postgraduate School Monterey, CA 93943-5002	2
3.	Professor P.M. Ligrani Code 69SLi Department of Mechanical Engineering Naval Postgraduate School Monterey, CA 93943	6
4.	Department Chariman Code 69 Department of Mechanical Engineering Naval Postgraduate School Monterey, CA 93943	1
5.	Dr. Charles MacArthur Project Engineer Components Branch Turbine Engine Division Aero Propulsion Laboratory Department of the Air Force Air Force Wright Aeronautical Laboratories Wright-Patterson Air Force Base, OH 45433	10
6.	LT. Stephen L. Joseph, USN 15 Brewster Road Milford, CT 06460	1
7.	LCDR. David L. Evans, USN 7103 N. 26th Drive Phoenix, AZ 85021	4

END

9-87

Dtic